THE

LONDON, EDINBURGH AND DUBLIN

PHILOSOPHICAL MAGAZINE

AND

JOURNAL OF SCIENCE.

[SEVENTH SERIES.]

APRIL 1937.

L. *Effect of Thunderstorms and Magnetic Storms on the Ionization of the Kennelly-Heaviside Layer.*

By J. N. BHAR, *M.Sc., Sir Rashbehary Ghose Research Scholar in Physics, University of Calcutta, and* P. SYAM, *M.Sc., Lecturer in Physics, Cotton College, Gauhati (Assam)* *.

1. *Introduction.*

MEASUREMENTS carried over long periods on the temporal variation of the ionization of the ionosphere have proved definitely that the ultra-violet radiation from the sun is the chief agency responsible for the production and maintenance of the ionization. The average variation of ionization is found to follow the diurnal and seasonal variation of the sun's altitude. Besides such regular variations—which may be called normal variations,—there are other variations, particularly in the lower Kennelly-Heaviside region of the ionosphere, of more or less erratic nature, the origin of which cannot be traced to ultra-violet solar radiation. Observations made by various workers [1] seem to show that a large number of these are probably connected with thunderstorms or/and magnetic storms.

It is obvious that the irregular nature of these disturbances, complicated by the fact that both of these

* Communicated by Prof. S. K. Mitra, D.Sc.

might occur simultaneously, makes it difficult to study their relationship with abnormal changes in ionospheric conditions. A subtropical region like Bengal, however, presents certain advantages in the study of one of the disturbances—the thunderstorms. In the first place the thunderstorms occur here more or less regularly in certain parts of the day during certain months of the year. In the second place, on account of the low latitude, the influence of magnetic storms may be expected to be much less here than at higher latitudes, since the charged particles from the sun responsible for magnetic storms are concentrated mostly in higher latitudes by the action of the earth's magnetic field. In view of these facts, and also because regular and systematic observations of thunderstorm effect on the ionosphere seem to be lacking, it was decided to keep regular records of the ion content of the Kennelly-Heaviside layer at Calcutta (lat. 22° 33′ N., long. 88° 23′ E.) during the months of April-July 1935, when the thunderstorms are of frequent occurrence, mostly in the afternoon. The records were then compared with thunderstorm and magnetic storm data obtained from the Meteorological Observatories at Alipore, Calcutta, and at Colaba, Bombay, respectively.

2. *Theoretical Considerations.*

The exact manner in which thunderstorms may influence the ionization of the ionospheric regions is not yet fully understood. Two processes have been pictured by Prof. C. T. R. Wilson which we shall discuss here in a little detail.

If, according to Wilson [2], we suppose that the upper part of a thundercloud is positively electrified, then an electric field is produced between the cloud and the Kennelly-Heaviside layer. This field may at times be so intense as to exceed the critical sparking value in the region immediately below the layer, where the pressure is much lower than that near the cloud. A very simple calculation made by Appleton [3] shows that even when the field near the cloud is only 1/27th of the sparking value, the field at a distance of 7 km. below the layer may reach the sparking value and the production of intense ionization currents may take place. He therefore suggested that the first effect of a thundercloud,

if it is sufficiently electrified, would be to produce a subsidiary region of ionization nearly 7 km. below the already existing ionized layer and vertically above the cloud. If, however, the cloud moves away from below the point of observation in the ionosphere, the ionizing effect at this point would gradually diminish until it becomes inappreciable. We shall attempt to estimate, from this point of view, the maximum probable distance from which thunderclouds can exert just appreciable influence on the particular portion under investigation of the Kennelly-Heaviside layer.

According to Wilson a thundercloud may be supposed to have an electric moment, say M, which is the resultant of the moments due to its upper and lower charges and their respective images in the earth. Such a cloud would

Fig. 1.

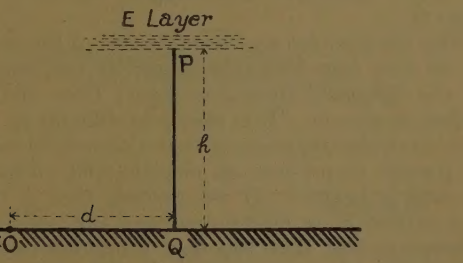

O. Position of the cloud ; Q. Place of observation ;
P. Portion of the ionized layer under investigation.

produce an electric field $\frac{2M}{h^3}$ at a point vertically above it and at a height h from the ground. Let P be the portion of the ionized layer under investigation and Q the point on the ground immediately below it so that PQ$=h$. If a thundercloud of electric moment M is above the point O at a horizontal distance d from Q, the vertical intensity of the electric field at P due to this cloud is easily seen to be

$$\frac{M}{(h^2+d^2)^{5/2}}(2h^2+d^2).$$

This expression enables us to make an estimate of the rate at which the field at P diminishes as the thundercloud recedes away from Q. The following table gives

the values of the electric field at P due to a thundercloud of electric moment M situated at different horizontal distances from Q.

TABLE I.

Variation of Electric Field with Distance.

Distance.	Field.	Distance.	Field.
$d=0$	$2M/h^3$	$d=3/2\,h$....	$2M/h^3.1/9$
$d=h/2$	$2M/h^3.1/1{\cdot}5$	$d=2h$	$2M/h^3.1/18{\cdot}5$
$d=h$	$2M/h^3.1/3{\cdot}7$	$d=5/2\,h$....	$2M/h^3.1/34$

It is evident from the above table that the electric force at P diminishes gradually as the cloud moves away from Q.

The composition and the pressure of the air at a height of 80 km. (the probable height of the lower boundary of the Kennelly-Heaviside layer) from the ground are rather uncertain. It is therefore difficult to estimate the minimum electric moment that a thundercloud is required to possess to produce an electric field of sparking value at such a height. If we assume that a thundercloud has ordinarily an electric moment not very far from this minimum, and that the field produced by it at a point vertically above it and at the height of the E layer does never exceed, say, 30 times the sparking value, it can be seen from the above table that thunderclouds situated beyond 200 km. would not produce appreciable effect at the point under investigation, for the intensity of the vertical electric field would then be less than 1/30th of that which it would produce if it were immediately below that point. Thus, to search for a correlation it seems enough, from this point of view, to take into account only those thunderstorms which might be in progress within a radius of about 200 km. around the place of observation.

There is another process, as pictured by Wilson, by which thunderclouds may indirectly affect upper atmospheric ionization. Consider an electron of radioactive origin or one produced inside the cloud by local discharges. On account of the intense electric field between the upper

and lower parts of the cloud (which is ordinarily assumed to be directed downward) it would travel upward and rapidly increase in energy, for the gain in energy during its travel in the electric field would exceed the loss of energy due to collision along its path. It has been shown [4] by Schonland that the energy acquired by these electrons cannot exceed 5×10^9e-volts. A stream of these runaway electrons moving upward past the upper boundary of the cloud would be attracted back into it owing to the strong upwardly directed electric field existing in the space between the upper part of the cloud and the lower boundary of the E layer. But when a spark discharge occurs the field is destroyed and the spray of " runaway electrons " moves upward with tremendous velocity

Fig. 2.

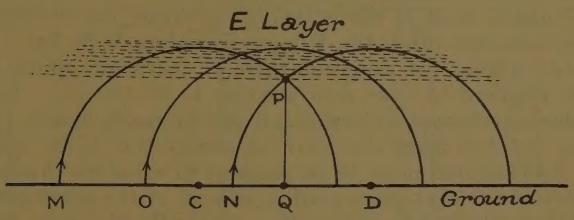

C, D, and Q—Centres of the circles, each of radius 100 km., described by electrons starting from M, N, and O respectively. An electron describing a circle of radius lying between limits 100 and 80 km. must start from some point within MN (and not outside) in order to have some portion of its trajectory at or above P. If PQ = 80 km., it can be shown from geometry that QM = 160 km., and QN = 40 km.

towards the ionosphere. Depending upon their initial velocity these would either be bent down by the earth's magnetic field or reach the E layer in due time. In the latter case the " runaway electrons " might possibly affect the ionization of the E layer.

If we neglect the effect of collision with neutral atoms and molecules, the only force that remains to act on these upward moving electrons is that exerted by the earth's magnetic field. It is therefore evident that they would describe circles, the radii of curvature of which would depend upon their initial velocity. Now, electrons of

such a high energy value as 5×10^9 e-volts will move with a velocity only a few metres per second less than that of light, so that their inertial mass becomes about 2000 times as great as their rest mass. Taking this fact into account, and remembering that the intensity of the earth's horizontal magnetic field at Calcutta is approximately ·3765 Gauss, it is easily seen that the radius of curvature of the path of the runaway electrons of the maximum possible energy value comes out to be about 100 km. If the energy is less the radius of curvature diminishes correspondingly. Again, if the force of friction arising from collision is taken into account the radius of curvature would also diminish. Thus it is clear that the maximum limit for the radius of curvature is about 100 km. Now since the runaway electrons are emitted vertically upward it is evident that they must describe semi-circles on the horizontal through their starting-point. As such the minimum value of the radius of curvature for which the electrons can reach the E layer boundary is 80 km. In other words, the range of radii of curvature which we are required to take into account is 80–100 km. Considering this range of values, it can be easily shown that the distance from the place of observation Q at which a thundercloud must be in progress to shoot up runaway electrons so that some portion at least of the upper parts of their trajectories are at P or vertically above it, must be within limits 160 and 40 km. nearly. If the distance of a cloud be outside these limits (*i. e.*, if its distance from Q is less than 40 km. or greater than 160 km.) electrons shot up from it would bend away from P without being able to affect the ionization at this point.

It should be noted that at places where the declination of the earth's field is very small (in Calcutta it is 1° West) electrons shot off in this way would affect the ionization of that portion of the ionosphere which lies to the east of the thundercloud. Thus as regards ionization produced by runaway electrons, we might only consider thunderclouds occurring due West of Calcutta and lying within a distance range of 160–40 km.

Considering all these points we have sought for the correlation between thunderstorm activity and abnormal increases of ionization by taking into account thunderstorms which were in progress within a radius of 200 km. round Calcutta.

3. *Experimental Arrangement.*

The method employed in our experiments was the group retardation method of Breit and Tuve. The interruptions were produced by the usual method of inserting a leaky condenser of suitable value in the grid circuit of the oscillator valve. It being not possible for us to transmit a continuous range of wave-lengths to find out the critical penetration frequency, we employed a large number of gradually increasing frequencies extending from ·7 to 9 Mc. per second, and the actual critical frequency was determined by interpolation. The receiver employed was placed by the side of the transmitter in the same room, but was connected to a separate aerial. The observations were all made in the Wireless Laboratory of the University College of Science, Calcutta.

Fig. 3.

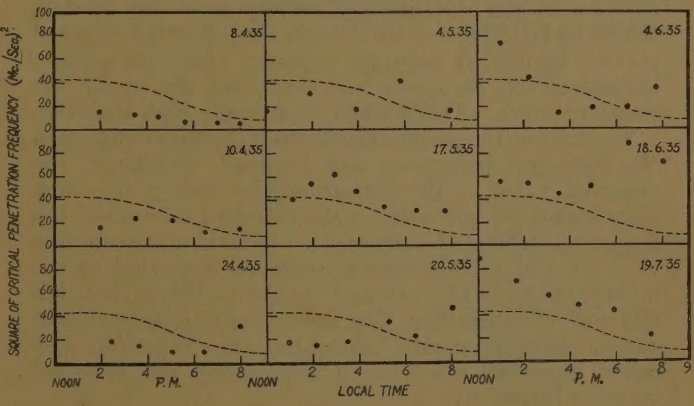

The dots represent the observed values of E layer ionization at different hours of the day. The broken line curves indicate the normal hourly variation of ionization calculated from Chapman's theoretical formula for summer solstice at Calcutta.

4. *Discussion of Results.*

The observations were usually made throughout the afternoon at intervals of about one hour and a half, thrice every week. The squares of the observed values of the critical penetration frequency were plotted against time for each day of observation. Some of these plots are represented in fig. 3. The points therefore represent

the values of the ionization density at different hours of the day. It is not possible to pick out from these points those which represent abnormal ionization without referring them to some standard curve indicating the normal variation of ionization during the hours of observation. Since the variation of ionization as caused by solar ultra-violet rays has been called the normal variation, we have drawn the standard ionization curve from Chapman's formula [5], starting from the observed value of the critical penetration frequency for the E layer at noon on summer solstice at Calcutta. This standard curve is drawn in broken lines, for comparison, in the diagram. It may be noted that Calcutta, being nearly on the Tropic of Cancer, the standard curve will represent the ionization and its variation due to the ultra-violet radiation from the sun alone fairly well for the months of May, June, and July. In the month of April, since the mid-day zenithal distance of the sun changes rapidly from day to day, the normal ionization will evidently not follow the standard curve. In fact, it may be expected that the average ionization will be much less than that shown by the standard curve. This is what has actually been observed.

To pick out the points representing abnormal ionization the following procedure was adopted. Whenever the observed value of the ionization was seen to be more than about 125 per cent. of the standard ionization, the former was taken to be abnormal. In making the selection we have had to take into account the fact that in the month of April the average ionization throughout the day was much less than that represented by the standard curve. In this month, therefore, the ionization was called abnormal whenever it approached the standard value or crossed it.

Having classified the abnormal ionizations in the above manner the data of thunderstorms and magnetic storms were consulted. The magnetic storm records, which were supplied to us by the Colaba Observatory, Bombay, only class the days as being magnetically quiet or of small or large magnetic disturbance without any reference as to the actual hours or the durations of the disturbances. It was, therefore, considered advisable to group separately, as a first step, the days of magnetic disturbance and the days of no magnetic disturbance. The thunderstorm records, which were supplied to us by the

Alipore Observatory, Calcutta, were next looked into to find whether thunderstorms and/or lightning discharges had been actually occurring or not at the hours of observation within a radius of 200 km. round Calcutta.

It seems necessary to explain why the records of lightning observed have also been taken into account together with thunderstorm records. The range of the different

TABLE II.

(*a*) Days of no Magnetic Disturbance.

Date.	Time of observation I.S.T.	Square of penetration frequency (Mc./sec.)^2.	Ionization.	Place and time of occurrence of thunderstorms and/or lightning discharges.
1.4.35	1606	16	Normal.	Nil.
	1806	25	Abnormal.	MDP (104 W) T1800–1900.
	1836	,,	,,	MDP (104 W) T 1800–1900.
12.4.35	1506	17	Normal.	Nil.
	1636	11	,,	,,
	1806	16	Abnormal.	,,
	1936	7	Normal.	,,
15.5.35	1306	18	Normal.	,,
	1410	14	,,	,,
	1520	18	,,	,,
	1636	22	,,	,,
	1806	25	Abnormal.	BLS (179 SW) T 1700–2036. KRG (98 N) T 1700–2036.
	1910	23	,,	Local T 1902–2027.
	1945	31	,,	MDP (104 W) T 1900–2000.
	2036	31	,,	STR (69 E) T 1900–2023.
etc.		etc.		etc.

observatories situated within a radius of 200 km. around Calcutta for the recording of thunderstorms is very small. They can record only those thunderstorms which are in progress locally. Hence, if we take into consideration the direct records of thunderstorms only, we are evidently sure to miss many that might occur at places intermediate between any two recording stations. To make up for this defect, the records of lightnings observed between stations have also been taken into account, for the

occurrence of lightning discharges must be due to the presence of highly charged thunderclouds which the observatories could not directly record. The whole set of data was then tabulated (Table II. (*a*) and (*b*)) as shown on pp. 521 and 522 :—

[The meanings of the symbols in the fifth column are as follows :—MDP, BLS etc. are the code names of the

TABLE II. (*cont.*).

(*b*) Days of Magnetic Disturbance.

Date.	Time of observation I.S.T.	Square of penetration frequency (Mc./sec.)².	Ionization.	Time and place of occurrence of thunderstorms and/or lightning discharges.
10.4.35	1336	14	Normal.	Nil.
	1506	26	Abnormal.	,,
	1636	21	,,	,,
	1806	11	Normal.	Local L 1805–1930.
	1936	15	Abnormal.	MDP (104 W) L 1900–1951. STR (69 E) T 1846–1921. BLS (179 SW) T 1930–1951.
1.5.35	1506	11	Normal.	Nil.
	1636	11	,,	,,
	1806	22	Abnormal.	,,
	1936	7	Normal.	,,
4.6.35	1236	72	Abnormal.	,,
	1350	50	,,	,,
	1510	13	Normal.	,,
	1636	20	,,	,,
	1806	20	Abnormal.	,,
	1920	50	,,	,,
etc.		etc.		etc.

observing stations, *e. g.*, MDP (Midnapore), BLS (Balasore) etc. The numerical figures and the letters within brackets give the distance of the observing station and its direction from Calcutta ; (104 W) stands for 104 km. west of Calcutta. The letters T and L signify thunderstorm and lightning. The hours of observation are given in Indian Standard Time, which is 24 minutes behind Calcutta time.]

The total number of observations on days of no magnetic disturbance was 122, and on days of magnetic disturbance was 68. Having thus tabulated the observations, the

results were summarized in the form of a four-fold table as follows :—

TABLE III.

Frequency Distribution of Ionization with and without Thunderstorms.

(*a*) Days of no Magnetic Disturbance.

	Ionization normal.	Ionization abnormal.	Total.
No thunderstorm ...	79	22	101
Thunderstorm	1	20	21
Total	80	42	122

(*b*) Days of Magnetic Disturbance.

	Ionization normal.	Ionization abnormal.	Total.
No thunderstorm ...	32	17	49
Thunderstorm	1	18	19
Total	33	35	68

These tables at once indicate some relation between thunderstorm activity and abnormal increases of E region ionization. In order to be definite about the association between the two we apply the statistical ($P\chi^2$) test of goodness of fit [6]. The values obtained are shown in Table IV.

TABLE IV.

($P\chi^2$) Test of Association between Thunderstorm and Abnormal Ionization.

	N.	χ^2.	C_1.	P.
No magnetic disturbance.	122	41·55	0·504	$<10^{-6}$
Magnetic disturbance ...	68	19·76	0·474	$<10^{-4}$
Total	190	62·38	0·497	$<10^{-6}$

The values under "total" are obtained by ignoring the absence or presence of magnetic disturbances.

The table shows that on magnetically quiet days the value of χ^2 is 41·55 and the value of $P<10^{-6}$, *i. e.*, the chance of obtaining a value of χ^2 equal to or greater than the observed value (41·55) on the assumption of complete independence between thunderstorm and abnormal E region ionization is less than 1 in 10^6. Hence it is reasonable to conclude that occurrences of thunderstorms and abnormal ionization must be associated to some extent. This is true of magnetically quiet days as well as of those of magnetic disturbance.

In order to make an estimate of the degree of association between the two variables (thunderstorm activity and abnormal ionization) which are classified in categories and not in quantitative measures, we may apply Pearson's method of Contingency Coefficient in which he defines C_1, *the coefficient of mean square contingency*, as follows :—

$$C_1=\sqrt{\frac{\phi^2}{1+\phi^2}}=\sqrt{\frac{\chi^2}{N+\chi^2}}$$

$$\left(\text{since the mean square contingency } \phi^2=\frac{\chi^2}{N}\right).$$

With normal distribution and certain restrictions as to grouping, Pearson has shown that C_1 ultimately becomes numerically equal to r, the well-known coefficient of correlation *. The values of C_1 between thunderstorm activity and abnormal ionization are shown in Table IV. col. 3, and it will be seen that these are approximately equal to 0·50. The values of this coefficient indicate a strong correlation between the two and are practically identical on both magnetically quiet as well as on disturbed days.

With a view to find out the association between magnetic disturbances and abnormal ionization, the occasions on which thunderstorms were acting were grouped separately

* In his paper "On the Theory of Contingency and its Relation to Association and Normal Correlation" (Drapers' Company Research Memoirs, Biometric series, I. pp. 1–35 (1904). Pearson shows that, provided the distribution is normal and the classes are sufficiently small to make it possible to replace integral values by groupings over small areas, the coefficient of correlation is given by the value $\pm\sqrt{\frac{\phi^2}{1+\phi^2}}$, where ϕ^2 is the mean square contingency.

from those on which there were no thunderstorms. In view of the fact that the hours and durations of the magnetic disturbances are not available, it was decided to assume, for the sake of simplicity, that such disturbances were operative throughout the days which are characterized as magnetically disturbed in the data supplied to us. Proceeding in this way the following tables were arrived at :—

TABLE V.

Frequency Distribution of Ionization with and without Magnetic Disturbances.

(1) Occasions of no Thunderstorms.

	Ionization normal.	Ionization abnormal.	Total.
No magnetic disturbance..	79	22	101
Magnetic disturbance	32	17	49
Total	111	39	150

(2) Occasions of Thunderstorm.

	Ionization normal.	Ionization abnormal.	Total.
No magnetic disturbance ..	1	20	21
Magnetic disturbance	1	18	19
Total.....	2	38	40

The ($P\chi^2$) test was applied to these tables, and the respective values of χ^2, C_1, and P are shown in Table VI.

The values under "total" are obtained, as before, by ignoring the presence or absence of thunderstorms.

The values of P and C_1 are evidently not adequate to evince a significant association between magnetic activity and abnormal increases of E region ionization.

Since magnetic disturbances are predominant during the dark hours of the night, it was next decided to divide our observations into two classes—daytime observations

and evening observations. By daytime observations we mean those that were carried out during the period from sunrise to sunset. All others are called evening observations. With the data in our hand the ($P\chi^2$) test was applied to find the association for the following cases, and the values of χ^2, C_1, and P are given in each case.

TABLE VI.

($P\chi^2$) Test of Association between Magnetic Disturbance and Abnormal Ionization.

	N.	χ^2.	C_1.	P.
No thunderstorm	150	2·859	0·137	·09
Thunderstorm	40	0·005	0·012	·94
Total	190	5·263	0·164	·03

TABLE VII.

	Association between abnormal ionization and	χ^2.	C_1.	P.
Daytime observations.	Thunderstorm	53·8	0·5470	$<10^{-6}$
	Magnetic disturbance ..	3·05	0·1538	·08
Evening observations.	Thunderstorm	7·8	0·3296	·02
	Magnetic disturbance ..	3·89	0·2396	·05

It will be seen from the above table that during daytime the association between thunderstorms and abnormal increases in E region ionization appears to be very strong. But in the evening the strength diminishes to some extent. But the case is quite otherwise with magnetic disturbances. The correlation between magnetic disturbances and abnormal increases of ionization is hardly perceptible during daytime, whereas in the evening it becomes appreciable. These facts are quite in agreement with one another in that some of the evening abnormalities which cannot be explained by the occurrence of thunderstorms might be caused by magnetic disturbances which

usually prevail during the dark hours. Finally, it is of interest to test the association, if any, between the occurrence of a thunderstorm and magnetic disturbance. Utilizing the data in our hand the following values of χ^2, C_1, and P were obtained.

TABLE VIII.

($P\chi^2$) Test of Association between Magnetic Disturbance and Thunderstorm.

	N.	χ^2.	C_1.	P.
Normal ionization	113	0·4259	0·061	·80
Abnormal ionization	77	0·1108	0·038	·75
Total	190	3·0235	0·125	·09

The values indicate no association between thunderstorms and magnetic disturbances.

Summary and Conclusion.

We may draw the following conclusions from the observations described above :—

(1) A marked association exists ($C_1 = 0·50$) between the occurrence of a thunderstorm and an abnormal increase in E region ionization.
(2) The association, if any, between magnetic disturbance and abnormal ionization of the E region is not very marked.
(3) There is no association between magnetic disturbances and thunderstorms.

It is thus evident that one or both of the processes pictured by Wilson might be at work when a strongly electrified cloud is present. It should be remembered, however, that all the thunderclouds recorded in our table might not have been responsible for producing abnormal increase of ionization ; there might have been some with electric moments too small to affect ionospheric conditions.

We also note that although the association between magnetic disturbances and abnormal increases of E region

ionization is not very marked, yet the values of the statistical coefficients obtained in the case of evening observations indicate that these are by no means independent of one another. More extended observations over longer periods, specially by the night and during that part of the year when thunderstorms are of rare occurrence, may possibly unveil the exact relationship between the two.

Acknowledgments.

It is our pleasant duty to acknowledge our sincere thanks to Dr. S. N. Sen, Meteorologist, Calcutta, for supplying the thunderstorm data, to Dr. S. C. Roy, Meteorologist, Bombay, for supplying the magnetic storm data, and to Prof. P. C. Mahalanobis and Mr. S. S. Bose, of the Statistical Laboratory, Presidency College, Calcutta, for much help in analysing the materials sent to them.

The investigation described here was undertaken at the suggestion of Prof. S. K. Mitra. We are indebted to him for his guidance and for many helpful discussions.

References.

(1) Appleton and Naismith, Proc. Roy. Soc. A, cxxxvii. p. 36 (1932). Ranzi, 'Nature,' cxxx. p. 368 (1932). Appleton, Naismith, and Builder, 'Nature,' cxxxii. p. 340 (1933). Appleton and Naismith, Proc. Phys. Soc. xlv. p. 389 (1933). Ratcliffe and White, Proc. Phys. Soc. xlv. p. 399 (1933). Ratcliffe, Sci. News Letter, 15th Sept. (1934). Colwell, 'Nature,' cxxxiii. p. 948 (1934). Ratcliffe and White, Proc. Phys. Soc. xlvi. p. 107 (1934).

(2) Wilson, Proc. Camb. Phil. Soc. xxii. p. 535 (1925); Proc. Phys. Soc. xxxvii. p. 32 D (1925); Proc. Roy. Soc. A, cxli. p. 697 (1933).

(3) Appleton and Naismith, Proc. Phys. Soc. xlv. p. 389 (1933).

(4) Schonland, 'Atmospheric Electricity;' Published by Methuen and Co. Ltd., 1932.

(5) Chapman, Proc. Phys. Soc. xliii. p. 26 (1931). *Ibid.* xliii. p. 483 (1931).

(6) See, for instance, 'Statistical Methods for Research Workers,' by R. A. Fisher, p. 80. Published by Oliver and Boyd, 1932.

Wireless Laboratory,
University College of Science,
Calcutta.
4th April, 1936.

LI. *Graphical Estimation of the Signal Handling Capacity of Screen-Grid Valves.* *By* ROBERT W. SLOANE, *M.A., Ph.D.* (Communication from the Research Staff of the M.O. Valve Company, Limited, at the G.E.C. Research Laboratories, Wembley, England *.)

Introduction.

DISTORTION of the envelope of a modulated carrier frequency wave occurs in screen-grid valves used as amplifiers or frequency changers. The distortion depends on the shape of the anode current-grid voltage characteristic of the valve, and increases with increasing carrier frequency voltage at the grid.

The carrier frequency voltage, E, at the grid of a valve which, under given conditions, produces a c.f. anode current which differs in some chosen way from g.E, g.E_1 being the current produced by an indefinitely small c.f. voltage E_1, may be taken as a measure of the signal handling capacity of the valve under these conditions.

In the case of variable-μ screen-grid valves, the variable condition is the mean potential, or bias, of the signal grid. The variation of signal handling capacity with bias of such a valve is important when the degree of amplification has to be controlled by varying the bias.

1. Let

$$i=f(v) \quad . \quad . \quad . \quad . \quad . \quad . \quad . \quad (1)$$

represent the anode current of a carrier frequency amplifying valve as a function of the grid-voltage only. This is justified for screen-grid and pentode valves except at very small values of grid-bias.

Then, by Taylor's Theorem,

$$\delta i = \frac{di}{dv}\delta v + \frac{1}{2}\frac{d^2i}{dv^2}(\delta v)^2 + \frac{1}{6}\frac{d^3i}{dv^3}(\delta v)^3 + \ldots \quad . \quad (2)$$

where the coefficients, written as derivatives, are the values of these derivatives at the point from which the variation takes place.

If

$$\delta v = e(1+m\cos pt)\cos \omega t,$$

* Communicated by C. C. Paterson, M.I.E.E.

and if the fifth and higher odd terms of (2) may be neglected, then, as is well known *, the expansion for δi contains the following terms of frequency of the order $\frac{\omega}{2\pi}$:

$$\delta i_\omega = g_m e \cos \omega t + \frac{1}{6}\frac{d^2 g_m}{dv^2}\left(\frac{3}{4} + \frac{9}{8}m^2\right)e^3 \cos \omega t$$

$$+ \frac{m}{2} g_m e \cos (\omega \pm p)t$$

$$+ \frac{1}{6}\frac{d^2 g_m}{dv^2}\left(\frac{9}{32}m^3 + \frac{9}{8}m\right)e^3 \cos (\omega \pm p)t$$

$$+ \frac{1}{6}\frac{d^2 g_m}{dv^2}\frac{9}{16}e^3 m^2 \cos (\omega \pm 2p)t$$

$$+ \frac{1}{6}\frac{d^2 g_m}{dv^2}\frac{3}{32}e^3 m^3 \cos (\omega \pm 3p)t, \quad . \quad . \quad (3)$$

where g_m has been written for $\frac{di}{dv}$ and $\cos (\omega \pm p)t$ means

$$\cos (\omega + p)t + \cos (\omega - p)t.$$

For a linear amplifier

$$\delta i = g_m e \cos \omega t + \frac{m}{2} g_m \cos (\omega \pm p)t \quad . \quad . \quad . \quad (4)$$

It is immediately obvious that any property of expression (3) which may be taken as a measure of departure from linearity or "distortion" is a function of m and $\frac{e^2}{g_m}\frac{d^2 g_m}{dv^2}$ only. For instance, the ratio of the amplitude of the first overtone (or second harmonic) sideband to the amplitude of the fundamental sideband is

$$s = \frac{\frac{3}{16}m\frac{e^2}{g_m}\frac{d^2 g_m}{dv^2}}{1 + \frac{3}{8}\left(1 + \frac{m^2}{4}\right)\frac{e^2}{g_m}\frac{d^2 g_m}{dv^2}},$$

or

$$s = \frac{\frac{3}{8}mk}{1 + \frac{3}{4}\left(1 + \frac{m^2}{4}\right)k}, \quad . \quad . \quad . \quad . \quad (5)$$

* C. S. Bull, W. E. E. W. vol. x. p. 83 (1933).

where k is written for $\frac{1}{2}\frac{e^2}{g_m}\frac{d^2 g_m}{dv^2}$.

2. The amplitude of the component of frequency $\frac{\omega_2-\omega_1}{2\pi}$ of the anode current of a valve with two control electrodes, to which voltages $v_1+e_1(1+m\cos pt)\cos\omega_1 t$ and $v_2+e_2\cos\omega_2 t$ respectively, are applied, is *

$$\begin{aligned}A = {} & \frac{1}{2}e_1(1+m\cos pt)\,e_2\frac{\partial^4 i}{\partial v_1\,\partial v_2} \\ & + \frac{1}{16}e_1{}^3(1+m\cos pt)^3\,e_2\frac{\partial^4 i}{\partial v_1{}^3\partial v_2} \\ & + \frac{1}{16}e_1(1+m\cos pt)\,e_2{}^3\frac{\partial^4 i}{\partial v_1\,\partial v_2{}^3}. \quad . \quad . \quad . \quad (6)\end{aligned}$$

Let

$$g_c = \operatorname*{Lim}_{e_1\to 0}\left[\frac{A}{e_1(1+m\cos pt)}\right] = \frac{1}{2}e_2\frac{\partial^2 i}{\partial v_1\,\partial v_2} + \frac{1}{16}e_2{}^3\frac{\partial^4 i}{\partial v_1\,\partial v_2{}^3} \quad . \quad . \quad . \quad (7)$$

If v_2 and e_2 are constant, g_c is a function of v_1 only.

Expressions representing the distortion of the signal envelope, $e_1(1+m\cos pt)$, may be found from expansion (6); such expressions may be shown to be functions of m and of $\frac{e_1{}^2}{g_c}\frac{d^2 g_1}{dv_1{}^2}$ only, provided that terms of the order $\frac{\partial^6 i}{\partial v_1{}^n\partial v_2{}^{6-n}}$ and higher may be ignored. For instance, the ratio of the amplitudes of second harmonic and fundamental of the modulation is

$$\left.\begin{aligned}s = {} & \frac{\frac{3}{2}m^2\frac{1}{16}e_1{}^3 e_2\frac{\partial^4 i}{\partial v_1{}^3\,\partial v_2}}{\frac{1}{2}e_1 e_2 m\frac{\partial^2 i}{\partial v_1\,\partial v_2} + \frac{1}{16}e_1 e_2{}^3 m\frac{\partial^4 i}{\partial v_1\,\partial v_2{}^3} + \frac{1}{16}e_1{}^3 e_2\left(3m+\frac{3m^3}{4}\right)\frac{\partial^4 i}{\partial v_1{}^3\,\partial v_2}}, \\ = {} & \frac{\frac{3}{16}me_1{}^2\frac{d^2 g_c}{dv_1{}^2}}{g_c + \frac{3}{8}\left(1+\frac{m^2}{4}\right)e_1{}^2\frac{d^2 g_c}{dv_1{}^2}},\end{aligned}\right\} \quad . \quad (8)$$

* A. C. Bartlett, Phil. Mag. xvi. p. 847 (1933).

which is the same as equation (5) with e_1, v_1, g_c for e, v, g_m.

The quantity g_m is the mutual conductance of a valve used as an amplifier and g_c is the conversion conductance for a given voltage injected on one grid, of a valve used as a frequency changer. These quantities may be measured experimentally.

The two cases have been made formally the same, so the subscripts are dropped.

Then $$k = \frac{1}{2}\frac{e^2}{g}\frac{d^2g}{dv^2} = \frac{16s}{6m - 3s(4+m^2)}, \quad \ldots \quad (9)$$

and k may be calculated for any given values of s and m.

3. Let the figure represent an experimental curve of g against v. It is required to find, without further experiment, the peak value, e, of a sinusoidal variation of v, modulated to a depth m, which will produce an output current containing 100 s per cent. second harmonic of the modulation.

Let (v_0, g_0) be the point, A, at which this operation is to be performed. Let the point B $(v_0, g_0(1+k))$ be plotted (k is known, because s and m are given) and the straight line through B, parallel to the tangent at A, be drawn. Then, referring to the figure,

$$kg_0 = \mathrm{A'B'} = \frac{1}{2}\left[\frac{d^2g}{dv^2}\right]_{v=v_0} \mathrm{AC}^2.$$

$$\therefore \quad k = \frac{1}{2}\frac{\mathrm{AC}^2}{g_0}\left[\frac{d^2g}{dv^2}\right]_{v=v_0}.$$

Comparison with (9) gives $e = \mathrm{AC}$ for $v = v_0$.

A curve of e against v may be obtained by repeating the above process at a series of values of v.

4. To deduce the characteristic of a valve that will give a particular e, v curve, $e = \mathrm{F}(v)$, it is necessary to solve the equation

$$\frac{1}{g}\frac{d^2g}{dv^2}[\mathrm{F}(v)]^2 = \text{constant}.$$

For e proportional to v the equation becomes

$$v^2\frac{d^2g}{dv^2} = cg,$$

of which the solution is

$$g = c_1 v^{\frac{1}{2}(1+\sqrt{1+4c})} + c_2 v^{\frac{1}{2}(-\sqrt{1+4c})}.$$

In the amplifier case

$$g_m = \frac{di}{dv}$$

and $$i = c_3 v^{\frac{1}{2}(3+\sqrt{1+4c})} + c_4 v^{\frac{1}{2}(3-\sqrt{1+4c})} + c_5.$$

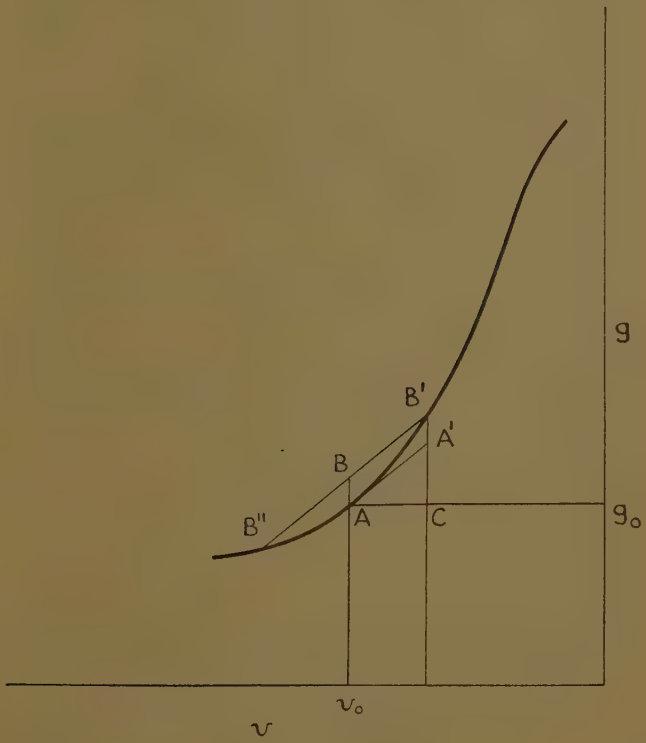

Illustration of Graphical Method :—

$$AB = kg_0,$$

$$CB' = CA' + A'B',$$

$$= AC\left(\frac{dg}{dv}\right)_0 + \frac{1}{2}AC^2\left(\frac{d^2g}{dv^2}\right)_0.$$

Any three of the constants, $c_1 \ldots c_5$, are disposable to satisfy other conditions.

5. The degree of agreement between values of signal handling capacity obtained graphically and experimentally depends on the degree of accuracy with which δi and A are represented by the first three terms of series (2) and (6) respectively. Obviously, the graphical method fails for values of v near the points of inflexion at the ends of the curve, and is inaccurate at sharp bends in the curve. At such points, the difference in length between BB′ and BB″ is an indication of the degree of inaccuracy.

The following figures, obtained with a variable-μ h.f. pentode illustrate these remarks. At a bias of -8 volts, near the sharpest bend of the curve, the ratio of the signal handling capacity estimated graphically to that obtained experimentally was 1·6 : 1. At -16 volts, the ratio was unity and towards the " tail " at -24 volts the ratio was 1·3 : 1.

The graphical method is very useful if its limitations are respected and becomes important when limitations of time or equipment prevent the exhaustive experimental study of a valve.

In conclusion, the author desires to tender his acknowledgments to the General Electric Company and the Marconiphone Company, on whose behalf the work was done which has led to this publication, also to J. F. Ramsay, M.A., who applied this method to the case of the amplifying valve.

LII. *The Corona Discharge between Points in Hydrogen.* *By* Robert W. Sloane, *M.A., Ph.D., Natural Philosophy Department, The University, Glasgow* *.

[Plates V. & VI.]

Preliminary.

THE object of this paper is to describe the current-potential characteristics of a discharge between points in hydrogen, and to call attention to a new phenomenon observed in the course of the investigation.

* Communicated by Prof. Taylor Jones.

Preliminary experiments showed that, to obtain repeatable results, it was necessary to use very dry hydrogen and that, to avoid effects due to charges on the dry glass walls of the discharge-tube, the tube had to be very large.

Apparatus.

The discharge-tube was a glass bulb, 15 cm. in diameter, with two open necks opposite each other, each 2·5 cm. in diameter. One of these served as an inlet for hydrogen which passed through drying tubes and a capillary from an electrolysis apparatus; the gas could be admitted to the tube by a tap. The other neck led to a mercury manometer and, through another stopcock, to a Hyvac pump. The electrodes were tungsten wires, ·5 mm. in diameter, their ends separated by a 2 mm. gap. Each was jammed tightly between the inside of a neck of the tube and the outside of the glass tube connecting the discharge-tube to the vacuum system. These joints were sealed with vacuum wax.

The tube was thoroughly washed with hydrogen and cleaned up by passing a high-frequency discharge in hydrogen in it. The ends of the tungsten electrodes were cleaned by passing a small arc between them when there was hydrogen at a pressure of 16 cm. of mercury in the tube.

Meter Measurements.

The tube was connected in the circuit shown in fig. 1. T is the discharge-tube across which a high potential was maintained by the potentiometer, R, of 12,000 ohms across a 3000 volt D.C. generator. A was a current meter, and V an electrostatic voltmeter. At P and Q were devices to prevent a large current flowing through the tube, either from the generator or from the capacity of the electrostatic instrument. The permutations of two valves and two high resistances taken two at a time were tried at P and Q. When there was a valve either at P or at Q it was not found possible to prevent the tube from flashing when the mean current through the tube was less than that necessary to maintain a normal glow discharge. High resistances, in the form of short lengths of slate pencil, were found suitable.

Fig. 1.

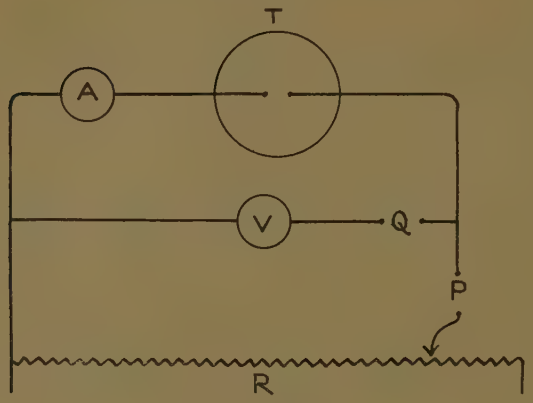

Circuit diagram.

Fig. 2.

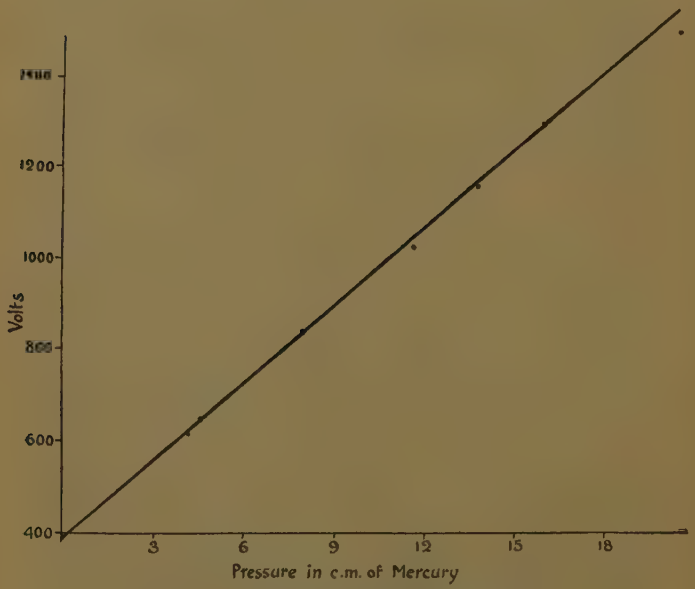

Graph of sparking potential of the tube against pressure of hydrogen.

In fig. 2 the sparking potential of the tube is plotted against pressure of hydrogen in the tube. The gradient of the straight line is 28·3 volts per cm. of mercury per mm. of gap-width. The apparent initial cathode fall is 380 volts.

The sequence of phenomena, as the potentiometer potential was increased, was as follows :—At some value of the potential, flashes of current began to pass through the tube. The smallest potential at which this can occur is the sparking potential of the tube. It did occur at the sparking potential if a discharge had been passed through the tube recently. If not, there was a lag in the striking of the tube, sometimes as long as ten minutes, even with the potential raised to twice the sparking potential.

As the supply of power to the tube was further increased the tube continued to flash, the potential rising to a value higher than the sparking potential before each flash *, until, at some particular value of the mean current, the potential across the tube dropped suddenly and the current and tube voltage became apparently steady.

By still further increasing the supply of power to the tube, a series of steady readings of the current through the tube, and the corresponding potential across the tube, was obtained. The curves plotted in fig. 3 show results obtained in this way at various pressures. These curves illustrate the following experimental facts concerning this point discharge in hydrogen :—

(1) At a given pressure there is a definite sparking potential.

(2) A steady corona discharge may be caused to pass across the gap, provided that the current is within a certain range of values, this range depending on the pressure.

(3) The steady corona current-potential characteristics have a negative slope.

(4) There are regions between the sparking potential and the corona characteristic, and between the corona characteristic and the glow characteristic, in which a static characteristic cannot be obtained.

* This rise in apparent sparking potential and its connexion with time lag have been studied by W. Clarkson, Phil. Mag. iv. p. 121 (1927).

It must be observed that the word "steady" means "apparently steady on measuring instruments with ponderous moving parts." The electrostatic voltmeter used had a period of about a fifth of a second and was almost dead beat. In the experiments described below it is shown that, though each point on a characteristic of fig. 3 corresponds to a stable and repeatable condition, the points represent mean values of current and potential during a periodic variation of these quantities.

Fig. 3.

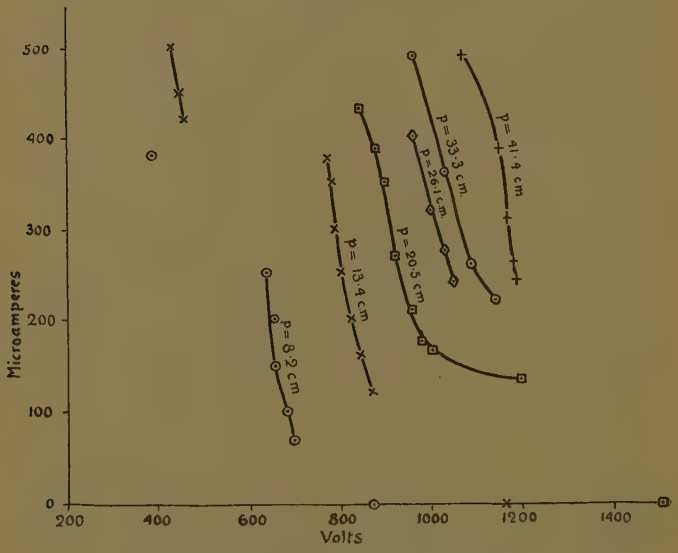

Current-potential characteristics of the tube filled with hydrogen to various pressures.

Oscillograph Measurements.

To investigate the variation of the current through the tube, and the potential across it, while an apparently steady corona current was passing, some oscillograph records of these quantities were obtained. A cathode-ray oscillograph was connected so that the pattern on the fluorescent screen was the graph of the current through the tube, as ordinate, against the potential across the

tube, as abscissa. The arrangement is shown in fig. 4. T is the discharge-tube, R_1 and R_2 were slate or "metalized" resistances, and r a wire-wound resistance. C represents the deflecting system of the cathode-ray oscillograph. The point A was connected to the high potential (negative) end of a well smoothed high tension supply. Current and potential meters could be con-

Fig. 4.

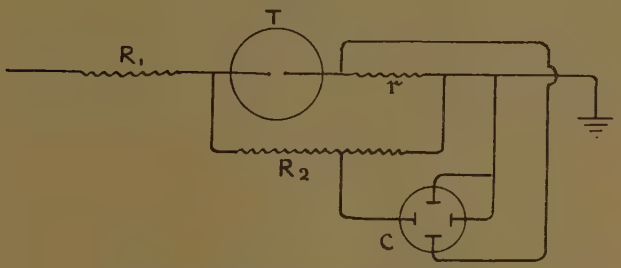

Diagram of tube and oscillograph connexions.

Fig. 5.

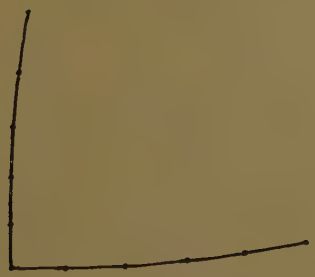

Shape of oscillograph axes.

nected as before. The potential difference across r (10,000 ohms) was always small compared to the potential difference across the tube.

Since the oscillograph was not magnetically shielded, and the zero position of the spot was adjusted magnetically, the axes on the screen were curved. Fig. 5, showing the shape of the axes, is drawn from a photograph obtained by applying steady potential to the deflecting plates.

Tube characteristics were photographed in the following manner :—The camera shutter was opened while the oscillograph spot was in its zero position. The high tension supply was then switched on and, as the smoothing system charged up, the spot moved along the potential axis until a discharge started in the tube. When the discharge was steady—that is to say, when the current through the tube and the potential across it had constant values—the spot on the screen took up a position corresponding to those values. The high voltage was varied in steps, so that a series of points was photographed, and the shutter was closed.

When the discharge was not steady the pattern traced out by the periodic movement of the oscillograph spot

Fig. 6.

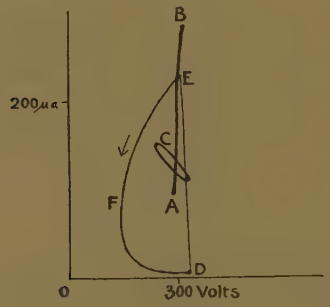

Dynamic characteristic at 5 mm. of mercury.

was photographed in the same way. The static characteristics and one or more dynamic characteristics could be photographed on the same plate, and the current axis could be obtained by short-circuiting the potential plates of the oscillograph while a periodic discharge was passing through the tube.

The characteristics so obtained, at pressures from 5 mm. to 2 cm., showed no unusual features, and fig. 6 may be taken as typical. In this case the pressure in the tube was 5 mm. of mercury. The resistance in series with the tube (R_1, fig. 4) was varied in steps between one and seven megohms. The line AB (fig. 6) represents that part of the static glow characteristic on which points were obtained. Increasing the series resistance from

one to seven megohms only lowered the lower current limit for steady discharge from 135 microamperes to 120 microamperes. The loops at C were obtained with one megohm in series and a mean current of 130 microamperes. When the supply of electrical energy was reduced until the mean current was less than 120 microamperes "flashing" set in. The curve DEF shows the cycle of repeated values assumed by the current and potential when the mean current through the tube was 60 microamperes. It will be observed that this curve confirms the assumption of previous workers, that the discharge "builds up" when the representative point is to the right of the static characteristic, and "clears up" when the point is to the left. It will be shown below that this is not always the case. It is interesting to compare the curve DEF with curves assumed and drawn by W. Clarkson *. No static corona characteristic could be found.

At slightly higher pressures a new and surprising phenomenon was observed. It was found that the current through the tube and the potential across it could vary through a cycle of values without crossing the stable characteristic, although during part of the cycle, the current was considerably larger than the smallest obtainable stable current. To explain this result it is only necessary to assume that the discharge through a given tube at a particular pressure does not assume the glow form immediately the current through the tube reaches a particular value, but that a current of this value, or in excess of it, must be maintained for some time before the space-charge distribution associated with the glow form of discharge is built up. If the duration of a flash is shorter than this time, a large current may flow while the discharge remains in the corona form.

This effect is shown very clearly in fig. 7 (Pl. V.), which is a contact print from the negative exposed to the oscillograph pattern. The pressure in the tube was 3·4 cm. of mercury and the series resistance was one megohm. The short line, A, on the glow characteristic, and the corona dynamic characteristic, B, were visible at the same time, showing that the discharge was alternating rapidly between the glow and corona forms. Increasing

* Phil. Mag. iv. p. 1002 (1927).

the mean current moved the representative point up the glow characteristic. Other dynamic corona characteristics were obtained by decreasing the mean current.

As the pressure was still further increased the whole pattern retained its form and increased in size. That the form of dynamic corona characteristics is the same at a pressure of 45·5 cm. of mercury, as at lower pressures, is shown in fig. 8, which is from a photograph taken at this pressure, the highest used. Curve A corresponds to a mean current of 600 microamperes and curve B to a mean current of 450 microamperes. The "spark" or "build up" parts of the characteristics are not shown

Fig. 8.

Dynamic corona characteristics (pressure 45·5 cm. of mercury).

because they were traversed too quickly to appear on the screen.

To compare the photographed characteristics with the characteristics plotted from meter readings, meter readings taken while the photograph (Pl. VI. fig. 9) was being exposed are plotted in fig. 10, curves A, A^1. Each point on curve A gives the steady voltage and current reading corresponding to one of the dynamic corona characteristics of the photograph. The part A^1 corresponds to steady values of the current and voltage. The pressure was 7·9 cm. of mercury. Curve B is taken from fig. 3 and represents measurements taken at a pressure of 8·2 cm. of mercury. Two months elapsed between the recordings of the curves B and A. The closeness in

shape and position of the two curves indicates good constancy of gas and electrode conditions.

It must now be concluded that each point on the corona characteristics drawn in fig. 3 represents mean values of current and potential during the traversal, by the representative point, of a particular dynamic corona characteristic.

Fig. 10.

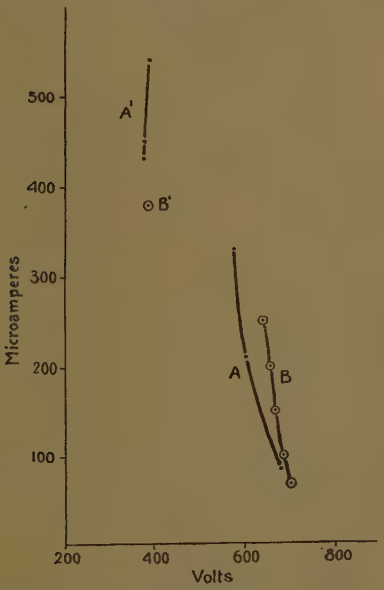

A, A^1. Plot of meter readings taken while fig. 9 (Pl. VI.) was being exposed (pressure 7·9 cm. of mercury).
B, B^1. Characteristic from fig. 3 (pressure 8·2 cm. of mercury).

Appendix.

For comparison with the characteristics of the discharge between points, the cathode-ray oscillograph traces of the characteristics of a neon discharge-lamp were photographed. The circuit is shown in fig. 11, L being the lamp, C the oscillograph deflecting system, r a high resistance, and R a potentiometer across the 250 volt D.C. mains.

Fig. 11.

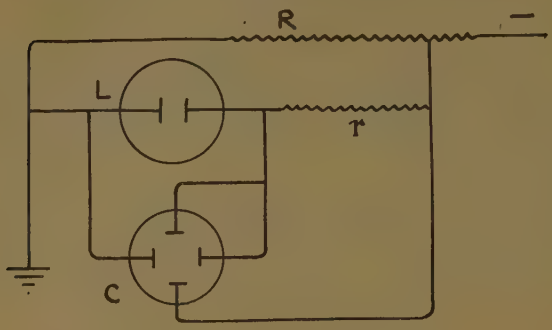

Lamp and oscillograph connexions.

Fig. 12.

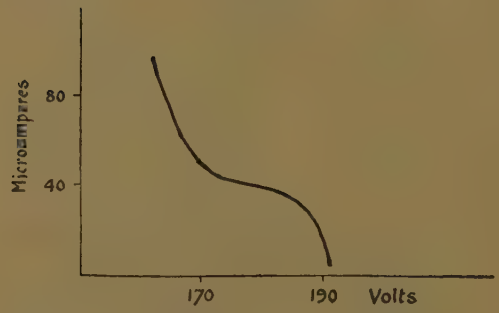

Static corona characteristic of neon lamp.

Fig. 13.

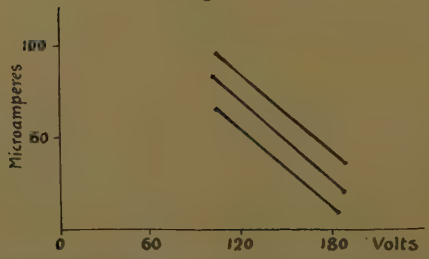

Dynamic characteristics of neon lamp across a condenser (capacity 160 $\mu\mu$f.).

When r was one megohm, the discharge in the lamp took the corona form and was steady, so that the representative point remained on the static boundary characteristic. The static characteristic was photographed by increasing the supply voltage slowly from 0 to 250 volts while the camera shutter was open. This characteristic is shown in fig. 12. Fig. 13 shows the result of following the same procedure when a condenser of 160$\mu\mu$f. capacity was connected across the tube. The parallel lines represent dynamic characteristics (probably very narrow loops) for different mean currents.

Summary.

A discharge-tube with tungsten point electrodes is described, and results of measurements of the sparking potential and the current-potential characteristics of the tube, containing hydrogen at various pressures, are given.

It is shown that apparent "static" corona characteristics, obtained by measuring current and potential with instruments with massive moving parts, are in this case the loci of the centroids of dynamic characteristics.

Results are given which show that, under certain conditions, the discharge may remain in the corona form, although the current rises for a short time to values much greater than the least stable glow current.

The general form of the characteristics is the same at all pressures from 0·5 cm. to 45 cm. of mercury.

This work was carried out while the author was a Thomson Experimental Scholar in Glasgow University, and he takes this opportunity of thanking Professor E. Taylor Jones for his help and encouragement.

LIII. *The Lattice Spacing of Iron-Nickel Alloys.* *By* A. J. Bradley, *D.Sc.*, *Royal Society Warren Research Fellow*, A. H. Jay, *Ph.D.*, *and* A. Taylor, *M.Sc.*, *Darbishire Research Fellow* *.

IRON-NICKEL alloys are either body-centred cubic like iron, or face-centred cubic like nickel. In spite of the comparative simplicity of the system, it has not

* Communicated by Prof. W. L. Bragg, F.R.S.

yet been possible to decide even approximate positions for the phase boundaries. This is due to the sluggish character of those iron-rich alloys in which two phases may exist. On cooling from high temperatures certain transition effects are recorded supposed to represent the beginning and end of the transformation from the face-centred cubic to the body-centred cubic type of structure. However, the reverse process, *i. e.*, the transformation of the body-centred cubic to the face-centred cubic structure does not give transition temperatures which agree even roughly with those obtained on cooling. For

Fig. 1.

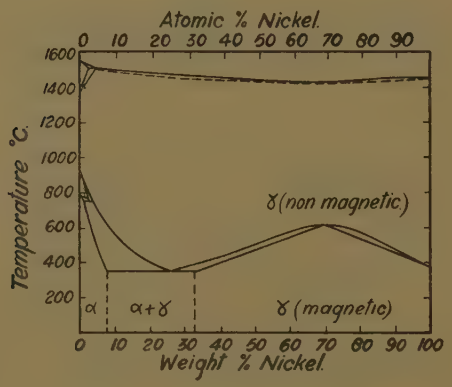

Fe.-Ni. HANSON & FREEMAN.

this reason the alloys are said to be "irreversible" (Hopkinson [1], Guertler and Tammann [2]).

At the nickel-rich end of the equilibrium diagram only the face-centred cubic structure exists. Although it was formerly believed that a phase-change occurred there, it is now known that this is merely the Curie point. Since the disappearance of magnetism on heating takes place at approximately the same temperature as its reappearance on cooling, these alloys are said to be "reversible."

The earliest equilibrium diagram is due to F. Osmond and G. Cartaud [3], and it was constructed from a study

of meteoritic alloys. These were found to contain three constituents, namely, kamacite corresponding to ferrite, the body-centred cubic material of the artificial alloys; tænite, corresponding to austenite, the face-centred cubic material; and plessite, a mixture of kamacite and tænite. Osmond and Cartaud considered that plessite contained a eutectoid mixture and proposed an equilibrium diagram of the type shown in fig. 1. The diagram shown here has been modified to its present form by Hanson and Freeman [4] as a result of careful experiments on artificial alloys, but owing to the difficulties experienced

Fig. 2.

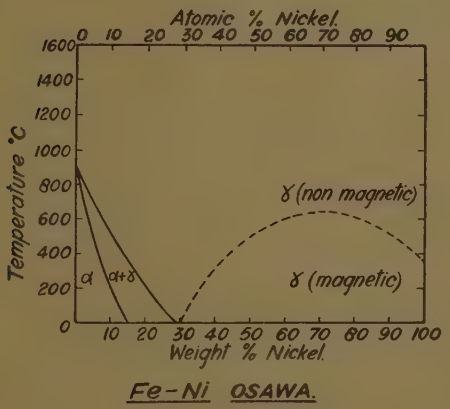

in obtaining equilibrium it was impossible to fix the real positions of the phase-boundaries.

In the light of current knowledge about the crystal structure of the iron-nickel alloys it is difficult to accept the eutectoid theory. An alternative equilibrium diagram has been published by the American Bureau of Standards [5] which has since been modified by Honda and others A diagram of the type shown in fig. 2, taken from a paper by Osawa [6], will explain the facts quite well. It is still impossible to state exactly where the phase-boundaries should be placed, but the nature of the diagram seems more reasonable since there are only two types of crystal

structure, not three, as would be expected from the eutectoid theory.

X-ray work on iron-nickel alloys has been done by M. R. Andrews [7], who found body-centred cubic structures up to 22 per cent. of nickel, and face-centred cubic structures beyond 30 per cent. nickel. L. W. McKeehan [8] found that the lattice spacings of the body-centred cubic alloys increased from 2·872 Å. to 2·88 Å. on the addition of nickel to iron; those of the face-centred cubic alloys increased from 3·510 Å. for pure nickel to 3·60 Å. for an alloy with 70 per cent. of iron. Osawa [9] measured lattice-spacing changes for both the reversible and the irreversible alloys and compared the results with density measurements. The first accurate measurements of lattice spacing are due to Phragmén [10], who investigated the region between 30 per cent. nickel and 40 per cent. nickel, with the object of explaining the invar phenomenon. Invar is an alloy containing 34·5 per cent. of nickel which has an abnormally low coefficient of expansion at room-temperatures. Phragmén showed that this was due to the slight expansion of the face-centred cubic lattice and not to any phase change, as had been suggested by Benedicks [11]. He also showed that the reversible alloys had a maximum spacing at about 38 per cent. of nickel.

Jette and Foote [12] have recently made very accurate measurements of lattice spacings and found a maximum lattice spacing for the face-centred cubic alloys at 39 per cent. nickel. From 100 to 43 atomic per cent. nickel the lattice spacing varies according to the equation $a_0 = 3{\cdot}64033 - 0{\cdot}0012379$ (atomic per cent. nickel). The body-centred cubic alloys show an increase of lattice spacing with the addition of nickel to iron, although a decrease would be expected, since nickel is a smaller atom than iron. Above 450° C. no single phase α alloy was found with more than 5 per cent. of nickel.

Owen and Yates [13] have just published an account of X-ray work on pure nickel which shows that the coefficient of expansion is abnormal near the magnetic change point (370° C.). The lattice spacing of pure nickel found for manganese radiation is 3·5172 Å. at 16° C. Dehlinger [14] has investigated the transformation of the face-centred cubic structure to the body-centred

cubic structure on cooling a 30 per cent. nickel alloy in liquid air.

The Present Work.

The lattice spacings of 35 different alloys were measured at room-temperature, using the method of Bradley and Jay [15]. The usual accuracy of these measurements is 1 part in 30,000, but differences much greater than this were found in the lattice spacing of the same alloy after different methods of heat-treatment. The most consistent results were obtained after slowly cooling. In this case the body-centred cubic alloys increase in spacing from pure iron to 6 per cent. atomic of nickel. There is, then, an unaccountable fall to the two-phase region where the values are constant. The face-centred cubic alloys on slow cooling show a steep increase in spacing with the addition of iron to nickel, to a maximum at about 39 per cent. of nickel, followed by a fall to the phase-boundary at about 28 per cent. atomic of nickel. Quenching experiments made on the face-centred cubic alloys gave inconsistent results.

It was the especial object of the present investigation to find out whether the lattice spacings of slowly cooled alloys gave anomalous results in the neighbourhood of "permalloy," *i. e.*, about 78 per cent. of nickel. Alloys near this composition are known to possess remarkable magnetic properties, which are brought out by special methods of heat treatment. After a preliminary heating at 900°, the alloy is reheated to 600°, and air cooled down to room-temperature [16]. Very high initial permeability is then obtained, the maximum value so far recorded being 13,000 [17].

We have succeeded in noting a definite peculiarity in the lattice spacing of alloys near the composition of "permalloy." Whereas Jette and Foote state that the dimensions change linearly with the addition of iron to nickel over the whole range between nickel and FeNi, we find that in slowly cooled alloys there is a definite break in the curve at about 78 per cent. of nickel. The spacing composition curve has two distinct linear ranges, one extends from about 50 per cent. nickel to 78 per cent. nickel, the other from 79 per cent. nickel to pure nickel.

In the neighbourhood of the intersection of the lines the results are somewhat erratic.

Experimental.

The iron-rich alloys were made from Hilger metal of 99·97 per cent. purity (batch nos. 8038 and 7636). Some of the first alloys examined at the nickel-rich end were made from rather less pure materials, but no systematic deviation can be found in the results due to this cause. The metals were melted together in alumina lined crucibles to prevent silicon contamination. The melts were made in a high frequency induction furnace under a low pressure of hydrogen. The gas was pumped off before solidification, leaving the alloys comparatively free from blow-holes.

The iron-rich alloys were lump annealed at 1300°, the remainder at 900° C. After three days the alloys so homogenized were slowly cooled to room-temperature and powdered by filing. The compositions of the alloys were partly checked by analysis, but were found to agree closely with the weighed out compositions. The powders were heated to 900° C. and cooled to room-temperature in three days in an evacuated furnace. In some cases alternative heat treatments were given to the filings. They were quenched from 900°, 800°, or 700°, by allowing a stream of water to rush into the evacuated furnace.

The heat treated powders were photographed in a Debye Scherrer camera, using cobalt radiation for the iron-rich alloys and copper radiation for the nickel-rich alloys. The lattice spacings were then determined by the method of Bradley and Jay. The use of cobalt radiation gives very accurate measurements for the body-centred cubic alloys which predominate at the iron-rich end, owing to the high angle of the 310 reflexion. It is not possible to obtain accurate measurements beyond above 12 per cent. of nickel because this line becomes extremely diffuse.

The lattice spacing measurements of the face-centred cubic alloys are very accurate at the high nickel concentrations where copper radiation give clear photographs with strong lines and faint backgrounds. There are two lines (331 and 420) which are well placed at high angles, no difficulty being experienced in applying the spacing

technique. As the iron-content increases the specimen absorbs copper radiation much more strongly, and ultimately at the iron-rich end it is no longer possible to get satisfactory results. The background becomes very dark and the lines are difficult to measure. We have, accordingly, not got many measurements of the face-centred cubic phase in the two-phase region.

Irreversible Alloys, 0–30 per cent. of Nickel.

Some results for slowly cooled alloys with body-centred cubic structures are tabulated below.

TABLE I.

The Lattice Spacings of slowly cooled Body-centred Cubic Iron-Nickel Alloys.

Atomic per cent. nickel.	Lattice spacing, Å.	Notes.
10·5	2·8634	Two-phase.
8·6	2·8635	
7·1	2·8635	
5·7	2·8644	Single-phase.
2·8	2·8624	
0.....	2·8605	

These results are shown graphically in fig. 3. The lattice spacing of the body-centred cubic alloys increases linearly with the addition of iron to nickel, though the rate of change is slow. The maximum value observed was from an alloy containing 5·7 per cent. of nickel. The three alloys from the two-phase region have equal spacings for the body-centred cubic structure as one would expect. This value, 2·8635, corresponds to a point on the single-phase curve at 4·4 per cent. nickel. The phase boundary, as deduced from the two-phase alloys, should therefore be at 4·4 per cent. nickel. This composition is confirmed by the amount of the face-centred cubic structure which is visible from powder photographs of the two-phase alloys. On the other hand, no trace of a face-centred cubic pattern is visible in the 5·7 per cent. alloy. Moreover, its higher spacing confirms the conclusion that we

are dealing with a genuine single-phase alloy. It must therefore be supposed that the 5·7 per cent. alloy has

Fig. 3.

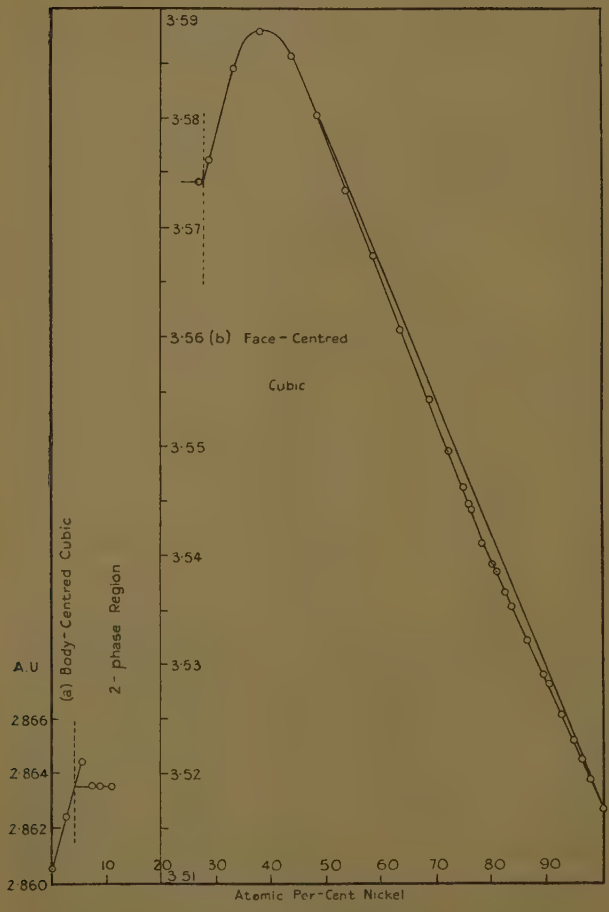

transformed completely from the face-centred cubic to the body-centred cubic structure during slow cooling, whereas with the higher nickel content this process has been checked at a higher temperature. We offer no

explanation for this observation, which is the more remarkable in view of the fact that all the iron-rich alloys were heat treated together.

Although we do not publish results of any measurements beyond 10·5 per cent. nickel, as these photographs have very diffuse lines, we have obtained a certain amount of information with regard to the state of these alloys. As would be expected, the proportion of the face-centred cubic phase steadily increases with the nickel content. The face-centred cubic pattern in the powder photographs is never sharp, which shows that this phase is present in a fine state of subdivision. The body-centred cubic lines are very sharp in the single-phase region, but gradually become more diffuse as the nickel content increases beyond the two-phase boundary. Beyond about 11 per cent. of nickel the lines are so broad as to indicate that the particles are probably of colloidal dimensions.

Some of the filings of the two-phase alloys were plunged in liquid air. With the exception of the alloy nearest the phase boundary (7·13 per cent. nickel), all gave powder photographs showing an increase in the proportion of the body-centred cubic phase. As in the slowly cooled alloys all the lines were extremely diffuse. In no case was there a complete transformation to the body-centred cubic pattern as was suggested by previous writers (*e. g.*, M. R. Andrews).

An alloy with 28·9 per cent. of nickel, which was entirely face-centred cubic at room-temperatures, was photographed at the temperature of liquid air. It gave both the face-centred and the body-centred cubic lines, the latter predominating. The body-centred cubic lines were again diffuse.

"*Reversible*" *Alloys*, 30–100 *per cent. Nickel.*

Fig. 3 (*b*) shows the results of lattice spacing measurements for the face-centred cubic alloys after slow cooling. The general trend of the curve is in agreement with the results of Jette and Foote. The spacing rises steadily from a value of 3·5168 Å. for pure nickel to a maximum of 3·5878 Å. recorded at 38·0 atomic per cent. of nickel. It then falls to 3·5741 Å. at the end of the face-centred cubic phase. A closer inspection of the results shows that the spacing changes from 50 to 100 per cent. of nickel do not conform very well to the linear relationship

given by Jette and Foote. In fig. 3 (*b*) a straight line between these two points is shown. The observed values fall consistently below this line. They conform

TABLE II.

Lattice Spacing Measurements for slowly cooled Iron-Nickel Alloys.

Atomic per cent. Ni.	Observed spacing, Å.	Calculated spacing, Å.*	Difference Å.
100	3·5169	3·5170	−·0001
97·9	3·5195	3·5193	+·0002
96·3	3·5215	3·5213	+·0002
94·8	3·5232	3·5230	+·0002
92·5	3·5255	3·5257	−·0002
90·5	3·5284	3·5280	+·0004
89·6	3·5293	3·5291	+·0002
86·7	3·5322	3·5324	−·0002
84·4	3·5354	3·5351	+·0003
82·8	3·5367	3·5370	−·0003
81·3	3·5387	3·5386	+·0001
80·2	3·5392	3·5399	−·0007
79·1	3·5412	3·5412	
78·1† ...	3·5418	3·5425	−·0007
76·6	3·5444	3·5445	−·0001
76·1	3·5445	3·5451	−·0006
75·0	3·5464	3·5465	−·0001
72·5	3·5497	3·5496	+·0001
69·0	3·5544	3·5542	+·0002
63·9	3·5606	3·5607	−·0001
58·7	3·5673	3·5673	
53·9	3·5734	3·5735	−·0001

* Above the line the spacing is calculated from the formula 3·5170+·00116 (atomic per cent. iron).
Below the line the spacing is calculated from the formula 3·5145+·00128 (atomic per cent. iron).
† Composition of permalloy.

much more closely to the two separate branches shown in the figure. One straight line begins at pure nickel, the other begins near 50 atomic per cent. of nickel. They

intersect at about 79 atomic per cent. of nickel. Near the point of intersection, which is, of course, the point of maximum deviation from the linear relation, the points diverge somewhat from the smooth curves. This is shown also by the preceding table (Table II.), where the observed values are compared with those calculated to lie on two straight lines. Normally the difference between observed and calculated values does not exceed ·0003 Å., but between 76 and 80 atomic per cent. nickel the differences rise to ·0007 Å. It is interesting to note that the composition of permalloy (indicated by †) falls right in the centre of this region.

Quenching Experiments on " Reversible " Alloys, 30–100 per cent. Nickel.

Drastic quenching gave different results for the lattice spacing measurements. Three series of experiments were carried out, in which the alloys were quenched from 700° C., 800° C., and 900° C. respectively. It was found that the spacings were on the whole greater after this treatment, though in a few cases smaller values were observed than in the slow cooling experiments, especially where slow cooling had given higher results than the calculated values for the two straight lines.

It was difficult to detect any general trend in the differences. In some cases the same alloy gave different values with very slight modifications in the quenching technique, even when the quenching temperature was unaltered. This shows that the initial quenching temperature is comparatively unimportant. The vital point appears to be the rate of cooling, which is not easy to control. Probably the exact lattice spacing depends on the way in which the alloy cools through the Curie point. There is corroborative evidence for this theory in experiments with nickel-aluminium alloys. We have found that the spacing of Ni_3Al is 1 per cent. smaller after quenching from above the Curie point than after slow cooling through the Curie point.

Some of the results of the quenching experiments on iron-nickel alloys are summarized in Table III. These results are not reproducible on quenching from the given temperatures, but are typical of the observed range of variations.

TABLE III.

Lattice Spacing of the Iron-Nickel Alloys.

Alloy at. per cent. Ni.	Annealed.	Quenched. 700° C.	Quenched. 800° C.	Quenched. 900° C.
100·0.....	3·5169	3·5170	3·5168	3·5168
97·9.....	195	189	189	186
96·3.....	215	..	203	206
94·8.....	232	227 244	243 235	229
92·5.....	255	259	254	254
90·5.....	284	..	277	
89·6.....	293	292	..	290
86·7.....	322	321	322	320
			318	319
84·4.....	354	356	348	348
82·8.....	367	366	363	365
81·3.....	387	387	..	390
80·2.....	392	404	395	408 406
79·1.....	412	414	422	414
78·1.....	418	424		425
76·6.....	444	447	443	438
76·1.....	449 445	..	445 442	453
75·0.....	464	472	472	468
74·0.....	..	..		483
72·5.....	497	501	502	501
69·0.....	544	551	557	564
66·4.....	..	..	..	576
63·9.....	606	612	620	615
58·7.....	673	679	686	687
53·9.....	734	746	743	743
48·8.....	803	803	804	806
43·8.....	857	..	859	853
38·0.....	878	..	880	880
33·3.....	846	..	839	840
29·0.....	761	..	741	742
27·0.....	741	..	743	724

Summary.

We have determined the lattice spacings of 35 iron-nickel alloys after slow cooling to room-temperature. The lattice spacings of the iron-rich body-centred cubic alloys increase from 2·8605 Å. for pure iron to 2·8644 Å. for 5·7 atomic per cent. of nickel. In the two-phase region the lattice spacing is 2·8635 Å. The lattice spacings of the face-centred cubic nickel-rich alloys increase from 3·5169 Å. for pure nickel to a maximum of 3·5878 Å. at

38·69 atomic per cent. of nickel, and then fall to 3·5741 Å. at 28 atomic per cent. of nickel. This is the position of the phase boundary after slow cooling. The spacing change is linear from pure nickel to 78 per cent. nickel, and thence to 45 per cent. nickel. The break at 78 per cent. nickel corresponds approximately to the composition of the high permeability alloy "permalloy." In this neighbourhood the values are less regular than elsewhere.

The face-centred cubic alloys were also examined after quenching from 700°, 800°, and 900°. The lattice spacings were found to be different from those in the slow cooling experiments, being on the whole decidedly higher. It is thought that this behaviour is connected with the magnetic properties of the alloy.

Acknowledgments.

We desire to thank Professor W. L. Bragg, F.R.S., for his kind interest in the work. One of us (A. T.) is indebted to the Department of Scientific and Industrial Research and to the Permanent Magnet Association for grants which enabled him to continue with the research.

References.

(1) B. Hopkinson, "Magnetic Properties of Alloys of Iron and Nickel," Proc. Roy. Soc. A, xlviii. p. 1 (1890).
(2) W. Guertler and G. Tammann, *Z. Anorg. Chem.* xlv. p. 205 (1905).
(3) F. Osmond and G. Cartaud, *Revue de Metallurgie*, i. p. 69 (1904).
(4) D. Hanson and J. R. Freeman, J. Iron and Steel Inst. cvii. p. 301 (1923).
(5) American Bureau of Standards, lviii. p. 3 (1916).
(6) A. Osawa, Sci. Rep. Tohoku, Imp. Univ. xv. p. 387 (1926).
(7) M. R. Andrews, Phys. Rev. xviii. p. 245 (1921).
(8) L. W. McKeehan, Phys. Rev. xxi. p. 402 (1923).
(9) A. Osawa, J. Iron and Steel Inst. cxiii. p. 447 (1926).
(10) G. Phragmén, J. Iron and Steel Inst. cxxiii. p. 465 (1931).
(11) C. Benedicks and Sederholm, *Arkiv for Matemtik, Astronomi och Fysik*, xix. B, no. 1 (1925).
(12) E. R. Jette and F. Foote, Amer. Inst. Min. &Met. Eng. Tech. Pub. 670, Jan. (1936).
(13) E. A. Owen and E. L. Yates, Phil. Mag. xxi. p. 809 (1936).
(14) U. Dehlinger and H. Bumm, *Zeits. f. Metallkunde*, xxvi. p. 112 (1934).
(15) A. J. Bradley and A. H. Jay, Proc. Phys. Soc. xliv. p. 563 (1932).
(16) J. D. Yensen, J. Franklin Inst. cxcix. p. 2 (1925).
(17) H. D. Arnold and G. W. Elmen, J. Franklin Inst. cxcv. p. 621 (1923).

LIV. *On the Fluorescence of Cyclohexane.* *By* S. M. Mitra, *Physics Department, Dacca University* *.

[Plate VII.]

Introduction.

WHILE investigating Raman effect in cyclohexane Habrel † noticed first the existence of continuous band, with a maximum at about λ 4000 Å. and another at about λ 2900 Å. These were also observed by Padmanabhan ‡. But the origin of these bands was a matter of a great controversy : while Habrel ascribed it to the fluorescence of pure cyclohexane, Padmanabhan reported the same to be due to the fluorescence of the products of a photochemical decomposition of cyclohexane brought about by the action of the intense ultra-violet radiation, and that pure cyclohexane has no fluorescence.

In view of the contradictory nature of the conclusion reached by the previous observers, a detailed investigation was undertaken in our laboratory. The present paper gives a report of a phase of our investigation.

Preparation of Pure Cyclohexane.

A quantity of cyclohexane (British Drug House) labelled pure was agitated thoroughly in a shaking machine with fuming sulphuric acid for 100 hours, and then neutralized with precipitated calcium carbonate and filtered. The filtrate was distilled and repeatedly washed with distilled water. After washing with water it was repeatedly recrystallized (m.p.—6·4° C), and these crystals were collected and used in the experiment.

Experimental Procedure.

The apparatus used for the present investigation is the continuous distillation apparatus with a cross-tube used in one of our previous investigations §, and which in principle is the same as that used by Pal and Sen Gupta ||

* Communicated by the Author.
† K. Habrel, *Ann. d. Phys.* xxi. p. 301 (1934).
‡ R. Padmanabhan, Proc. Ind. Acad. Sci. ii A, p. 209 (1935).
§ S. M. Mitra, *Zeits. für. Phys.* xcvi. p. 29 (1935).
|| N. Pal and P. Sen Gupta, Ind. J. Phys. v. p. 609 (1931).

in our laboratory. A diagram of the distillation apparatus is sketched below (fig. 1).

It is made of pyrex glass, with two quartz windows fitted on to the ends of the cross-tube. The cross-tube C is immersed in a bath B, the temperature of which can be kept constant at any desired degree. T_1, T_2 give the temperature of the liquid cyclohexane inside the cross-tubes and of the bath respectively.

Requisite amount of pure cyclohexane was introduced in the flask, which was then very carefully evacuated and finally sealed. If now the flask be kept immersed in a hot bath liquid vaporizes and is condensed by a system of bulb condensers of the usual type C_1 and C_2,

Fig. 1.

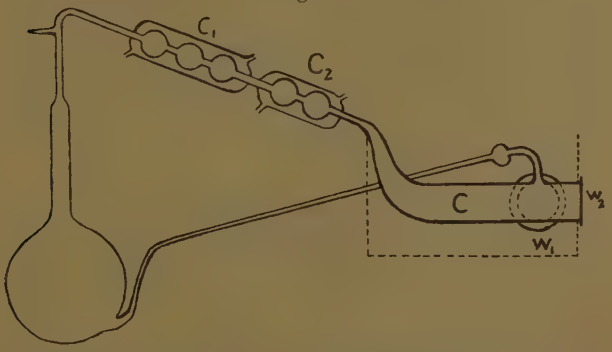

and then enters the cross-tube and finally flows out of it in continuous stream into the flask. By maintaining the temperature of the circulating water in the condensers C_1 and C_2 and that of the bath constant at any desired degree the temperature of the cyclohexane in the cross-tube may also be maintained at the desired point [$T_1 = T_2$].

Light from a mercury arc-lamp was focussed on the liquid through the window W_1 by a quartz lens, and the light scattered at right angles through the window W_2 was in turn focussed on the slit of a quartz spectrograph and photographed in the usual way.

Nature of the Fluorescent Spectrum.

The accompanying fig. 2 (Pl. VII.) shows the continuous bands of the cyclohexane at 16° C. when it is illuminated

by the light of the quartz mercury-lamp. It consists of an intense band extending from λ 3342 Å to λ 2650 Å. with a maximum at λ 2900 Å. and a very feeble one in the blue-violet region with a maximum at about λ 4000 Å. The ultra-violet band (U.V. band) is very sensitive to temperature; its intensity is maximum at about 16° C., but decreases as its temperature is increased or decreased. The aforesaid ultra-violet band persists undiminished in intensity whether we subject the liquid to the continuous distillation process or not, provided the temperature is favourable for its excitation. It is constant and reproducible, and long irradiation by the ultra-violet light has no influence. But the band in the blue-violet region (B.B. band) does not exhibit such a marked sensitiveness to temperature in contrast to its sister band (U.V.). Further, it was noticed that under identical conditions, such as time of exposure, intensity of the incident light, etc., the continuous band (B.V.) varied from experiment to experiment. At first a very feeble band in the blue-violet region makes its appearance, but it gains in intensity and broadens out a little with successive exposures.

Is Fluorescence characteristic of Pure Cyclohexane?

As regards the origin of the continuous band, it may be due to one of the following sources:—

(*a*) The band is due to the fluorescence of cyclohexane molecules themselves.

(*b*) It is due to the substance produced by the photochemical action of the ultra-violet light on the cyclohexane, which in turn fluoresces.

(*c*) It is due to the foreign fluorescent impurities; but in view of the fact that we have used absolutely pure material obtained by orthodox chemical processes this postulate is ruled out.

We have already seen that the ultra-violet band persists undiminished in intensity whether we subject the liquid to the continuous distillation process or not; so we are inclined to the view that this band is due to the fluorescence of the cyclohexane molecules themselves. The other in the blue-violet region, which appears very feeble when the continuous distillation is employed during

exposure but gains in intensity when the continuous distillation is stopped, is due to the product of the photochemical action of the ultra-violet on cyclohexane. These conclusions were verified by means of the following simple experiments: we took two sealed quartz bulbs containing freshly distilled cyclohexane; one was exposed to the mercury light for hours together and the other was kept in a dark room; then, keeping both the bulbs at the temperature 16° C., they were exposed to the exciting mercury light, and on spectrophotographing the scattered radiations we observed a great increase in the intensity of the blue-violet band, while the ultra-violet band was unchanged in intensity as a result of the previous exposure to the ultra-violet radiations. At ordinary temperature also the intensity of this band was decidedly increased, due to the previous exposure—in fact the intensity was so much increased that the light track, barely perceptible before, was clearly visible to the naked eye after exposure to the ultra-violet light.

Origin of the Fluorescence.

It is perhaps of some interest now to examine what wave-lengths are responsible for the excitation of the fluorescent band and for the photochemical decomposition of the cyclohexane as a result of which the visible (B.V.) band makes its appearance.

This was done by introducing various colour-filters in the path of the incident beam, and taking the picture of the scattered radiation every time with the spectrograph.

The introduction of a glass plate, which removes all the radiations of wave-lengths below λ 3000 Å., removes the fluorescent band altogether; so also carbon tetrachloride filter. These suggest that radiations of wave-lengths below λ 2600 Å. are responsible for the photo-decomposition of the cyclohexane, the product of which shows the fluorescent band in the blue-violet region. A similar experiment with the "Kishakowsky and Nelles" filter *, which transmits all light which is transmitted by quartz but less than λ 2400, shows the ultra-violet band.

* G. Kishakowsky and M. Nelles, Phys. Rev. xli. p. 595 (1932).

This conclusively proves that radiations of wave-length between λ 2400–2600 are responsible for the excitation of the ultra-violet band in cyclohexane. As in our experimental arrangement with the mercury arc the line λ 2537 is the most intense radiation, this is considered to be the chief source for the band in the ultra-violet as shown in fig. 2 (Pl. VII.).

As for the photo-decomposition, radiations of wave-lengths below λ 2600 Å., as we have already alluded to, are capable of decomposing cyclohexane photochemically.

Nature of the Compound Photochemically Produced.

In order to study further the nature of the photo-compound produced we exposed a quantity of pure cyclohexane to the ultra-violet light for a long time, at the end of which we found solid powder settled at the bottom of the container, evidently produced by photo-chemical action of the ultra-violet light on cyclohexane. This powder was isolated from the mother liquid in the usual way, and on examination the following points were revealed :—

Colour of the photo-compound : white powder, which on further exposure to ultra-violet turned a little brownish.

Fluorescence : the powder in solution when excited gives a fluorescent band in the blue-violet region with a maximum at about λ 4000 Å.

Odour : very bad smell.

Further study on the nature of the photo-compound, including its chemical properties, will be reported elsewhere in due course.

In conclusion, the author thanks Professor S. N. Bose for his kind interest in the work, and also the authorities of the University of Dacca for giving him full facility to carry out the investigation at the Physics Laboratory.

Physics Laboratory,
Dacca University,
India.

LV. *The Frequency of Transverse Vibration of a Loaded Fixed-Free Bar.—*III. *The Effect of the Rotatory Inertia of the Bar.* *By* R. M. Davies, *M.Sc., F.Inst.P., Lecturer in Physics, University College of Wales, Aberystwyth* *.

Notation.

ρ = Density of the bar.

E = Young's Modulus of the material of the bar.

l = Length of the bar.

k = Radius of gyration of the cross-section of the bar about an axis through the centre of gravity, perpendicular to the plane of motion.

$\beta = \frac{k}{l}$.

A = Area of cross-section of the bar.

$M' = \rho Al$ = Mass of the bar.

M = Mass of the load fixed to the free end of the bar.

$c = \frac{M}{M'}$.

κ = Radius of gyration of the load about an axis through the point of attachment of the load to the bar and perpendicular to the plane of motion.

$I = M\kappa^2$ = Moment of inertia of the load about this axis.

$d = \frac{I}{M'l^2} = \frac{c\kappa^2}{l^2}$.

n = Natural frequency of vibration of the bar when vibrating in the fundamental mode.

$\omega = 2\pi n$ = Natural pulsatance of the bar for this mode.

m = Frequency parameter, defined by the equation

$$m^4 = \frac{\rho\omega^2}{Ek^2}.$$

$z = ml$; $\alpha = z^4 = \frac{\rho\omega^2 l^4}{Ek^2}$.

γ, δ = Functions of β and z defined below.

---

* Communicated by Vice-Principal Gwilym Owen, M.A., D.Sc.

THE present paper is a continuation of the discussion given in two previous papers [1,2] of the fundamental frequency of transverse vibration of a loaded fixed-free bar, more especially in its bearing on a dynamical method developed in this laboratory [3] for the determination of Young's Modulus. In order to calculate the value of Young's Modulus from the data obtained experimentally with a loaded fixed-free bar vibrating transversely in its fundamental mode it is necessary to evaluate the quantity z which is a function of the constants of the bar and of its load. In order to avoid errors exceeding the experimental errors it is necessary that the calculated value of z should be accurate to within 1 in 4000.

In the first paper [1] of this series (hereafter quoted as D. 1) the load was considered as a point-mass, in which case z is a function of c only; the relation between z and c is a transcendental equation due to Prescott [4], and it was shown that an algebraic expression for z in terms of c could be derived from Prescott's equation by a method of expansion in series. In the second paper [2] (hereafter quoted as D. 2) the dynamical theory of the vibration of bars was extended so as to include the effect of the rotatory inertia of the load, and it was shown that z is, in this case, a function of c and d; the equation connecting z with c and d is a transcendental equation which can be made to give an algebraic expression for z in terms of c and d by the series method.

In these two papers the effect of the rotatory inertia of the vibrating bar was neglected, and the object of the present paper is to extend the theory so as to include the effect of the rotatory inertia of the bar as well as the effects of the translatory and rotatory inertia of the load.

The problem of the effect of the rotatory inertia of the bar has been investigated by Rayleigh [5] for the case of a fixed-free unloaded bar; the method employed is an energy method and the result is to be regarded as a first approximation. Considering a fixed-free unloaded bar vibrating transversely in the fundamental mode, if ω_0 be the natural pulsatance when the rotatory inertia is neglected, and if ω_r be the natural pulsatance when the rotatory inertia is small, but not negligibly small, then, in the present notation, Rayleigh's result may be written

$$\omega_r = \omega_0(1-2{\cdot}3241\,\beta^2). \quad . \quad . \quad . \quad . \quad . \quad (1)$$

If z_0 and z_r be the corresponding values of z, then, since $z^4 = \frac{\rho\omega^2 l^4}{Ek^2}$,

$$z_r^4 = z_0^4(1-2{\cdot}3241\beta^2)^2.$$

Since $z_0^4 = 12{\cdot}36_4$, and since β^2 is small in comparison with unity, this result may be written

$$z_r^4 = 12{\cdot}36_4(1-4{\cdot}6482\beta^2). \quad . \quad . \quad . \quad . \quad (2)$$

If necessary, Rayleigh's result could be extended to the case of a loaded bar by applying Dunkerley's Rule [6].

The method adopted in the present work for the evaluation of z consists in forming the differential equation of motion of the bar and then finding a solution which agrees with the boundary conditions at the free and fixed ends.

Let the axis of the bar (assumed straight when in equilibrium) be taken as the axis of x, and let the direction of the displacement of the bar be taken as the axis of y. Let the origin be taken at the fixed end of the bar. If the rotatory inertia of the bar is not negligible then the differential equation of motion is

$$\frac{Ek^2}{\rho}\frac{\partial^4 y}{\partial x^4} - k^2\frac{\partial^4 y}{\partial x^2 \partial t^2} + \frac{\partial^2 y}{\partial t^2} = 0, \quad . \quad . \quad . \quad (3)$$

where t denotes time. In this equation the effect of the rotatory inertia of the bar is represented by the second term.

To solve this equation we assume that, for a simple harmonic vibration of pulsatance ω, y is of the form $y = ue^{i\omega t}$, where $i = \sqrt{-1}$ and where the normal function u is a function of x only. This assumption gives the following differential equation for u :—

$$\frac{\partial^4 u}{\partial x^4} + m^4\left(k^2\frac{\partial^2 u}{\partial x^2} - u\right) = 0, \quad . \quad . \quad . \quad . \quad (4)$$

where $m^4 = \rho\omega^2/Ek^2$.

The particular integrals of this equation are of the form $u = e^{\lambda m x}$, where λ is given by the equation

$$\lambda^4 + k^2 m^2 \lambda^2 - 1 = 0.$$

Thus

$$\lambda^2 = -\tfrac{1}{2}k^2m^2 \pm (1+\tfrac{1}{4}k^4m^4)^{\frac{1}{2}} = -\frac{\beta^2 z^2}{2} \pm \left(1+\frac{\beta^4 z^4}{4}\right)^{\frac{1}{2}},$$

where

$$\beta = k/l \text{ and } z = ml,$$

and we may therefore write the possible values of λ as $\pm\gamma$ and $\pm i\delta$, where

$$\left.\begin{matrix}\delta\\ \gamma\end{matrix}\right\} = + \left\{ \left(1 + \frac{\beta^4 z^4}{4}\right)^{\frac{1}{2}} \pm \frac{\beta^2 z^2}{2} \right\}^{\frac{1}{2}}. \quad . \quad . \quad (5)$$

The general solution of equation (4) may thus be written

$$u = Ce^{\gamma mx} + De^{-\gamma mx} + C'e^{i\delta mx} + D'e^{-i\delta mx},$$

or, alternatively, as

$$u = P \cosh \gamma mx + P' \sinh \gamma mx + Q \cos \delta mx + Q' \sin \delta mx, \quad . \quad . \quad . \quad (6)$$

where C, C', . . . Q, Q' are integration constants which are determined by the boundary conditions.

It may be noted that if the rotatory inertia of the bar is neglected $\beta = 0$ and $\gamma = \delta = 1$, and equation (6) reduces to the form of equation (8) of D. 2.

The boundary conditions at the fixed end ($x = 0$) are

(i.) $y = u = 0$ for all values of t.

(ii.) $\partial y/\partial x = \partial u/\partial x = 0$ for all values of t.

Inserting these conditions in equation (6), we obtain

$$P + Q = 0 \; ; \; \gamma P' + \delta Q' = 0;$$

whence

$$u = P (\cosh \gamma mx - \cos \delta mx) + P' \left(\sinh \gamma mx - \frac{\gamma}{\delta} \sin \delta mx\right). \quad . \quad . \quad . \quad (7)$$

Using the sign-convention given by Prescott (*op. cit.*), chapter ix., the boundary conditions at the free end of the bar ($x = l$) are as follows :—

(i.) The product of the mass M of the load into its linear acceleration is equal to the reversed shearing force, *i. e.*,

$$F = -M \frac{\partial^2 y}{\partial t^2}, \quad . \quad . \quad . \quad . \quad . \quad . \quad . \quad (8)$$

where F is the shearing force, and in the case where the

rotatory inertia of the bar is not negligible F is given by the equation

$$\mathrm{F} = \rho \mathrm{A} k^2 \frac{\partial^3 y}{\partial x \partial t^2} - \frac{\partial \mathrm{M}_b}{\partial x} = \mathrm{A} k^2 \left(\rho \frac{\partial^3 y}{\partial x \partial t^2} - \mathrm{E} \frac{\partial^3 y}{\partial x^3} \right), \quad (9)$$

where $\mathrm{M}_b = k^2 \mathrm{EA} \frac{\partial^2 y}{\partial x^2}$ is the bending moment (*v.* Prescott, *op. cit.*, chapter ix., equations (9.3) and (9.7)). The effect of the rotatory inertia of the bar is represented by the $\frac{\partial^3 y}{\partial x \partial t^2}$ term in equation (9).

Combining equations (8) and (9) we obtain the following equation for u :

$$\mathrm{M} \omega^2 u = -\mathrm{A} k^2 \left[\rho \omega^2 \frac{\partial u}{\partial x} + \mathrm{E} \frac{\partial^3 u}{\partial x^3} \right],$$

or, in terms of c, m, and l,

$$\frac{\partial^3 u}{\partial x^3} = -m^4 \left(k^2 \frac{\partial u}{\partial x} + clu \right). \quad . \quad . \quad . \quad (10)$$

If $k=0$, *i. e.*, if the rotatory inertia of the bar is neglected, this equation reduces to equation (10) of D. 2.

(ii.) The secondary boundary condition at $x=l$ is that the product of the moment of inertia, I, of the load into its angular acceleration is equal to the reversed bending moment. Thus

$$\mathrm{I} \frac{\partial^3 y}{\partial x \partial t^2} = -\mathrm{M}_b = -\mathrm{EA} k^2 \frac{\partial^2 y}{\partial x^2},$$

which gives

$$\frac{\partial^2 u}{\partial x^2} = dm^4 l^3 \frac{\partial u}{\partial x}, \quad . \quad . \quad . \quad . \quad . \quad (11)$$

as in D. 2 equation (11).

Using the values of u, $\frac{\partial u}{\partial x}$ and $\frac{\partial^2 u}{\partial x^2}$ derived from equation (7), we obtain the following equation on substitution in equation (10) :

$$\mathrm{P}[(\delta \sinh \gamma ml - \gamma \sin \delta ml) + clm \, (\cosh \gamma ml - \cos \delta ml)]$$

$$= -\mathrm{P}' \Big[(\delta \cosh \gamma ml + \gamma^3 \cos \delta ml) + clm \, (\sinh \gamma ml - \frac{\gamma}{\delta} \sin \delta ml) \Big]. \quad (12)$$

Similarly we obtain the following equation from equation (11):

$$\begin{aligned}\mathrm{P}[(\gamma^2\cosh\gamma ml+\delta^2\cos\delta ml)-dm^3l^3(\gamma\sinh\gamma ml+\delta\sin\delta ml)]\\ =-\mathrm{P}'[(\gamma^2\sinh\gamma ml+\sin\delta ml)\\ -\gamma dm^3l^3(\cosh\gamma ml-\cos\delta ml)]. \quad (13)\end{aligned}$$

From equations (12) and (13) P and P′ can be eliminated by cross-multiplication, giving the required frequency equation as a transcendental equation connecting $z(=ml)$ with γ, δ, c, and d. This equation can be simplified if we note that, from equation (5),

$$\left.\begin{aligned}&\gamma\delta=1\,; \quad \delta^2-\gamma^2=k^2m^2=\beta^2z^2\,;\\ &\gamma^2+\delta^2=2(1+\tfrac{1}{4}k^4m^4)^{\frac{1}{2}}=2(1+\tfrac{1}{4}\beta^4z^4)^{\frac{1}{2}}\,;\\ &\gamma^4+\delta^4=2+k^4m^4=2+\beta^4z^4.\end{aligned}\right\} \quad . \quad . \quad (14)$$

Carrying out the necessary reduction from the frequency equation, we find ultimately that

$$\begin{aligned}\{1+\left(1+\frac{\beta^4z^4}{2}\right)\cosh\gamma z\cos\delta z-\tfrac{1}{2}\beta^2z^2\sinh\gamma z\sin\delta z\}\\ =\left\{\frac{cz}{2}(\gamma^2+\delta^2)\left[\frac{1}{\delta}\cosh\gamma z\sin\delta z-\frac{1}{\gamma}\sinh\gamma z\cos\delta z\right]\right.\\ +\frac{dz^3}{2}(\gamma^2+\delta^2)\left[\frac{1}{\gamma}\cosh\gamma z\sin\delta z+\frac{1}{\delta}\sinh\gamma z\cos\delta z\right]\\ \left.+cdz^4\left[\cosh\gamma z\cos\delta z-1+\tfrac{1}{2}\beta^2z^2\sinh\gamma z\sin\delta z\right]\right\}.\\ \quad . \quad . \quad . \quad (15)\end{aligned}$$

It should be noted that equation (15) reduces to equation (12) of D. 2 if $\beta=0$ and $\gamma=\delta=1$, *i. e.*, if the rotatory inertia of the bar is neglected.

We have next to derive an explicit algebraic relationship giving z in terms of the parameters β, c, and d, and this can be done by expanding the products of the trigonometric and hyperbolic functions in series. As in the simpler cases considered in D. 1 and D. 2, the required accuracy of about one in one thousand in z^4 is obtained if we reject terms involving z^{12} and higher powers of z. Using the well-known series for $\cosh\gamma z$, $\sinh\gamma z$, $\cos\delta z$, and $\sin\delta z$, it is permissible to form these products by multiplication of the series, since the series are uniformly convergent

in the region considered. In this way we obtain the following results :—

$$\left.\begin{aligned}
&1+\cosh\gamma z\cos\delta z = 2-\frac{z^4}{6}(1+3\beta^2)+\frac{z^8}{2520}(1+42\beta^2+105\beta^4),\\
&\tfrac{1}{2}\beta^1 z^1\cosh\gamma z\cos\delta z = \tfrac{1}{2}\beta^1 z^4\left[1-\frac{z^4}{6}(1+3\beta^2)\right],\\
&-\tfrac{1}{2}\beta^2 z^2\sinh\gamma z\sin\delta z = -\tfrac{1}{2}\beta^2 z^4\left[1-z^4\left(\frac{1}{90}+\frac{\beta^2}{6}\right)\right],\\
&\tfrac{1}{2}cz(\gamma^2+\delta^2)\left[\frac{1}{\gamma}\cosh\gamma z\sin\delta z-\frac{1}{\gamma}\sinh\gamma z\cos\delta z\right]\\
&\qquad = c\left[\frac{2z^4}{3}-\frac{z^8}{2520}(8+168\beta^2-420\beta^4)\right],\\
&\tfrac{1}{2}dz^3(\gamma^2+\delta^2)\left[\frac{1}{\gamma}\cosh\gamma z\sin\delta z+\frac{1}{\delta}\sinh\gamma z\cos\delta z\right]\\
&\qquad = d\left[2z^4-\frac{z^8}{2520}(168+840\beta^2-1260\beta^4)\right],\\
&cdz^4\left[\cosh\gamma z\cos\delta z-1+\frac{z^2\beta^2}{2}\sinh\gamma z\sin\delta z\right] = -420\,\frac{cdz^8}{2520}.
\end{aligned}\right\} \quad . \quad . \quad . \quad (16)$$

Using these results, and putting $z^4=\alpha$, equation (15) becomes

$$\frac{\alpha^2 A}{2520}-\frac{\alpha B}{6}+2=0, \quad . \quad . \quad . \quad . \quad . \quad (17)$$

where

$$\left.\begin{aligned}
A &= 1+8c+168d+420cd+56\beta^2(1+3c+15d)\\
&\quad +105\beta^4(1-4c-12d)-630\beta^6,\\
B &= 1+4c+12d+6\beta^2-3\beta^4.
\end{aligned}\right\} \quad (18)$$

If the rotatory inertia of the bar is neglected equations (17) and (18) reduce to equation (14) of D. 2 as far as terms in α and α^2 are concerned.

Regarding equation (17) as a quadratic equation in α, the smaller root corresponds to the fundamental mode of vibration and the larger root to the first overtone ; as shown in D. 1 and D. 2 the value of z given by this equation for the first overtone is likely to be in error since z in this case is large. On the other hand, the error in

z^4 for the fundamental is unlikely to exceed 1 in 1000 in cases which are likely to occur in practice. Confining our attention to the fundamental mode, we find that

$$\alpha = z^4 = \frac{210}{A}\left(B - \sqrt{B^2 - \frac{4A}{35}}\right), \quad . \quad . \quad (19)$$

which, in conjunction with equation (18), gives the value of z in terms of c, d, and β.

In discussing these results it will be convenient to take first the particular case of an *unloaded bar*. If A_0 and B_0 be the values of the coefficients A and B of equations (18) and (19) for this particular case,

$$\left.\begin{aligned} A_0 &= 1+56\beta^2+105\beta^4-630\beta^6, \\ B_0 &= 1+6\beta^2-3\beta^4. \end{aligned}\right\} \quad . \quad . \quad . \quad (20)$$

If β is sufficiently small to allow β^4 and higher powers of β to be neglected then $A_0 = 1+56\beta^2$ and $B_0 = 1+6\beta^2$, and from equation (19) it can be shown that in this case

$$\alpha = z^4 = 12{\cdot}36_4(1-4{\cdot}624\beta^2), \quad . \quad . \quad . \quad (21)$$

which is in good agreement with the approximate value given in equation (2). The variation of z with β is shown graphically in the figure, where β is plotted as abscissa and z as ordinate. The full-line curve gives the value of z derived from the accurate equations (19) and (20), whilst the dotted-line curve gives the value of z deduced from the approximate formula of equation (21). It is clear that the two values do not differ greatly for small values of β, and calculation shows that the difference between the accurate and approximate values of z amounts to about 0·1 per cent. for $\beta = 0{\cdot}1$. In this connexion it may be added that $\beta = 0{\cdot}1$ corresponds to a bar whose thickness is about 0·3465 times its length if the cross-section of the bar is rectangular, and to a bar whose radius is 0·2 times its length if the cross-section of the bar is circular. Thus in most cases encountered in practice z is generally given to a sufficient degree of approximation by the approximate formula of equation (21).

Turning next to the case of *loaded bars*, it is of interest to consider the effect of the rotatory inertia of the bar in the experiments of Davies and James and of Davies and Thomas [3]. In the latter paper the values of z were

calculated using equation (9) of D. 1, and thus the effects of the rotatory inertia of the bar and of the load were neglected. The magnitude of the effect in question may be illustrated by reference to the two cases quoted in D. 2.

The first case is one in which the value of c is comparatively small; in this case $l=2{\cdot}568$ cm. and $c=0{\cdot}03663$,

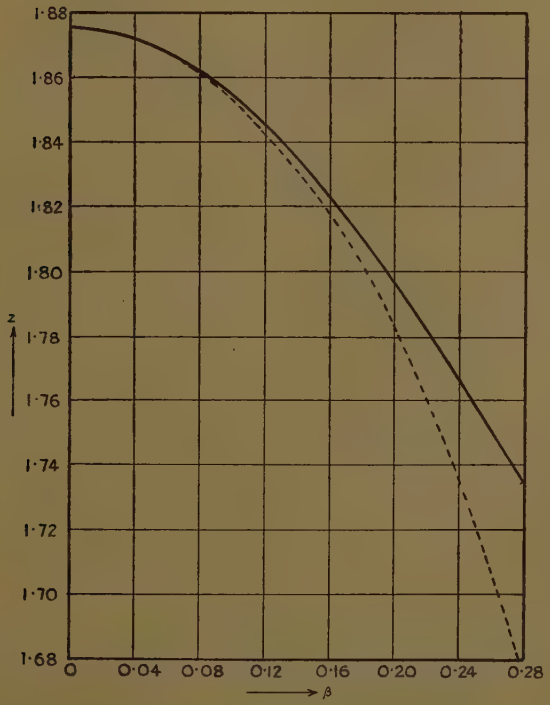

Variation of z with β for an unloaded bar. Full-line curve: accurate values of z, using equations (20) and (19). Dotted line curve: approximate values of z, using equation (21).

and, neglecting the rotatory inertia of both bar and load, $z^4=10{\cdot}77_9$. Assuming the width of the load in the direction of vibration to be 0·5 cm., as in D. 2, $d=1{\cdot}157\times 10^{-4}$; taking into account the rotatory inertia of the

load, but neglecting that of the bar, *i. e.*, calculating z according to equation (16) of D. 2, we find $z^4=10{\cdot}77_1$. The thickness of the bar was 0·0765 cm., hence $k^2=(0{\cdot}0765)^2/12$ cm.^{2} and $\beta^2=7{\cdot}399\times10^{-5}$. Using equations (18) and (19) it is found that $z^4=10{\cdot}76_7$; thus, taking the rotatory inertia of the load and of the bar into account reduces the value of z^4 by about 0·12 per cent.—a difference which is of the same order as the experimental error, when it is remembered that E varies inversely as z^4.

The second case is one in which the value of c is comparatively large; for this case $l=2{\cdot}321$ cm. and $c=0{\cdot}1153$; neglecting the rotatory inertia of both bar and load it is found that $z^4=8{\cdot}435_5$. If the width of the load in the direction of vibration is taken to be 0·5 cm., then $d=4{\cdot}458\times10^{-4}$, and taking into account the rotatory inertia of the load, but neglecting that of the bar, it is found that $z^4=8{\cdot}414_6$. The thickness of the bar was 0·0727 cm., and thus $\beta^2=8{\cdot}175\times10^{-5}$, and taking into account the rotatory inertia of both bar and load $z^4=8{\cdot}412_5$; in this case the error in z^4 or E due to neglect of the rotatory inertia of the load and of the bar amounts to 0·3 per cent.

In the actual experiments, as pointed out in D. 2, the width of the load did not exceed 0·3 cm. and $d=1{\cdot}605\times10^{-4}$ for this value of the width; neglecting the effect of the rotatory inertia of the bar, but allowing for that of the load, it is found that $z^4=8{\cdot}425_7$. Finally, taking the rotatory inertia of both load and bar into account it is found that $z^4=8{\cdot}425_7$. In this case the rotatory inertia of the bar and load reduce the value of z^4 from $8{\cdot}435_5$ to $8{\cdot}425_7$; this corresponds to an error of about 0·12 per cent. in the calculation of z or E.

As far as the results contained in the paper of Davies and Thomas are concerned it may be concluded that the neglect of the rotatory inertia of the bar and load does give rise to some uncertainty in the final values of E; from the extreme case discussed above it appears that this uncertainty is not likely to exceed 0·12 per cent.

In conclusion, the author wishes to express his sincere thanks to Vice-Principal Gwilym Owen for his interest and encouragement, and to Mr. Thomas Lewis, Head of the Department of Applied Mathematics, for discussing and checking the results.

References.

(1) Davies, Phil. Mag. xxii. p. 892 (1936).
(2) Davies, Phil. Mag. xxiii. p. 464 (1937)
(3) Davies and James, Phil. Mag. xviii. p. 1023 (1934); James and Davies, Phil. Mag. xviii. p. 1053 (1934); Davies and Thomas, Phil. Mag. xxiii. p. 361 (1937).
(4) J. Prescott, 'Applied Elasticity,' p. 213 (London, 1924).
(5) Lord Rayleigh, 'Theory of Sound,' vol i. p. 294 (London, 1894).
(6) Dunkerley, Phil. Trans. Roy. Soc. A, clxxxv. p. 279 (1894); Temple and Bickley, 'Rayleigh's Principle,' p. 117 (Oxford, 1933); Prescott, *op. cit.* p. 234.

November 1936.

LVI. *On the Motion of an Extensible Membrane in a given Curved Surface.* *By* C. E. Weatherburn, *M.A., D.Sc., Professor of Mathematics in the University of Western Australia* *.

WE propose to consider the equations governing the motion of a thin membrane or film in a fixed surface. If there are any material guides to keep the film in the given surface they are supposed to be smooth, so that the action between them and the film is normal to the surface. The film is assumed capable of finite distortion without rupture. We employ the differential geometry of the surface, and make use of the surface invariants † (gradient, divergence, curl, etc.) of functions on the surface. These invariants involve only two parameters, and differ from those frequently employed in the case of three dimensions.

Kinematics.

1. The velocity **v** of a particle of the membrane is a point function on the surface. With reference to any scalar or vector point function ψ on the surface, we have to distinguish between the time-rate of change of the function at a fixed point, *i. e.*, the *local* rate of change

* Communicated by the Author.

† *Cf.* a paper by the author "On Differential Invariants in Geometry of Surfaces, with some Applications to Mathematical Physics," 'Quarterly Journal of Pure and Applied Mathematics,' l. (1925), pp. 230–269. This paper will be referred to briefly as Q. J. An account of these is also given in the author's 'Differential Geometry,' vol. i. chap. xii. (Camb. Univ. Press, 1927). This will be indicated briefly by D. G.

$\partial\psi/\partial t$, and the rate of change of the value of ψ associated with a definite particle of the membrane, *i. e.*, the *individual* rate of change $d\psi/dt$. The value of ψ associated with a particle at any instant is that of the point instantaneously occupied by the particle. These two rates of change are connected by the relation *

$$\frac{d\psi}{dt} = \frac{\partial\psi}{\partial t} + \mathbf{v}.\nabla\psi. \quad . \quad . \quad . \quad . \quad . \quad (1)$$

The *equation of continuity* is obtained by equating the rate of increase of mass within a fixed closed curve on the surface to the rate at which matter is flowing into this region. In terms of the surface density ρ of the membrane (which is a point function as well as a function of t) and the surface divergence for a vector function this equation of continuity is expressible in the alternative forms †

$$\frac{\partial\rho}{\partial t} + \operatorname{div}(\rho\mathbf{v}) = 0 \quad . \quad . \quad . \quad . \quad . \quad (2)$$

or

$$\frac{d\rho}{dt} + \rho \operatorname{div}\mathbf{v} = 0. \quad . \quad . \quad . \quad . \quad . \quad (3)$$

The physical meaning of div $\mathbf{v}$ may be seen as follows. Consider a definite element of the membrane, consisting always of the same particles. As it moves its mass remains constant, so that $\rho\, d\mathrm{S} = \text{const.}$, where $d\mathrm{S}$ is the area of the element. From this relation it follows that

$$\frac{1}{\rho}\frac{d\rho}{dt} = -\frac{1}{d\mathrm{S}}\frac{d}{dt}(d\mathrm{S}),$$

and (3) then gives

$$\operatorname{div}\mathbf{v} = \frac{1}{d\mathrm{S}}\frac{d}{dt}(d\mathrm{S}).$$

Thus the divergence of the velocity is equal to the time-rate of increase of area per unit area ‡.

If the motion is such that div $\mathbf{v} = 0$ it follows from (3) that $d\rho/dt = 0$. This does not mean that the membrane is necessarily inextensible. The shape of the above element $d\mathrm{S}$ may change, but its area is constant, so that

* Q. J. p. 266.
† Q. J. p. 267.
‡ This also follows from Q. J. p. 255 (45), or D. G. p. 240 (25).

its *density is invariable* in the sense that its individual rate of change is zero. We may write $\mathbf{v}=v\mathbf{t}$, where v is the speed of the particle and $\mathbf{t}$ the unit tangent to the line of flow. Then

$$\operatorname{div}\mathbf{v}=\mathbf{t}.\nabla v+v\operatorname{div}\mathbf{t}.$$

Now if div $\mathbf{t}$ vanishes the lines of flow are parallels * on the surface. If $\mathbf{t}.\nabla v$ is zero v is constant along a line of flow, while $\operatorname{div}\bar{\mathbf{v}}=0$ is the condition that ρ be invariable. Hence the theorem :

If the motion of the membrane has two of the following properties it will also have the third : (a) *that the lines of flow are parallels*, (b) *that the speed is constant along a line of flow*, (c) *that the surface density of an element is invariable.*

Another particular case deserves mention. The velocity $\mathbf{v}$ will be the surface gradient of some scalar function if the resolved part of the surface curl of $\mathbf{v}$ normal to the surface is zero †, *i. e.*, if $\mathbf{n}.\operatorname{curl}\mathbf{v}=0$, where $\mathbf{n}$ is the unit vector normal to the surface. We may then write

$$\mathbf{v}=-\nabla\phi \quad . \quad . \quad . \quad . \quad . \quad . \quad . \quad . \quad (4)$$

and speak of ϕ as the *velocity potential*. The circulation round any closed curve C on the membrane is then zero. For ‡

$$\int_c \mathbf{v}.d\mathbf{r}=\iint \mathbf{n}.\operatorname{curl}\mathbf{v}\,dS=0.$$

Such motion, possessing a velocity potential, will be called *irrotational*. Also, since $\mathbf{v}=v\mathbf{t}$, we have

$$\mathbf{n}.\operatorname{curl}\mathbf{v}=\mathbf{n}.(\nabla v\times\mathbf{t}+v\operatorname{curl}\mathbf{t})$$

$$=v(\mathbf{n}.\operatorname{curl}\mathbf{t})-\mathbf{b}.\nabla v,$$

where $\mathbf{b}$ is a unit surface vector perpendicular to $\mathbf{t}$. Now $\mathbf{n}.\operatorname{curl}\mathbf{t}=0$ is the condition that the lines of flow be geodesics §. If $\mathbf{b}.\nabla v$ is zero, the lines $v=$const. are orthogonal to the lines of flow ; and if $\mathbf{n}.\operatorname{curl}\mathbf{v}$ vanishes the motion is irrotational. Hence the theorem :

If the motion of the membrane has two of the following properties it will also have the third : (a) *that the motion*

* D. G. p. 258.
† Q. J. p. 258, or D. G. p. 244.
‡ Q. J. p. 257, or D. G. p. 243.
§ Q. J. p. 247, or D. G. p. 250.

is irrotational, (b) *that the lines of flow are geodesics*, (c) *that the lines v=const. are orthogonal to the lines of flow.*

Dynamics.

2. *Equation of Motion.*—Suppose first that the tension at a point across any line in the membrane is perpendicular to it, there being no action tangential to the line. Then it follows, as in the case of three dimensions *, that the tension or pull per unit length across a line is a point function p, being the same for all directions of the line through the point.

Consider the motion of the portion of the membrane bounded by a closed curve C, which moves with the membrane, containing always the same particles and therefore always the same mass. Let $d\mathrm{S}$ be the area of an element of the enclosed portion, also moving with the membrane, so that the mass $\rho\, d\mathrm{S}$ of the element remains constant. Since the acceleration of a particle is the individual rate of increase of $\mathbf{v}$, *i. e.*, $d\mathbf{v}/dt$, the rate of increase of the momentum of the above element is $\dfrac{d\mathbf{v}}{dt}\rho\, d\mathrm{S}$.

The bodily force on this element is $\mathbf{F}\rho\, d\mathrm{S}$, where $\mathbf{F}$ is the force per unit mass. Let R be the resultant force per unit area on the sides of the membrane. We assume the constraints (if any) to be frictionless, so that $\mathrm{R}\mathbf{n}\, d\mathrm{S}$ is the lateral force on the above element. Let ds be the length of an element of the boundary curve C and $\mathbf{m}$ the unit surface vector perpendicular to this element and directed outward from the enclosed region. Then $p\mathbf{m}\, ds$ is the tension across the element. Equating the rate of increase of the momentum of the portion of the membrane enclosed by C to the vector sum of all the forces on it we have

$$\iint \frac{d\mathbf{v}}{dt}\rho\, d\mathrm{S} = \iint (\rho\mathbf{F}+\mathrm{R}\mathbf{n})\, d\mathrm{S} + \int_c p\mathbf{m}\, ds.$$

Transforming the line integral in the last term by the formula †

$$\int_c p\mathbf{m}\, ds = \iint (\nabla p + \mathrm{J}p\mathbf{n})\, d\mathrm{S},$$

* *Cf.* the author's 'Advanced Vector Analysis,' p. 58 (G. Bell & Sons, 1924).

† Q. J. p. 255 (46), or D. G. p. 240 (26).

where J is the mean curvature (or first curvature) of the surface, we obtain

$$\iint \frac{d\mathbf{v}}{dt}\rho\, dS = \iint (\rho\mathbf{F}+\mathrm{R}\mathbf{n}+\nabla p+\mathrm{J}p\mathbf{n})\, dS.$$

Since this relation holds for the region bounded by any closed curve drawn on the surface the integrands must be identical, so that

$$\left.\begin{aligned}\rho\mathbf{F}+\nabla p+(\mathrm{R}+\mathrm{J}p)\mathbf{n} &= \rho\frac{d\mathbf{v}}{dt}\\ &= \rho\left(\frac{\partial\mathbf{v}}{\partial t}+\mathbf{v}.\nabla\mathbf{v}\right).\end{aligned}\right\} \quad . \quad (5)$$

This is the *equation of motion* of the membrane. By resolving all the vectors into components normal to the surface or tangential to it we may replace this equation by two. Thus if we write $\mathbf{F}=\mathbf{G}+\mathrm{H}\mathbf{n}$, where $\mathbf{G}$ is the tangential component of $\mathbf{F}$, we obtain the equivalent relations

$$\rho\mathrm{H}+\mathrm{R}+\mathrm{J}p=\kappa_n v^2\rho \quad . \quad . \quad . \quad . \quad . \quad (6)$$

and

$$\rho\mathbf{G}+\nabla p=\rho\left(\frac{\partial\mathbf{v}}{\partial t}+\frac{dv^2}{ds}\mathbf{t}+\gamma v^2\mathbf{b}\right), \quad . \quad . \quad . \quad (7)$$

in which κ_n is the normal curvature of the surface in the direction of $\mathbf{v}$, γ is the geodesic curvature of the line of flow, and d/ds denotes differentiation in the direction of this line. We shall not give the details of this transformation.

The conditions of *equilibrium* of the membrane follow from the above on putting $\mathbf{v}$ and $\frac{d\mathbf{v}}{dt}$ equal to zero. In particular, if $\mathbf{F}$ is everywhere normal to the surface it follows from (5) that $\nabla p=0$, and therefore p is constant over the membrane. Similarly, if $\mathbf{F}$ is a surface vector at all points and R is zero, we must have $\mathrm{J}=0$. We thus see that *

For the equilibrium of a stretched membrane with normal tension if the external force is everywhere normal to the membrane, the tension is the same at all points. If, however, the external force is at all points tangential to the membrane

* *Cf.* Q. J. p. 261.

(or zero) the shape of the membrane is that of a minimal surface.

Also, since the curl of a gradient and the curl of a normal vector are both tangential to the surface *, it follows from (5) in the case of equilibrium that curl ($\rho\mathbf{F}$) is also a surface vector. Consequently for the equilibrium of a membrane the bodily force and the density must satisfy the relation

$$\mathbf{n}.\operatorname{curl}(\rho\mathbf{F})=0.$$

3. *Vorticity.*—We may call the quantity $\frac{1}{2}\mathbf{n}.\operatorname{curl}\mathbf{v}$ the "vorticity" at the point considered and its surface integral over any portion of the membrane the total vorticity of that portion. Since for any closed curve C on the surface and the region enclosed by it

$$\int_C \mathbf{v}.d\mathbf{r}=\iint \mathbf{n}.\operatorname{curl}\mathbf{v}\,dS,$$

it follows that the circulation round any closed curve on the membrane is equal to twice the vorticity of the region enclosed. Kelvin's Circulation theorem for fluid motion is proved on the assumption that the density of the fluid is a function of the pressure. No such relation between p and ρ exists in the present instance. Films, however, do exist for which the tension is constant, and in such cases $\nabla p=0$. If, in addition, the bodily force $\mathbf{F}$ is a surface gradient we may prove that the circulation round any closed curve moving with the membrane does not change with elapse of time. This may be done just as in the case of three dimensions †. Or we may proceed by showing that the vorticity of an element moving with the membrane does not alter. Thus twice the individual rate of change of the vorticity

$$=\frac{d}{dt}(\mathbf{n}.\operatorname{curl}\mathbf{v})=\frac{d\mathbf{n}}{dt}.\operatorname{curl}\mathbf{v}+\mathbf{n}.\operatorname{curl}\frac{d\mathbf{v}}{dt}.$$

Now each of these terms is equal to zero. For

$$\frac{d\mathbf{n}}{dt}.\operatorname{curl}\mathbf{v}=\left(\frac{\partial\mathbf{n}}{\partial t}+\mathbf{v}.\nabla\mathbf{n}\right).\operatorname{curl}(v\mathbf{t})$$

$$=-v(\kappa_n\mathbf{t}+\tau\mathbf{b}).(\nabla v\times\mathbf{t}+v\operatorname{curl}\mathbf{t})$$

* Q. J. pp. 240, 241, or D. G. pp. 229, 230.

† *Cf.* 'Advanced Vector Analysis,' p. 73.

$$= -v^2(\kappa_n \mathbf{t}.\operatorname{curl}\mathbf{t} + \tau \mathbf{b}.\operatorname{curl}\mathbf{t})$$

$$= -v^2(\kappa_n\tau - \tau\kappa_n) = 0,$$

τ being the geodesic torsion * of a line of flow. Also, since $\mathbf{F}$ is a surface gradient $-\nabla V$, and $\nabla p = 0$,

$$\mathbf{n}.\operatorname{curl}\frac{d\mathbf{v}}{dt} = \mathbf{n}.\operatorname{curl}\left[-\nabla V + \frac{1}{\rho}(R + Jp)\mathbf{n}\right],$$

and this expression vanishes since both the curl of a gradient and the curl of a normal vector are tangential to the surface. Thus the vorticity of an element moving with the film is invariable ; and we have the theorem :

In the motion of a film of constant tension, if the bodily force is tangential and conservative, the vorticity of a particle is invariable, and therefore the circulation round a closed curve moving with the film is also invariable.

Under these conditions the total vorticity of any region moving with the film remains constant, and, in particular, if the motion is irrotational at any instant it remains so.

4. *General Tension.*—Now let us remove the restriction that the tension at any point across a line is normal to that line. If tangential action is possible the tension at a point across a line depends upon the direction of the line through the point. This direction is specified by a unit surface vector $\mathbf{m}$ orthogonal to the line. The tension across the line will be denoted by $\mathbf{T}_m$, this being the force per unit length acting on the material at the back of the line relative to $\mathbf{m}$. We have shown elsewhere † that $\mathbf{T}_m$ is a linear vector function of $\mathbf{m}$ given by

$$\mathbf{T}_m = \mathbf{m}.\Psi, \quad \ldots\ldots \quad (8)$$

where Ψ is the dyadic (or tensor) defined by

$$\Psi = \mathbf{a}\mathbf{T}_a + \mathbf{b}\mathbf{T}_b, \quad \ldots\ldots \quad (9)$$

$\mathbf{a}$ and $\mathbf{b}$ being any two perpendicular unit surface vectors, and $\mathbf{T}_a$ and $\mathbf{T}_b$ the tensions corresponding to the directions of $\mathbf{a}$ and $\mathbf{b}$ respectively.

Considering, as in § 2, the motion of the portion of the membrane enclosed by the curve C, we have now to replace

* D. G. p. 250.
† Q. J. p. 263

the integral $\int_c p\mathbf{m}\,ds$ by $\int_c \mathbf{m}.\Psi\,ds$. The transformation represented in the Divergence Theorem * is also applicable to this integral, so that

$$\iint \nabla.\Psi\,d\mathrm{S} = \int_c \mathbf{m}.\Psi\,ds - \iint \mathbf{J}\mathbf{n}.\Psi\,d\mathrm{S}.$$

But $\mathbf{n}.\Psi$ is zero in virtue of (9), so that for the motion of the portion of the membrane enclosed by C we have

$$\iint \frac{d\mathbf{v}}{dt}\rho\,d\mathrm{S} = \iint (\rho\mathbf{F} + \mathrm{R}\mathbf{n} + \nabla.\Psi)\,d\mathrm{S}.$$

And since this relation holds for any portion of the membrane the integrands are identically equal, and we have the *equation of motion*

$$\rho\mathbf{F} + \nabla.\Psi + \mathrm{R}\mathbf{n} = \rho\frac{d\mathbf{v}}{dt}. \quad . \quad . \quad . \quad . \quad (10)$$

LVII. *The Deflexion of Unsupported Beams under Variable Loads.* *By* R. A. Fairthorne, *B.Sc.*†

Contents.

1. *Introduction.*

THE problem of the deflexion of beams under dynamic loads, being of great technical importance, is studied in considerable detail in text-books. A complete and rigorous solution for the case of a simply supported uniform beam under any form of variable load has been given by A. N. Lowan [1]. The problem of the unsupported beam seems, however, to have been neglected, possibly because it is scarcely of practical importance in the design of bridges and similar structures. Nevertheless all

* Q. J. p. 255, or D.G. p. 239.

† Communicated by the Author.

structures, such as ships and aircraft, that are not anchored to a rigid base come under this category.

In this paper, it is shown that, if the motion of the beam in pitch is small, the deflexion equations have the same form as those of Lowan. A rule is given for the upper limit of the strain energy due to a variable force, of which the rule that, for a system of one degree of freedom, the deflexion due to a load suddenly applied is twice the static deflexion, is a particular case. Finally, the practical limitations of the theory are discussed.

2. *General Theory.*

Suppose that an imperfectly rigid body is moving under the action of any forces, and that rotating axes are taken through the instantaneous position of the mass centre of the deformed body. If these axes are given angular velocities such that the sum of the squares of the deviations of the particles of the body from the positions they would occupy if fixed relative to these axes is, throughout any small portion of time, a minimum, then the equations of motion referred to these axes will have the same form as if the body were rigid [(2)]. The inertia coefficients, however, will now be variable.

It is not difficult to show that this condition for the motion of the axes is equivalent to saying that the angular momentum relative to them must be zero, or the kinetic energy relative to them must be a minimum. Axes chosen to fulfil this condition will be termed "mean axes."

The condition being fulfilled, any change in the co-ordinates relative to the mean axes must necessarily involve a change of shape, that is, a change of strain energy, alone; for if it involved a translation or rotation of the body as a whole the kinetic energy of the relative motion could be further reduced by giving the same translation or rotation to the mean axes. But, by hypothesis, the kinetic energy of the relative motion is already a minimum.

If the body is moving under the action of external forces F, these forces will be in equilibrium with the reversed inertia forces I. These inertia forces can be split in two parts: i_R, the inertia relative to the mean axes, and i, the inertia that would result if the particles were frozen round the mean axes, that is, if the body were rigid

and moving in step with the mean axes. Now i is equal to forces f, so distributed as to produce motion without deformation in the body, and to have the same resultants as F,—that is, their components must be of the form $m(A_1+B_1y+C_1z)$, $m(A_2+B_2z+C_2x)$, $m(A_3+B_3x+C_3y)$ at each particle of mass m, and coordinates xyz, and their resultant force and moments must be equal to those of F. The body can now be considered as being in equilibrium under the force system $(F-i_R)-f$.

Now suppose that the body is acted upon by a unit load at ξ say, and by a reaction $f(1)$, so distributed as to produce motion without deformation in the absence of the unit load, and having a resultant equal and opposite to that load. This type of reaction conforms with the criterion that a reaction does no work. Let $G(x, \xi)$ be the deflexion at x due to this combined loading, with respect to axes through the mass centre of the deformed body. Then the deflexion $y(x)$ at x, due to a distributed load $F(\xi)$, and the corresponding distributed reaction $f(\xi)$, will be

$$y(x) = \int G(x, \xi).F(\xi).d\xi, \quad . \quad . \quad . \quad . \quad (1)$$

the integration extending over all the particles of the body.

In the dynamical problem F must be replaced by the sum of the applied forces and the reversed inertia forces relative to the mean axes. This will give an integral equation for the deflexions. The motion of the mean axes is given, as stated above, by equations of the same form as if the body were rigid, but with variable inertia coefficients which involve the deflexions. In many applications the deflexions are very small, and the inertia coefficients that enter into the equations of motion may be taken as constant. The motion of the mean axes is then the same as if the body were rigid. It should be noticed that only the motion of the mean axes is required; their absolute position is arbitrary, though they are generally taken to coincide initially with the principal axes of inertia.

3. *Deflexion of a Free Beam under Forces Perpendicular to its Length, when the Motion in Pitch is Small.*

Let the length of the beam be 2L, the line density $\sigma(x)$, and the flexural rigidity $EI(x)$, the last two being

variable along the length of the beam. Suppose it to be acted upon by external forces $\phi(x, t)$, perpendicular to its length and variable along it and in time. Take the initial position of the mean axis of x to lie along the undeformed centre line and the axis of y perpendicular thereto through the mass centre. If the deflexions y are small the inertia about the mass centre may be taken as constant, and the motion of the mean axes will be the same as that of a similar rigid beam. Therefore, if

θ = angle between mean axis and the horizontal,
$\mathrm{M}k^2$ = polar moment of inertia about the mass centre,

then $\mathrm{M}k^2\ddot{\theta} = h(t)$,

where $h(t)$ = applied moment $= \int u.\phi(u, t)du$,

the integration extending over the whole length of the beam. These will be the limits of all integrals unless otherwise stated.

The acceleration of any element of the beam relative and perpendicular to the instantaneous position of the mean axes is

$$x\ddot{\theta}+\ddot{y}-y\dot{\theta}^2$$

or, taking y and $\dot{\theta} << 1$,

$$x\ddot{\theta}+\ddot{y}.$$

The force distribution along the beam, that is the sum of the applied forces and the reversed inertia forces, is then, neglecting the rotational inertia of deformation,

$$\mathrm{F}(x, t) = \phi(x, t)-\sigma x.h(t)/\mathrm{M}k^2-\sigma\ddot{y}(x, t). \quad . \quad (2)$$

Substituting in (1), we have

$$y(x, t) = \int \mathrm{G}(x, \xi).f(\xi, t)d\xi - \frac{h(t)}{\mathrm{M}k^2}\int \sigma\xi.\mathrm{G}(x\xi)d\xi, \quad (3)$$

where $$f(x, t) = \phi(x, t)-\sigma\ddot{y}(x, t). \quad . \quad . \quad . \quad . \quad (4)$$

Since a load distribution of σx produces rotation without deformation, the second integral on the right-hand side of (3) vanishes, by virtue of equation (1), or, more shortly, reactions, concentrated or distributed, do no work.

Therefore

$$y(x, t) = \int \mathrm{G}(x, \xi)\{\phi(\xi, t)-\sigma(\xi).\ddot{y}(\xi, t)\}d\xi \quad . \quad (5)$$

when the deflexions and the motion in pitch are small.

Application of (5) to the case of no applied forces shows that $G(x\xi)$ can be written in the form

$$G(x, \xi) = \Sigma_n \frac{1}{w_n^2} u_n(x).u_n(\xi), \quad . \quad . \quad . \quad (6)$$

where the w's are the frequencies of free vibration of the beam and the u's are the normal modes of vibration. Another way of regarding the u's, which is sometimes useful, is to take them as those force distributions which, in conjunction with the reactions, bend the beam into a curve which, when the ordinates are divided by factors corresponding to the corresponding densities, has the same profile as the loading curve. More shortly, the normal modes u_n are the possible shapes of the beam when bent by transverse forces proportional to the product of the density and the deflexion. The functions u_n have the normal property that

$$\left.\begin{aligned} \int \sigma(x).u_n(x).u_m(x)dx &= 0, \quad \text{if } n \neq m \\ &= 1, \quad \text{if } n = m \end{aligned}\right\} . \quad . \quad . \quad (7)$$

On the assumption that y and ϕ/σ can be represented, within the length of the beam, as series of the functions $u_n(x)$ with coefficients that are functions of the time, (7) allows us to write

$$\begin{aligned} y(x, t) &= \Sigma_n u_n(x).\int \sigma(\xi).y(\xi, t)u_n(\xi)\,d\xi \\ &= \Sigma_n \alpha_n(t).u_n(x), \quad \text{say} \end{aligned}$$

$$\begin{aligned} \frac{\phi(x, t)}{\sigma(x)} &= \Sigma_n u_n(x) \int \phi(\xi, t).u_n(\xi)\,d\xi + \frac{R(t)}{M} + x\frac{h(t)}{Mk^2} \\ &= \Sigma_n a_n(t)u_n(x) + \frac{R(t)}{M} + x\frac{h(t)}{Mk^2}, \quad \text{say}, \quad . \quad . \quad (8) \end{aligned}$$

where

$R(t) =$ resultant of $\phi = \int \phi(x, t)\,dx$,

$h(t) =$ moment of $\phi = \int x.\phi(x, t)\,dx$.

The terms in the expansion for ϕ/σ containing the resultant force and moment are necessary, because neither u_n nor y can contain constant terms or terms proportional to x, for these would correspond not to deflexions but to a translation or rotation of the beam as a whole.

Substituting the values of y and ϕ given by (8) in equation (5), we have

$$\ddot{\alpha}_n + w_n^2 . \alpha_n = a_n. \quad . \quad . \quad . \quad . \quad . \quad (9)$$

The solution of this equation is

$$\alpha_n(t) = \frac{1}{w_n}\int_0^t a_n(\xi) . \sin w_n(t-\xi)\, d\xi + \alpha_n(0) . \cos w_n t + \frac{\dot{\alpha}_n(0)}{w_n} \sin w_n t,$$

$\alpha_n(0)$, $\dot{\alpha}(0)$ being the values of α_n, $\dot{\alpha}_n$ when t is zero. Whence, by substitution in the first equation of (8),

$$y(x, t) = \sum_n \frac{u_n(x)}{w_n}\int_0^t d\xi_1 \int \phi(\xi_2, \xi_1) . u_n(\xi_2) . \sin w_n(t-\xi_1) . d\xi_2 + \sum_n u_n(x) \int \sigma(\xi) . y(\xi, 0) . u_n(\xi) . d\xi . \cos w_n t + \sum_n \frac{u_n(x)}{w_n} \int \sigma(\xi) . \dot{y}(\xi, 0) . u_n(\xi) . d\xi . \sin w_n t, \quad (10)$$

where $y(x, o)$ = initial distribution of deflexions, $\dot{y}(x, o)$ = initial distribution of velocity of deflexions *relative to mean axes.*

This expression (10) is the complete formal solution of the problem of the free beam when the motion in pitch is small. It is also the solution for a beam anchored in any manner, the normal functions and frequencies, u_n, w_n, being in this case those appropriate to the boundary conditions.

4. *Strain Energy.*

For many purposes it is convenient to have an expression for the total energy of deformation at any instant. To obtain this it will be assumed that the initial deformation and velocities of deformation are zero. Then U, the kinetic energy of deformation, is given by

$$2\mathrm{U} = \int \sigma \left(\frac{dy}{dt}\right)^2 dx = \sum_n \left\{ \int_0^{\mathrm{T}} dt \int \phi(x, t) . u_n(x) . \cos w_n(\mathrm{T}-t)\, dx \right\}^2 . \quad . \quad (11)$$

The strain energy of deformation, V, is given by

$$2\mathrm{V} = \int \mathrm{EI} \left(\frac{d^2y}{dx^2}\right)^2 dx. \quad . \quad . \quad . \quad . \quad (12)$$

This can be evaluated from (10) by using the relations

$$\left.\begin{aligned}\int \mathrm{EI}\,\frac{d^2}{dx^2}u_n(x).\,\frac{d^2}{dx^2}u_m(x)\,dx &= 0, \text{ if } m\neq n\\ &= w_n, \text{ if } m=n.\end{aligned}\right\} \quad (13)$$

These, like the normal relations (7), are a consequence of the fact that the modes of free vibration can be derived from the variational problem

$$\int\left\{\mathrm{EI}\left(\frac{d^2y}{dx^2}\right)^2+\sigma\left(\frac{dy}{dt}\right)^2\right\}dx = \text{minimum}.$$

From (13), (12), and (10) we have

$$2\mathrm{V}=\sum_n\left\{\int_0^{\mathrm{T}}dt\int\phi(x,\,t).u_n(x).\sin w\,(\mathrm{T}-t)\,dx\right\}^2. \quad (14)$$

The total energy of deformation, W, can therefore be written as

$$\mathrm{W}=\mathrm{U}+\mathrm{V}=\frac{1}{2}\sum_n\left\{\int_0^{\mathrm{T}}dt\int\phi(x,\,t).u_n(x).e^{iw_n\mathrm{T}-t)}\,dx\right\}\times\left\{\int_0^{\mathrm{T}}dt\int\phi(x,\,t).u_n(x).e^{-iw_n(\mathrm{T}-t)}\,dx\right\}, \quad (15)$$

or

$$\mathrm{W}=\sum_n\left\{\int_0^{\mathrm{T}}dt_1\int_0^{t_1}dt_2\iint\phi(x_1,\,t_1).\phi(x_2,\,t_2).u_n(x_1).u_n(x_2).\times\cos w_n(t_1-t_2)\,dx_1\,dx_2\right\}, \quad . \quad . \quad . \quad (15a)$$

or

$$\mathrm{W}=\frac{1}{2}\sum_n\left\{w_n{}^2\alpha_n{}^2+\dot{\alpha}_n{}^2\right\}, \quad . \quad . \quad . \quad (15b)$$

where α_n is the coefficient of $u_n(x)$ in the expansion for $y(x)$.

In the same way can be derived an expression for the strain energy of the beam when deformed by a static load. The "static loading" of an unsupported beam has no direct significance, but it will be defined as in § 2 —that is, the applied load is supposed balanced by a distributed reaction that would produce, in the absence

of the applied load, motion of the beam without deformation. The deflexion is then given by (1)

$$y(x) = \int G(x_1, \xi) . F(\xi) . d\xi$$

$$= \sum_n \frac{u_n(x)}{w_n^2} \int F(\xi) . u_n(\xi) \, d\xi \quad . \quad . \quad . \quad . \quad (16)$$

from (6);

whence

$$2V = \int EI \left(\frac{d^2y}{dx^2}\right)^2 dx$$

$$= \sum_n \left\{ \frac{1}{w_n} \int F(x) . u_n(x) . dx \right\}^2 . \quad . \quad . \quad (17)$$

from (13).

5. *The Upper Limit of the Energy due to Transient Loading.*

The calculation of the deflexions of beams due to transient loads, and equivalent quantities in mechanics and electricity, is complicated by the integration with respect to the time in equation (10)—that is, by the product of composition of the loading with the sine of appropriate frequencies.

It would be useful to have some method of comparison by which it could be said that the deflexions or the energy of the beam due to a given transient load cannot exceed that due to a certain static load. Of this kind is the well-known statement that "The deflexion due to a load suddenly applied is twice that due to the same static load."

This statement is a particular case of a rule now to be proved. The rule is applicable to all linear systems, but is especially appropriate to unsupported mechanical systems, for with them the applied loads are necessarily variable in time, since the loads must have at least a definite duration.

The "static loading" of an unsupported system will be defined as in §§ 2 and 4, the applied load being supposed balanced by a reaction that would of itself produce motion without deformation.

In this case the deflexion due to a load F at ξ will be

$$y(x)=\overline{F}\sum_n \frac{u_n(x).u_n(\xi)}{w_n^2},$$

and the strain energy will be

$$V=\frac{\overline{F}^2}{2}\sum_n \frac{u_n^2(\xi)}{w_n^2} \quad \text{from (16) and (17).}$$

If then $F(t)$ is the transient load at ξ, the strain energy due to it will be less than that due to the " static " load F, if

$$\overline{F} \geqslant \left| \int_0^t F(T).w_n \sin w_n(t-T).dT \right|$$

for all values of n. . (18)

To find $\overline{F}$ split up the range of integration into parts bounded by the initial and final instants and by those instants at which the force has a maximum or minimum with respect to the time. In each of these durations the force will be always increasing or always decreasing. Applying the second mean value theorem of the integral calculus to such a subdivision, we have

$$\int_{t_1}^{t_2} F(T).w \sin w(t-T).dT$$

$$= \left\{ F(t_1)\int_{t_1}^{\tau} + F(t_2)\int_{\tau}^{t_2} \right\} w \sin w(t-T)\,dt,$$

where τ has some definite value between t_1 and t_2,

$$= F(t_1)\left[\cos w(t-T) \right]_{t_1}^{\tau} + F(t_2)\left[\cos w(t-T) \right]_{\tau}^{t_2}.$$

Hence

$$\left| \int_{t_1}^{t_2} F(T).w \sin w(t-T)\,dT \right| \leqslant 2\left| F(t_1) \right| + 2\left| F(t_2) \right|$$

for all values of w. . (19)

Adding the results of all the subdivisions,

$$\left| \int_0^t F(T).w \sin w(t-T)\,dT \right| \leqslant 2\left| F(0) \right|$$

$$+ 4\sum_m \left| F(t_m) \right| + 2\left| F(t) \right| = \overline{F}, \quad \text{say,} \quad (20)$$

where $F(t_m)$ are the maximum or minimum values of F(T), excluding the values at the initial and final instants.

This upper value, $\bar{F}$, may be in certain cases very drastic; for instance, if there is a slight and rapid ripple in time of the force at every point all the maxima and minima must be included, and $\bar{F}$ will consequently be enormous. This arises from the fact that there is, *à priori*, nothing to guarantee that the ripple does not coincide with a period of free vibration, when there would be resonance. In this case, however, the upper limit can be drawn more closely by means of the following device.

The form of (10) shows that the Principle of Superposition is valid in this problem. Therefore the effect of the force at any point can be regarded as the sum of the effects of any parts into which it may be convenient to divide it. The force-time curve at any point can therefore be expressed as the sum of several successively "smoothed" curves, each of which represents the deviation from the smoother curve following it. Thus in the case mentioned the ripple is first smoothed out, and (20) is applied to the amplitudes relative to the smooth curve, giving a maximum value $\bar{F}_1$. The smooth curve is then smoothed relative to any waviness it may possess, and (20) is applied to its amplitudes relative to this smoothed curve, giving $\bar{F}_2$, and so on. This process is applied to all points of the beam, and the maximum value of the strain energy can then be found from (17), where $F(x)=F_1(x)+F_2(x)+\ldots$, etc. The value of $\bar{F}$ will still depend on the number of maxima and minima, for the possibility of resonance remains.

A common method of estimating the stresses in the case of unsupported structures, used in practical engineering, is to calculate the general motion of the structure as if it were rigid, and then to estimate the stresses as if they were due to the applied forces and the reversed inertia forces of the rigid body motion. The comparison theorem just proved shows that this method may be seriously in error unless the applied forces are monotonic in time, a conclusion that is confirmed by common sense.

6. *Practical Deficiencies of the Theory.*

So far the rotational inertia due to deformation and the deflexion due to shear have been neglected. In theory at least these could be allowed for without any alteration

of the method. There are implicit assumptions, however, that make caution necessary in practical applications.

The assumption that the deflexions are small is nearly always correct in technical applications, but the implication that the dispersion of the material of the beam is such that the speed of propagation increases without limit with the frequency of the disturbance cannot be correct; for not only does internal damping predominate at high frequencies, but physical and, in particular, engineering structures have periodicities that act as filters.

Equally fundamental defects are shown up by a consideration of the effect of an impulse. It will be found that, though the deflexions are everywhere finite, the total energy is not. There will be a cusp at the point of application of the impulse. Impulses are not physically possible, for when applied to non-rigid and continuous bodies they imply a source of infinite energy, but the strain energy of the beam increases rapidly with a decrease of the regions of space and of time over which a blow of given momentum acts. The conclusion is that the macroscopic effects of a load confined within microscopic limits of space and time cannot be determined without the taking into account of the actual stress distribution due to the load in the region where it acts.

Actual experience confirms that the effects of such loads are localized and almost independent of the flexural stiffness and boundary conditions.

References.

(1) A. N. Lowan, "The Transverse Oscillations of Beams under the Action of Moving Variable Loads," Phil. Mag. xix. no. 127 (March 1935).

(2) H. Lamb, 'Higher Mechanics' (Cambridge, 1920).

Farnborough, Hants,
July 1936.

LVIII. *The Vibrations of a Face-centred Cubic Lattice.* *By* C. Strachan, *Department of Natural Philosophy, University of Aberdeen* *.

IN theoretical investigations of phenomena occurring at the surface of a solid it is often necessary to find the sum over all the normal modes of vibration

* Communicated by Prof. J. E. Lennard-Jones.

of a crystal of a function of these modes. An example which occurs frequently is the function which gives the probability that the oscillator corresponding to a normal mode will emit or absorb a quantum of energy. A type of crystal of great practical interest is the face-centred cubic lattice. The general theory of crystal lattices as developed by Born and others * can be applied, but a somewhat different analysis has advantages which will be mentioned later.

The rectangular coordinates of the atoms in the face-centred lattice may be written $(l_1a,\ l_2a,\ l_3a)$, where a is a constant length and $l_1,\ l_2,\ l_3$ are of the forms $(2m_1,\ 2m_2,\ 2m_3)$, $(2m_1,\ 2m_2+1,\ 2m_3+1)$, $(2m_1+1,\ 2m_2,\ 2m_3+1)$, $(2m_1+1,\ 2m_2+1,\ 2m_3)$, $m_1,\ m_2,\ m_3$ being positive or negative integers or zero.

In the usual notation the increase of potential energy for small displacements $\mathbf{u}^l$ of the atom $(l_1,\ l_2,\ l_3)$ may be written †

$$\Phi_2=-\tfrac{1}{2}\mathop{\mathrm{S}}_{ll'}\sum_{xy}(\phi^{l-\nu})_{xy}\mathbf{u}_x^l\mathbf{u}_y^{l'}, \quad . \quad . \quad . \quad . \quad . \quad (1)$$

since the linear terms vanish in the neighbourhood of the equilibrium position. In (1)

$$(\phi^{-l})_{xy}=(\phi^l)_{xy}. \quad . \quad . \quad . \quad . \quad . \quad . \quad . \quad (2)$$

The kinetic energy is

$$\mathrm{T}=\tfrac{1}{2}\mathop{\mathrm{S}}_{l}\sum_{x}m(\dot{\mathbf{u}}_x^l)^2, \quad . \quad . \quad . \quad . \quad . \quad . \quad (3)$$

m being the mass of an atom. We suppose that all the atoms are the same. Then the equations of motion are

$$m\ddot{\mathbf{u}}_x^l-\mathop{\mathrm{S}}_{l'}\sum_{y}(\phi^{l-l'})_{xy}\mathbf{u}_y^{l'}=0, \text{ etc.} \quad . \quad . \quad . \quad (4)$$

As an assumption which is justified by each atom being situated with regard to its neighbours in exactly the same way as any other, we take as solution

$$\mathbf{u}^l=\frac{\mathbf{C}}{\sqrt{m}}e^{-i\omega t+i(l,\,\phi)}; \quad (l,\phi)=(l_1\phi_1+l_2\phi_2+l_3\phi_3). \quad (5)$$

* *Cf.* Lennard-Jones and Strachan, Proc. Roy. Soc. A, vol. cl. p. 442 (1935); Lennard-Jones and Devonshire, *ibid.* vol. clvi. p. 6 (1936).

† Born, *Enc. der Math. Wiss.* vol. v. pt. 3, p. 527; Waller, *Uppsala Univ. Arsskrift.* (1925).

Writing

$$\phi_1=\tau(\mathbf{s}, \mathbf{a}_1), \quad \phi_2=\tau(\mathbf{s}, \mathbf{a}_2), \quad \phi_3=\tau(\mathbf{s}, \mathbf{a}_3),$$

where $\mathbf{s}$ is a unit vector in the direction of the wave-normal corresponding to (5), and $\mathbf{a}_1$, $\mathbf{a}_2$, $\mathbf{a}_3$ are vectors of length a in the directions of the axes, (5) becomes

$$\mathbf{u}^l=\frac{\mathbf{C}}{\sqrt{m}}e^{-i\omega t+i\tau(\mathbf{s}, l_1\mathbf{a}_1+l_2\mathbf{a}_2+l_3\mathbf{a}_3)}.$$

Thus $\lambda=2\pi/\tau$, $(\mathbf{s}, \mathbf{a}_1)=a\cos\alpha$, etc., where α, β, γ are the angles between the wave-normal and the axes. Then

$$\sqrt{(\phi_1^2+\phi_2^2+\phi_3^2)}=\tau a,$$

and, by analogy with elastic waves in a continuum, the frequency

$$\nu=\frac{c}{\lambda}=\frac{c\tau}{2\pi}=\frac{c}{2\pi a}\sqrt{(\phi_1^2+\phi_2^2+\phi_3^2)}, \quad . \quad . \quad (6)$$

c being the velocity of the wave.

From (4) and (5)

$$\omega^2\mathbf{C}_x+\Sigma(x, y)\mathbf{C}_y=0, \quad \text{etc.}, \quad . \quad . \quad . \quad . \quad (4a)$$

where

$$(x, y)=\frac{1}{m}\mathrm{S}_l(\phi^l)_{xy}e^{-i(l, \phi)}. \quad . \quad . \quad . \quad . \quad (7)$$

By (2) the coefficients of (4 a) are real, so that the $\mathbf{C}$ are real. Choose $\mathbf{C}$ for purposes of normalization, so that

$$\mathbf{C}_{1x}\mathbf{C}_{1y}+\mathbf{C}_{2x}\mathbf{C}_{2y}+\mathbf{C}_{3x}\mathbf{C}_{3y}=\delta_{xy}, \quad . \quad . \quad . \quad . \quad (8)$$

where $\mathbf{C}_1$, $\mathbf{C}_2$, $\mathbf{C}_3$ are the three vectors which are solutions of equations (4 a) corresponding to values ω_1^2, ω_2^2, ω_3^2 of ω^2 which make (4 a) consistent. From (4 a) and (8) it follows that

$$\omega_1^2\mathbf{C}_{1x}\mathbf{C}_{1y}+\omega_2^2\mathbf{C}_{2x}\mathbf{C}_{2y}+\omega_3^2\mathbf{C}_{3x}\mathbf{C}_{3y}=-(x, y). \quad . \quad . \quad (9)$$

Since $\omega(\phi)=\omega(-\phi)$ the following standing waves are possible :

$$\left.\begin{aligned}\mathbf{u}^l&=\frac{\mathbf{C}_j}{\sqrt{m}}\cos(l, \phi)e^{-i\omega_j t},\\ \mathbf{u}^l&=\frac{\mathbf{C}_j}{\sqrt{m}}\sin(l, \phi)e^{-i\omega_j t},\end{aligned}\right\} \quad j=1, 2, 3. \quad . \quad . \quad (10)$$

Suppose that $2k\pi$ is the periodicity of (x, y). Then $k_1l_1+k_2l_2+k_3l_3$ is an integer for all possible l_1, l_2, l_3. If the latter could take all integral values then it would be necessary for k_1, k_2, k_3 to be integers, and, as usual *, we should obtain all possible solutions of $(4\,a)$ by restricting the values of ϕ_1, ϕ_2, ϕ_3 to lie in the phase-cube $-\pi<\phi_1,\ \phi_2,\ \phi_3<\pi$. Here, however, the fact that $l_1+l_2+l_3$ is always even introduces a modification of the domain of ϕ_1, ϕ_2, ϕ_3. Taking values $(2m_1, 2m_2, 2m_3)$, $(2m_1, 2m_2+1, 2m_3+1)$ of l_1, l_2, l_3, we see that k_2+k_3 must be an integer. Similarly for k_3+k_1, k_1+k_2. If

$$k_1=\text{integer}+f,$$

Fig. 1.

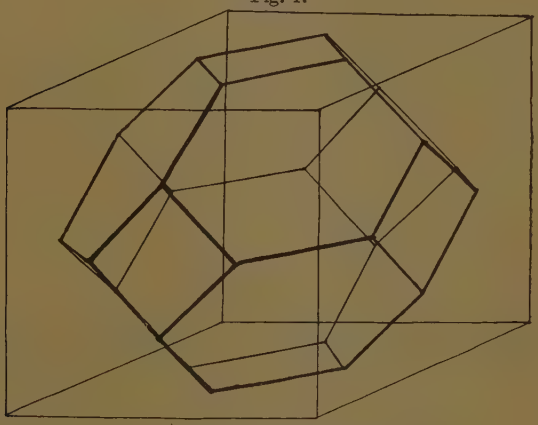

The phase-figure and phase-cube.

where $0\leqslant f\leqslant 1$, then

$$k_2=\text{integer}-f,\ k_3=\text{integer}-f,$$

and since k_2+k_3 is an integer, $f=1/2$. If we increase ϕ_1, ϕ_2, ϕ_3 each by π the increase in $(l,\ \phi)$ is an even multiple of π, and no other increase gives the necessary periodicity of the coefficients of $(4\,a)$ except one of 2π for ϕ_1, ϕ_2, ϕ_3. Hence we must restrict the domain of ϕ_1, ϕ_2, ϕ_3 to the regions of the phase-cube for which

$$\pm\phi_1\pm\phi_2\pm\phi_3\leqslant\frac{3\pi}{2}.$$

Fig. 1 shows the phase-figure.

* Born, Waller, *loc. cit.*

Adopting Waller's notation, we write

$$\mathbf{v}_j^{l\phi}=\mathbf{C}_{j\phi}\cos(l,\phi)\,;\quad \mathbf{w}_j^{l\phi}=\mathbf{C}_{j\phi}\sin(l,\phi),\quad .\quad . \quad (11)$$

the suffix ϕ indicating the dependence of $\mathbf{C}_j$ on ϕ. It is easily verified that the substitution

$$\mathbf{u}_l=\sum_{\phi}{}'\sum_j(\mathbf{v}_j^{l\phi}a_{\phi j}+\mathbf{w}_j^{l\phi}b_{\phi j})\ *\quad .\quad .\quad .\quad .\quad (12)$$

transforms (1) and (3) into

$$\mathrm{T}=\frac{1}{2}\left(\frac{m\mathrm{N}}{2}\right)\sum_{\phi}{}'\sum_j(\dot{a}_{\phi j}^2+\dot{b}_{\phi j}^2),\quad .\quad .\quad .\quad (1a)$$

$$\Phi_2=\frac{1}{2}\left(\frac{m\mathrm{N}}{2}\right)\sum_{\phi}{}'\sum_j\omega_{\phi j}^2(a_{\phi j}^2+b_{\phi j}^2),\quad .\quad .\quad (3a)$$

provided that †

$$\left.\begin{aligned}\sum_l\sum_x\mathbf{v}_{jx}^{l\phi}\mathbf{v}_{j'x}^{l\phi'}&=\frac{\mathrm{N}}{2}\delta_{\phi\phi'}\delta_{jj'},\\ \sum_l\sum_x\mathbf{w}_{jx}^{l\phi}\mathbf{w}_{j'x}^{l\phi'}&=\frac{\mathrm{N}}{2}\delta_{\phi\phi'}\delta_{jj'},\\ \sum_l\sum_x\mathbf{v}_{jx}^{l\phi}\mathbf{w}_{j'x}^{l\phi'}&=0,\end{aligned}\right\}\quad .\quad .\quad .\quad .\quad (13)$$

where N is the number of atoms in the lattice.

To prove the relations (13) we distribute G^3 points in the phase-cube at the points

$$\phi_1=(p_1+\tfrac{1}{2})\frac{2\pi}{\mathrm{G}}-\pi,\qquad p_1=0,\,1,\,\ldots\,\mathrm{G}-1,\ \text{etc.},\quad (14)$$

where $\mathrm{G}^3=2\mathrm{N}$.

It is equivalent to (13) to prove that

$$\sum_j\sum_{\phi}{}'(\mathbf{v}_{jx}^{l\phi}\mathbf{v}_{jy}^{l'\phi}+\mathbf{w}_{jx}^{l\phi}\mathbf{w}_{jy}^{l'\phi})=\frac{\mathrm{N}}{2}\delta_{xy}\delta_{ll'}.\quad .\quad .\quad (13a)$$

By (8) and (11) this is equal to

$$\sum_j\sum_{\phi}{}'(\mathbf{C}_{j\phi x}\mathbf{C}_{j\phi y}\cos(l-l',\phi)=\delta_{xy}\sum_{\phi}{}'\cos(l-l',\phi).\quad (15)$$

* Σ' denotes summation over the values (14) of ϕ_1, ϕ_2, ϕ_3 lying in one-half of the phase-figure (Waller, *loc. cit.* p. 14).

† The normalization conditions (8) differ from those of Waller.

As mentioned above Σ'_{ϕ} implies summation over half of the phase-figure, since, as Waller pointed out, that is sufficient to give all the independent normal modes. Consider OD′ in fig. 2, an octant of the phase-figure. The plane EGH separates those parts of the phase-cube which belong to the phase-figure from those which do not. Thus, for example, the tetrahedron OAEK belongs to the phase-figure, while D′B′GH does not. For every point

Fig. 2.

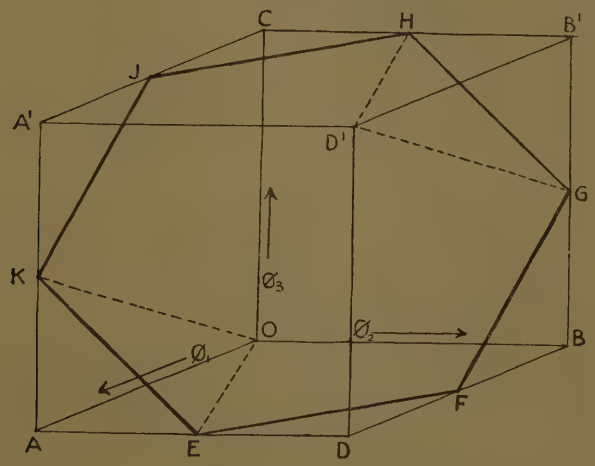

An octant of the phase-figure.

ϕ_1, ϕ_2, ϕ_3 in the former we get a point $\pi-\phi_1$, $\pi-\phi_2$, $\pi-\phi_3$ in the latter, as is evident from (14). The values of $\cos(l,\ \phi)$ and $e^{i(l,\ \phi)}$ for these points are equal, since $l_1+l_2+l_3$ is even. Also the two tetrahedra have equal volumes. Similar results hold for the pairs of tetrahedra D′DEF, OCHJ and OBGF, D′A′JK. Also the volumes of OEFGHJK and D′EFGHJK are equal, and for each point ϕ_1, ϕ_2, ϕ_3 in the former we have a corresponding point $\pi-\phi_1$, $\pi-\phi_2$, $\pi-\phi_3$ in the latter, giving the same values for $\cos(l,\ \phi)$ and $e^{i(l,\ \phi)}$. The volume of the phase-

figure is therefore one-half of that of the phase-cube, *i. e.*, is $4\pi^3$, and

$$\sum_{\phi}' e^{i(l,\phi)} \quad \text{over half of the phase-figure}$$

$$= \tfrac{1}{2} \sum_{\phi}' e^{i(l,\phi)} \quad \text{over half of the phase-cube}$$

$$= \tfrac{1}{4} \sum_{\phi} e^{i(l,\phi)} \quad \text{over the whole of the phase-cube}$$

$$= \tfrac{1}{4} e^{\frac{i\pi}{G}(l_1+l_2+l_3)} \sum_{p_1,p_2,p_3=0}^{G-1} e^{\frac{2\pi i}{G}(p_1 l_1 + p_2 l_2 + p_3 l_3)}.$$

This is zero unless l_1, l_2, l_3 are integral multiples of G. In the summations with which we deal l_1, l_2, l_3 are the differences in the l values of two atoms in the lattice. Since there are $G^3/2$ atoms in the lattice and a cube of side $2a$ contains four atoms the number of cubes of side a in the lattice is G^3. Hence l_1, l_2, l_3 must each be less than G. The above is therefore zero unless $l_1=l_2=l_3=0$. When this is so the sum becomes one-quarter of the number of points in the phase-cube $=G^3/4=N/2$ *. The sum we have just evaluated is found necessary in the reduction of the potential energy to the sum of squares, and if we take the real part of the summation we have proved (13 a).

The face-centred lattice can of course be treated as a simple lattice with its fundamental cell rhombohedral. The above method, however, has the advantage that, in problems in which the solid has to provide one quantum of definite energy †, the normal modes which can supply this quantum are represented by points lying about the surface of a hemisphere in the phase-figure. This makes the mathematical treatment much simpler. It is also clear how to estimate the energy of the largest available quantum. From equation (6) and fig. 1 the appropriate value of $\sqrt{(\phi_1^2+\phi_2^2+\phi_3^2)}$ is the distance between the points (0, 0, 0) and (0, $\pi/2$, π) in the phase-figure, corresponding to the distance OH in fig. 2. Thus

$$h\nu_{\max} = \frac{hc}{a}\frac{\sqrt{5}}{4}.$$

* When N is very large any points (14) which happen to lie on the faces of the above solid figures will give a negligible contribution to the sum.

† *E.g.*, in the theory of accommodation coefficients, surface adsorption, etc. For references, see, *e.g.*, Lennard-Jones and Strachan, Proc. Roy. Soc. A, vol. cl. p. 442 (1935).

In the case of copper where

$$c = 3{\cdot}984 \,.\, 10^5 \text{ cm./sec.},$$

$$a = 1{\cdot}80 \,.\, 10^{-8} \text{ cm.},$$

$$h\nu_{\max.} = 8{\cdot}095 \,.\, 10^{-14} \text{ ergs.}$$

It may also be mentioned that, when the phase-figure is replaced, for reasons of convenience, by a phase-sphere of equal content *, the alteration in the distribution of phase-points and their corresponding frequencies is less marked for the above figure than for a phase-cube. The radius of this sphere is given by

$$\frac{4\pi}{3}(\phi_1^2+\phi_2^2+\phi_3^2)^{3/2} = 4\pi^3,$$

corresponding to

$$h\nu_{\max.} = 7{\cdot}14 \,.\, 10^{-14} \text{ ergs, for copper.}$$

LIX. *The Radial and Spiral Flow of a Compressible Fluid.* *By* A. M. Binnie, *M.A.*, *and* S. G. Hooker, *D.Phil.*†

Summary.

In the radial or spiral flow of an inviscid compressible fluid two velocity fields are possible, one in which the fluid velocity at infinite radius is zero and the other in which the velocity is everywhere greater than the local velocity of sound, reaching at infinity the maximum possible to a compressible fluid. The former we term convergent flow and the latter expanding flow. Our numerical work refers to air.

In radial flow the velocity distributions for both cases have been computed directly, and it is shown numerically that for convergent flow the method of successive approximations (suggested by G. I. Taylor) converges to the correct result. Taylor's process can never be made to yield the solution for expanding flow, and we have therefore suggested an alternative sequence which will converge under these conditions.

* *E. g.*, in the theory of specific heats; *cf.* also Strachan, Proc. Roy. Soc. A, vol. cl. p. 456 (1935), in particular § 3.

† Communicated by R. V. Southwell, M.A., F.R.S.

It has been supposed that Taylor's process will diverge whenever the fluid velocity exceeds the local speed of sound at any point in the velocity field. This supposition is found to be incorrect in the case of convergent spiral flow. Here there exist regions in which the fluid velocity considerably exceeds the local velocity of sound: yet Taylor's process is shown to yield the correct result.

Radial Flow.

1. *Introduction: Direct Calculation for Convergent Two-Dimensional Flow.*—Radial flow is one of the few special cases of compressible inviscid fluid motion which is completely soluble. If the flow is two-dimensional and derivable from a potential ϕ, the same mass of fluid must cross every circle, and the equation of continuity becomes

$$2\pi r\rho\frac{\partial\phi}{\partial r}=\text{constant}=2\pi r^*\rho^*\left(\frac{\partial\phi}{\partial r}\right)^*, \quad . \quad (1.1)$$

where the variables are functions of r only, ρ being the density at a radius where the fluid velocity is $\partial\phi/\partial r$. The "starred" variables refer to the condition in which the local velocity of sound is just attained by the fluid, or, in other words,

$$\left(\frac{\partial\phi}{\partial r}\right)^*=a^*.$$

Thus (1.1) can be written

$$\frac{\rho}{\rho^*}\mathrm{R}\theta=1, \quad . \quad . \quad . \quad . \quad . \quad . \quad (1.2)$$

where $\mathrm{R}=r/r^*$, and θ is the fluid velocity measured as a fraction of a^*.

The combination of the adiabatic relation $p=\mathrm{A}\rho^\gamma$ with Bernoulli's equation leads to the well-known formula †

$$\frac{\rho}{\rho^*}=\left[1-\tfrac{1}{2}(\gamma-1)(\theta^2-1)\right]^{\frac{1}{\gamma-1}}, \quad . \quad . \quad (1.3)$$

and, eliminating ρ/ρ^* between (1.2) and (1.3), we have

$$\mathrm{R}\theta\left[1-\tfrac{1}{2}(\gamma-1)(\theta^2-1\right]^{\frac{1}{\gamma-1}}=1. \quad . \quad . \quad (1.4)$$

† Durand, 'Aerodynamic Theory,' 1935, vol. iii. p. 223.

In the work which follows we shall be dealing with the flow of air, for which $\gamma=1{\cdot}408$. Equation (1.4) can be regarded as an equation determining a value of R corresponding to a given value of θ. Both the "expanding flow" (in which the velocity is everywhere greater than the local velocity of sound) and the slower converging flow are contained in (1.4), but in this part we are inter-

Fig. 1.

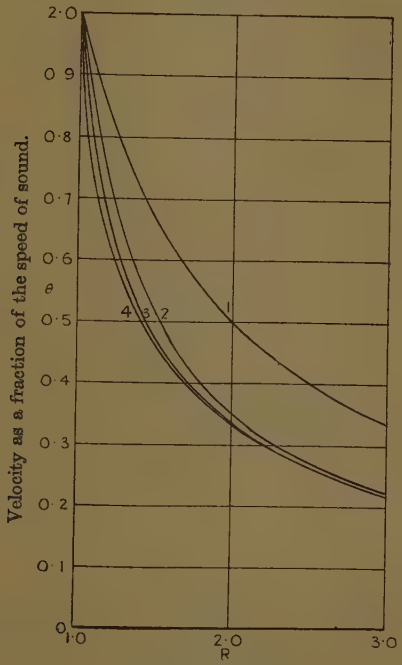

Radial convergent flow.

ested only in the latter, for which θ never exceeds unity. Values of R corresponding to given values of θ in the range

$$1 \geqslant \theta \geqslant 0$$

have therefore been computed from (1.4), and the result is shown by curve 4 in fig. 1.

2. *Successive Approximations for Convergent Two-Dimensional Flow.*—Let us now turn to the mechanical method

for solving problems of two-dimensional flow in compressible fluids which has been developed by G. I. Taylor †. In this apparatus the fluid is represented by an electric current flowing through an electrolyte, and variations in density are represented by proportional variations in the depth of the conducting medium. Taylor proposed a sequence by means of which he could approximate to the flow of a compressible fluid, and deduced from his experiments that the method was convergent so long as the local velocity of sound was not exceeded at any point in the velocity field.

This last condition is realized in the radial flow we have just considered ; so it is of interest to examine numerically (as we can in this particular case) the successive steps of Taylor's sequence.

Taking units of velocity and length as in §(1), the sequence proposed by Taylor, when applied to our problem, can be written in the analytical form

$$\frac{\rho_n}{\rho^*}.\mathrm{R}\theta_n=1, \quad . \quad . \quad . \quad . \quad . \quad . \quad (2.1)$$

$$\frac{\rho_{n+1}}{\rho^*}=\left[1-\tfrac{1}{2}(\gamma-1)(\theta_n^2-1)\right]^{\frac{1}{\gamma-1}}. \quad . \quad . \quad (2.2)$$

The starting form of the sequence (corresponding to $n=1$) is conveniently taken to be the flow of an incompressible fluid, in which case the corresponding density ρ_1 is independent of the speed and $\frac{\rho_1}{\rho^*}=1$. Thus from (2.1)

$$\theta_1=\frac{1}{\mathrm{R}},$$

and, inserting numerical values for θ_1 in (2.2), we deduce from that equation the second distribution of density ρ_2/ρ^*. The use of this result in (2.1) gives us a new velocity distribution θ_2, and the process can be repeated indefinitely.

The successive approximations are shown by the curves numbered 1, 2, 3, 4 on fig. 1. Curve 4 is indistinguishable from the result obtained directly from (1 4). Thus the ideal process suggested by Taylor converges rapidly to the true solution over the whole range of R in the case we are considering.

† Taylor and Sharman, R. & M. 1195, Aug. 1928, and Proc. Roy. Soc. A, Vol. cxxi. (Nov. 1928), p. 194.

3. *Direct Calculation for Two-Dimensional Expanding Flow.*—In this type of flow the velocity is everywhere greater than the local speed of sound, and the pressure and density fall continuously as the radial distance increases. It has been pointed out in §1 that the solution of this expanding flow is also contained in the equation

$$\mathrm{R}\theta\left[1-\tfrac{1}{2}(\gamma-1)(\theta^2-1)\right]^{\frac{1}{\gamma-1}}=1. \quad . \quad (1.4)\,bis$$

As before, it is more convenient to postulate a value of θ in the range

$$1\leqslant\theta\leqslant\sqrt{\frac{\gamma+1}{\gamma-1}},$$

and to calculate from (1.4) the corresponding value of R. When this is done for various values of θ the broken curve shown in fig. 2 is obtained for air. Again, this velocity curve has an infinite slope at $\mathrm{R}=1{\cdot}0$, while no real solution is possible inside this limiting radius.

4. *Successive Approximations for Two-Dimensional Expanding Flow.*—In §2 Taylor's sequence was employed to proceed in steps from the incompressible to the compressible radial flow in which the velocity is zero at $\mathrm{R}=\infty$. A few numerical steps will readily demonstrate that the process is divergent if values of θ greater than unity are assumed, although such a solution exists and can be calculated, as the previous section shows. The experimental work of Taylor and Sharman † suggests that this is a general property of Taylor's sequence, viz., it becomes divergent for those regions in which the local speed of sound is exceeded. No matter what initial approximation is taken the sequence (2.1) cannot be made to converge to the expanding flow solution in which the velocities everywhere exceed the local speed of sound. But it is easy to see that the sequence which will converge to this answer is

$$\frac{\rho_n}{\rho^*}.\mathrm{R}\theta_n=1, \quad . \quad . \quad . \quad . \quad . \quad (4.1)$$

where

$$\theta_{n+1}=\sqrt{1+\frac{2}{\gamma-1}\left(1-\left(\frac{\rho_n}{\rho^*}\right)^{\gamma-1}\right)}. \quad . \quad . \quad (4.2)$$

† *Loc. cit.*

Equation (4.2) is merely the density-velocity relation given in (1.3) transformed so that the velocity is given as a function of the density.

The process is to assume any initial velocity distribution (*e. g.*, $\theta_1=1{\cdot}0$ for all values of R), and then to calculate from (4.1) the corresponding value of ρ_1/ρ^* satisfying

Fig. 2.

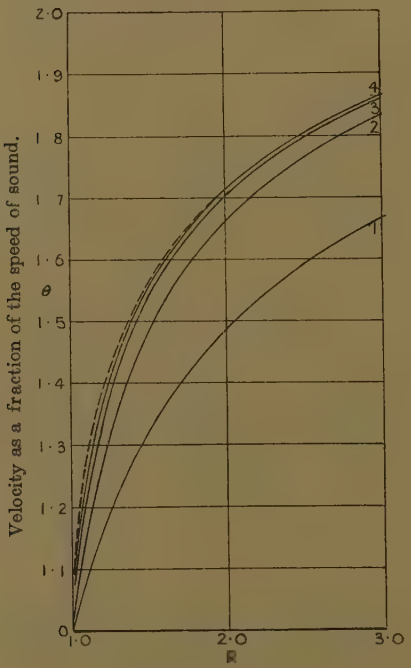

Radial expanding flow.

this equation. Substituting this in (4.2), we obtain new values for θ_2, the second velocity distribution, which can then be put into (4.1) to obtain ρ_2/ρ^*. The cycle can be repeated indefinitely. It will be seen from curves 1–4 in fig. 2, where the successive approximations for air are shown in graphical form, that the process rapidly converges to the correct solution of the expanding flow as calculated from (1.4) in §3.

The condition for convergency appears to be that the velocity must now exceed the local speed of sound. Solutions of this type could therefore be found by the electrical tank developed by Taylor, but the experimental technique would probably be much more difficult. Instead of carving the wax bottom to a specified shape at each step, it would be necessary so to model the bottom that a distribution of potential gradient prescribed by the previous approximation was obtained in the electrolyte. Measurement of the depth of the electrolyte at various points would then give the new velocity distribution to be obtained in the next approximation by recarving the bottom.

Spiral Flow.—Radial Flow combined with Circulation.

5. *Direct Computation.*—This type of flow has been discussed by G. I. Taylor in a lecture to the London Mathematical Society †. The appropriate form, in polar co-ordinates $r\theta$, of the velocity potential is

$$\phi = A\theta + Bf(r), \quad . \quad . \quad . \quad . \quad . \quad (5.1)$$

from which it follows that the velocity, pressure, and density of the fluid are functions of r only, and that the circumferential velocity is independent of compressibility effects.

Taylor discussed the form of $f(r)$ by graphical methods, but a simpler solution of the problem can be obtained by writing the equation of continuity in the form

$$2\pi r \frac{\partial \phi}{\partial r} \rho = \text{constant} = 2\pi r^* \left(\frac{\partial \phi}{\partial r}\right)^* \rho^*$$

or

$$\frac{\rho}{\rho^*} \mathrm{R} . \frac{\partial \phi}{\partial \mathrm{R}} \Big/ \left(\frac{\partial \phi}{\partial \mathrm{R}}\right)^* = 1. \quad . \quad . \quad . \quad (5.2)$$

Considering the case when the stream-lines make an angle of 45° with the circle $r=r^*$, we have the relations

$$\left(\frac{\partial \phi}{r \partial \theta}\right)^* \Big/ \left(\frac{\partial \phi}{\partial r}\right)^* = 1$$

and

$$\left(\frac{\partial \phi}{\partial r}\right)^{*2} + \left(\frac{\partial \phi}{r \partial \theta}\right)^{*2} = 1,$$

† Journ. London Math. Soc. v. p. 224 (1930).

whence it follows that

$$\left(\frac{\partial\phi}{\partial r}\right)^* = \left(\frac{\partial\phi}{r\partial\theta}\right)^* = \frac{1}{\sqrt{2}}. \quad . \quad . \quad . \quad (5.3)$$

The resultant velocity θ is given by

$$\theta^2 = \left(\frac{\partial\phi}{\partial \mathrm{R}}\right)^2 + \frac{1}{2\mathrm{R}^2}, \quad . \quad . \quad . \quad . \quad (5.4)$$

and eliminating $\dfrac{\partial\phi}{\partial \mathrm{R}} \Big/ \left(\dfrac{\partial\phi}{\partial \mathrm{R}}\right)^*$ between (5.2), (5.3), and (5.4), we obtain

$$\frac{\rho}{\rho^*}\sqrt{2\mathrm{R}^2\theta^2 - 1} = 1. \quad . \quad . \quad . \quad . \quad (5.5)$$

Using this equation together with the density-velocity relation (1.3) we can compute values of R corresponding with assigned values of θ, and thus obtain the values shown by the full line in fig. 3. It will be seen that in convergent flow (*i. e.*, when the velocity at infinite radius is zero) a maximum speed 1·22 times that of the local speed of sound is attained at a radius R=0·947. It can be shown that at this limiting condition the radial component of velocity is just equal to the local speed of sound †.

6. *Successive Approximations for Spiral Flow.*—In the previous section it has been demonstrated that the speed of the fluid in convergent spiral flow increases continuously from below to above that of sound with decreasing radial distance. In the particular case worked out it is found that a maximum speed 1·22 times that of sound is attained by the fluid, and it is of interest to see whether Taylor's process of successive approximations will converge for spiral flow in the regions where the speed of sound is exceeded. The sequence to be employed is, evidently, from (5.2)

$$\sqrt{2}\mathrm{R}\left(\frac{\partial\phi}{\partial \mathrm{R}}\right)_n = \frac{1}{\left(\dfrac{\rho}{\rho^*}\right)_{n-1}}, \quad . \quad . \quad . \quad . \quad (6.1)$$

where

$$\left(\frac{\rho}{\rho^*}\right)_{n-1} = \left[1 - \tfrac{1}{2}(\gamma-1)(\theta^2_{n-1} - 1)\right]^{\frac{1}{\gamma-1}},$$

† S. G. Hooker, Ae. Tech. p. 601 (F. M. 62), 1932.

Successive Approximations to Spiral Flow.

R.	0·90.	0·92.	0·94.	0·95.	0·96.	0·97.	0·98.	1·00.	1·05.	1·10.
1st Approximation, θ_1	1·11	1·086	1·065	..	1·040	..	1·02	1·00	0·953	0·91
2nd Approximation, θ_2	1·182	1·137	1·10	..	1·062	..	1·033	1·00	0·928	0·87
3rd Approximation, θ_3	1·24	1·172	1·123	..	1·076	..	1·04	1·00	0·922	0·857
4th Approximation, θ_4	1·31	1·21	1·142	..	1·085	..	1·043	1·00		
5th Approximation, θ_5	1·41	1·248	1·155	..	1·09	..	1·045			
6th Approximation, θ_6	1·58	1·29	1·17	..	1·092	..				
7th Approximation, θ_7			1·182	1·129	1·096	1·068				
8th Approximation, θ_8			1·193	1·135	1·099	1·070				
9th Approximation, θ_9			1·203	1·140	1·101					
10th Approximation, θ_{10}			1·213	1·144						
11th Approximation, θ_{11}			1·224	1·147						
12th Approximation, θ_{12}			1·234	1·149						
13th Approximation, θ_{13}			1·245	1·151						
14th Approximation, θ_{14}			1·256	1·135						

DIVERGENT

CONVERGENT

and

$$\theta^2{}_{n-1} = \left(\frac{\partial\phi}{\partial R}\right)^2_{n-1} + \frac{1}{2R^2}.$$

The numerical values of the successive steps are given in the table, and the corresponding curves are displayed in fig. 3. It will be seen that the process converges at all points to the answer as directly computed—even, let it be noted, in those regions for which the local speed of sound is considerably exceeded by the fluid.

Fig. 3.

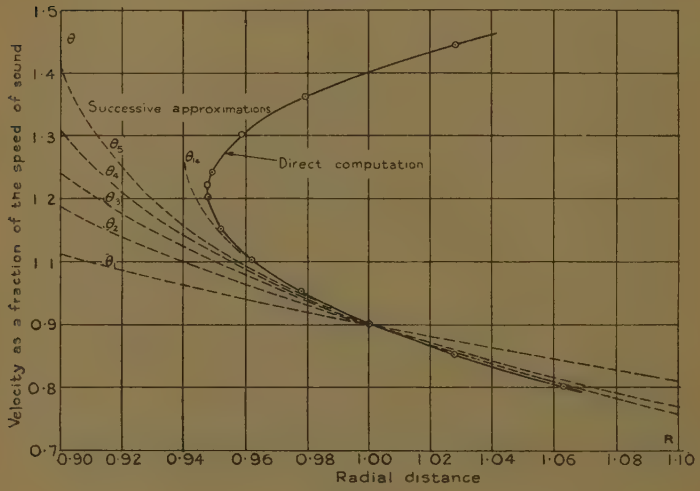

Spiral flow.

Here, then, is a type of flow for which a solution is known to exist involving an increase of fluid speed from below to above that of sound, and for which Taylor's process will converge at all points.

Although we have made no attempt here to pursue the calculations, the sequence of operations suggested in §4 will evidently converge to the expanding spiral flow solution, *i. e.*, to the upper part of the full curve in fig. 3 ; and thus the two processes can be made to cover the full range of velocities, namely, from zero to that corresponding to zero density and pressure of the air.

LX. *A General Proof of Saint-Venant's Principle.*

By J. N. Goodier, *M.A., Ph.D.**

1. THIS principle was enunciated by Saint-Venant as a generalization from experience, and it appears to be generally accepted as purely empirical, although it now plays an important part in the theory of elasticity, and can only be a necessary consequence of some or all of the postulates of that theory. The only published attempt to discover its theoretical foundation is, as far as I am aware, Southwell's [1] discussion of its relation to the theorem of minimum energy in the case of the prism strained by end loads. Saint-Venant was primarily concerned with this problem, and probably it still represents the most important application of the principle. It would now, however, be generally acknowledged that no restriction is necessary as to the shape of the body. Moreover, there can be no vital connection between the principle and Hooke's Law (or any particular stress-strain relation), since the former is certainly valid for materials such as rubber and cast iron, which do not obey the latter, and, in fact, there is every reason to suppose that the principle, especially as cited below in terms of *strain*, continues to hold good beyond failure of elasticity. Evidently it rests on some very general mechanical basis. The argument which follows exhibits it as a simple consequence of the conservation of energy.

2. Love's [2] statement of the principle is: "The strains that are produced in a body by the application to a small part of its surface of a system of forces statically equivalent to zero force and zero couple are of negligible magnitude at distances which are large compared with the linear dimensions of the part."

When such a system of forces is so applied the forces do work by reason of the *relative* displacements of points within the small loaded area. These relative displacements may be looked on as the cumulative effects of strains within the area. The strains are determined by the stress induced in the surface layer, and for reasons of equilibrium this stress has the same order of magnitude

* Communicated by the Author.

as the applied tractions. The relative displacements which such strains can build up within the loaded area must evidently be limited by the smallness of this area, and consequently the work done by the tractions is similarly limited.

The work done is either stored as strain energy within the body or else partly dissipated in plastic strain. In any case the strain cannot have appreciable magnitude throughout an unlimited volume, but only within a volume limited by the smallness of the loaded area—or, otherwise expressed, the strain must have diminished to insignificance at the boundary of some limited region within the body.

3. In order to arrive at an estimate of the size of this region we must have recourse to the relation between stress and strain, and we therefore consider the purely elastic solid. Hooke's Law is not assumed, since we use E to represent not Young's modulus but merely the order of magnitude of the slope of the stress-strain curves of the material.

Let p represent the order of magnitude of the applied surface tractions, a a representative linear dimension of the loaded area. Since the tractions are self-equilibrating, those acting in a definite sense will combine to give a resultant of order pa^2, and those acting in the opposite sense will form an equal and opposite resultant. The points of application of these two forces will be two definite points within or near the area, and we have to evaluate the order of magnitude of their relative displacement.

They will be separated by a distance of order a. The stress induced in the surface layer within the loaded area will, for reasons of equilibrium, be of order p. The associated strains will therefore be of order p/E, and this implies (rigid body rotations being excluded) that all nine components ($\partial u/\partial x$, $\partial u/\partial y$, etc.) of the space-gradient of the displacement will also be of this order. The relative displacement we are concerned with will be the integral of such a space-gradient over a distance of order a, and will therefore be of the order $(p/\mathrm{E}) \,.\, a$.

The order of magnitude of the work done by the tractions is, then,

$$pa^2 \,.\, pa/\mathrm{E} \quad \text{or} \quad p^2a^3/\mathrm{E}.$$

If stress of order p or strain of order p/E exists within the body it contributes to the strain energy an amount of order p^2/E per unit volume. Since the total strain energy is of order p^2a^3/E, it follows that such stress and strain must be limited to a volume of order a^3. This is essentially what Saint-Venant's principle asserts. There is no difficulty in the identification of the volume with the immediate neighbourhood of the loaded area. Equilibrium requires that stress of order p should exist there, and it is impossible that there should be another such region elsewhere. For it could be cut off from the neighbourhood of the load by a surface (of area of order a^2) on which the stress is small. The work done by the stress over this surface represents the energy of the second stress-field, and the latter must consequently be insignificant.

References.

(1) R. V. Southwell, (i.) Phil. Mag. (6) xlv. p. 193 (1923); (ii.) Proc. Roy. Soc. A, vol. cliv. p. 4 (1936).
(2) A. E. H. Love, Math. Theory of Elasticity, p. 131 (1927).

Ontario Research Foundation, Toronto,
July 1936.

LXI. *Sensitiveness of a Geiger Point Counter in the Region between its Threshold Voltage and the Voltage for Constant Counting.* *By* B. Dasannacharya, *M.A., Ph.D., F.Inst.P., Professor of Physics, Benares Hindu University, Benares, and* T. S. Krishna Moorthy, *M.Sc., Benares Hindu University* *.

1. *Introduction.*

As is well known, when the positive voltage applied to the plate of a Geiger point counter is gradually increased, depending on the nature of the gas filling the counter and its pressure, as well as the size and shape of the needle, and the dimensions of the counter, no kicks on the entrance of a particle will be observed in the needle of an electrometer attached to the pointer, until the voltage rises beyond a certain value. This is the threshold voltage for the counter to "speak." As

* Communicated by Prof. A. W. Porter, D.Sc., F.R.S.

this voltage is increased, the number of counts also increase, until a certain value of the voltage is reached, beyond which, up to a certain region of voltage, called the saturation-range of counting, the number of counts remain the same. This number is taken as a quantitative indication of the number of particles that enter. As the voltage is still further raised the counts increase in a very complex way.

The object of the present investigation is to study the way in which the counts vary in the region of voltage between the threshold value and the beginning of the saturation region.

2. *Experimental Procedure.*

A radioactive source (an old radon tube) is moved perpendicularly across the axis of the counter at a certain distance from the counter window. The counts are measured as a function of the distance of the source from the axis. Next, similar measurements are made along lines across different points on the axis. It is found that the counts increase at points on either side of the axis, reach a maximum value, and then, for still greater distances, decrease gradually to a zero value. Certain simple relations are derived connecting the positions and magnitude of the maxima. These measurements are continued for different values of the applied voltage, keeping the counter unaltered in other respects. It is found, that with increase of voltage, the prominence of the maxima compared with the minima on the axis, becomes less and less and disappears entirely beyond a certain value of the voltage. The effect of using different filters, varying in the geometry of the source holder, and of the position of the filters with respect to the source and counter has been tried, on the disappearance of the axial minima.

3. *The Counter.*

The ebonite plug E (see fig. 1, drawn to scale) carries a needle at its centre and closes one end of a brass tube of internal diameter of 1·9 cm. The needle has its tip rounded and was heated to redness before it was fitted in. The inside of the brass tube was polished with sandpaper and cleaned with benzene. The front part of the tube is closed with a brass plate nearly 2 mm.

thick, and has a central circular hole 2·5 mm. in diameter and covered with a thin piece of mica, fixed with shellac varnish. The distance between the tip of the needle and the back of the front brass plate is 1·4 cm. A guard-ring on the inner surface of the ebonite block, and kept connected to the earth, prevents any surface-leaking of charge from the outer plate reaching the central

Fig. 1.

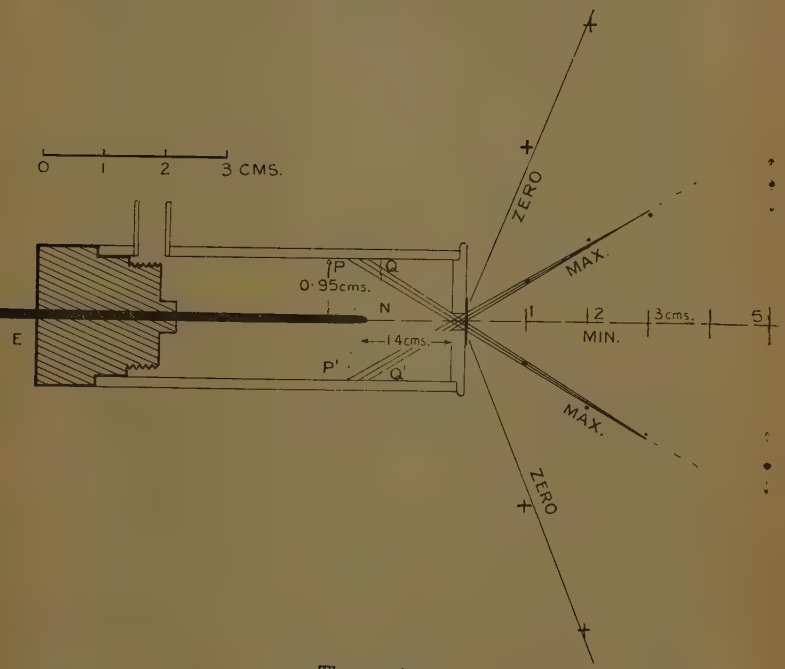

The counter.

needle. The counter is connected permanently with a 10 litre glass bottle containing a little P_2O_5 at its bottom for drying the gas in the counter.

The voltage to the counter is applied through a high water-resistance from a set of accumulator batteries. The needle was connected to a Lindemann electrometer, which, however, was used at its least sensitiveness,

since the voltage surge was quite large. The resistance which connects the needle to the earth is a mixture of alcohol and xylol, with an arrangement to vary the resistance.

4. *The Radioactive Source.*

Four thin-walled capillary tubes, each about 1 cm. long, containing radon. The radon and the short-lived A, B, and C, must have long disappeared, leaving the long-lived RaD and its transformation products E and F in the walls of the capillary. The tubes were mounted with bees'-wax in thin coating on a plate of brass 2·5 cm. diameter and about 5 mm. thick. A plate of lead 1 mm. thick covers the brass holder. A circular opening in the lead plate about 5 mm. diameter lets the rays through. The distance between the radon capillaries and this front opening is about 5 mm. The radioactive source is mounted on sliding supports, and can be moved by known amounts, accurately, along the axis of the counter or at right angles to it.

Results.

5. *Spatial Distribution of Counts.*

Counts are obtained, the voltage remaining the same, at a value slightly above the threshold, while the pressure, namely, 3 cm. Hg, air-filled is kept constant. The variations are only in the positions of the radioactive source. So as to avoid fluctuations of voltage to any great extent, all the measurements were made on the same day. The counts recorded are means per minute, taken in each case for an interval of 5 minutes.

The results are plotted in fig. 2. The abscissæ give the distance x in centimetres of the source from the axis along a line perpendicular to the axis. The distance y in centimetres of this line from the window of the counter, along the axis, is marked on each curve. The ordinates n give the observed number of counts per minute.

With y as 1 cm. the counts rise to a maximum at $x=-0{\cdot}5$ cm. and at $+0{\cdot}8$ cm. Along the axis itself, which is the position for $x=0$, the counts are less. The actual minimum occurs at about $+0{\cdot}3$ with $n=7{\cdot}8$. The maximum values are 12·3 and 10·4.

With $y=2$ cm., the maxima values of n are 3·2 and 2·7 at x, equal to $-1{\cdot}2$ and 1·6 respectively The minimum occurs at 0·4 for $n=1{\cdot}5$.

With $y=3$ cm., the maxima are farther apart and occur at $-2{\cdot}3$ and 1·7 cm. The minimum is not so pronounced for $y=5$, 7, 9, and 13 cm. Axial values for distances 20 and 30 cm. are indicated in fig. 2, they being 1 and 0·6 per min. respectively.

In fig. 1 the positions of the maxima and the zero edges are marked respectively by black dots and crosses, the position of the minima might be taken roughly as

Fig. 2.

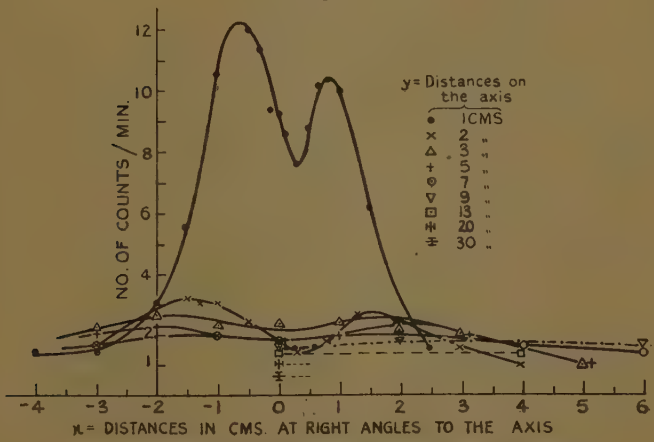

Variation of counts with position of source, voltage remaining constant.

falling on the axis. The positions of maxima fall nearly on a straight line passing through the window of the counter and reaching the cylindrical sides of the counter almost opposite to the needle-point. Similarly, the zero positions roughly fall on a line directed to the centre of the window, but not passing through into the interior of the counter.

6. *Influence of Voltage on the Spatial Distribution of Counts.*

The pressure of the gas remaining the same as before, the voltage is raised by steps and counts are taken, for

positions of the source varied on a cross-line at $y=0{\cdot}65$ cm. All the measurements were taken on a single day, 23rd Feb., 1936. They are illustrated in fig. 3. The values of voltage indicated are approximate, but the relative variations they indicate are correct.

Fig. 3.

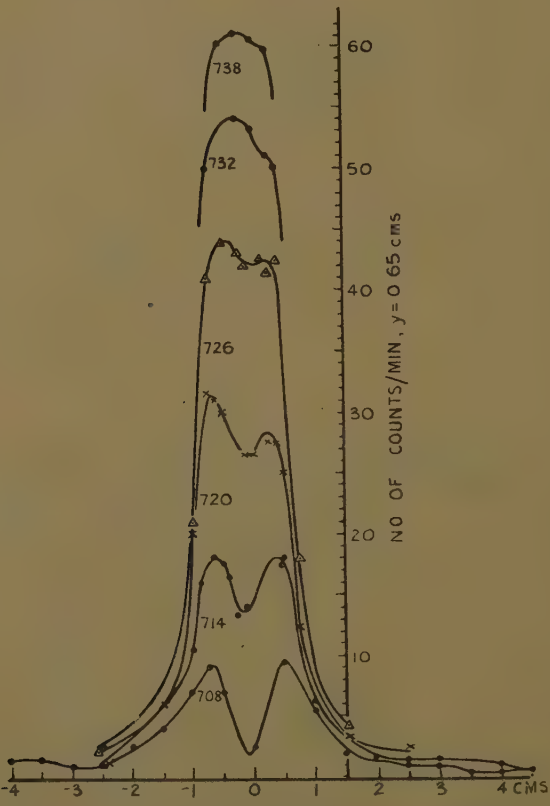

Variation of counts with voltage, $y=0{\cdot}65$ cm. on the axis at 0.

The curve for V=708 volts, shows the minimum in the centre very prominently. In the next curve, 6 volts higher up, the prominence diminishes. It is very small at 720 and 726, is noticeable at 732, but has disappeared

entirely at 738 volts The distances apart of the maxima also show a characteristic variation, and disappear as the voltage is increased to saturation value In fig 4 curves are drawn showing the distances apart of the maxima, as well as the magnitudes of the maxima and minima, in their relation to the corresponding voltages. It will be seen that the zero distance apart, or the disappearance of the minima roughly agrees with the voltage at which saturation value of the counting sets in, viz , at about 745 volts.*

It is now obvious that for certain voltages, the reading of counts along the axis must become nearly zero, with

Fig. 4.

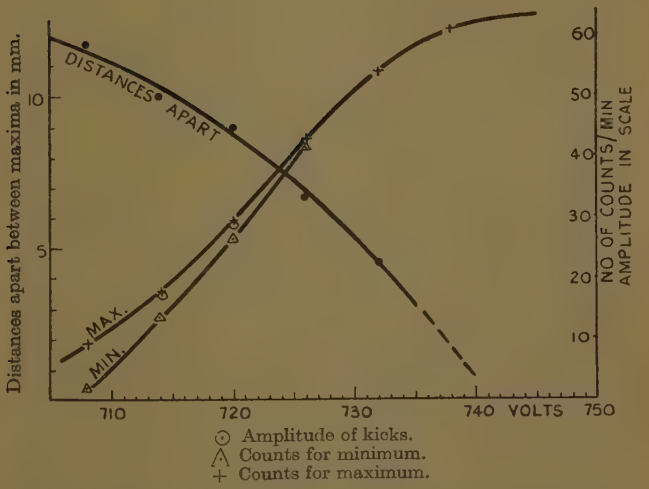

maxima on either side. We wanted also to see further if there will be any change, if the radon tubes, instead of being vertical and arranged in a vertical plane, as they have been mounted so far, are now rotated so that each tube is horizontal but arranged one over the other in

N.B.—*Added in reading Proof* :—

* It is very interesting to note that the amplitude of the kicks is proportional to the voltage above the threshold value, as the line joining the two circles for amplitude would pass roughly through the voltage axis at 705, fig. 4.

a vertical plane. As the counts become less with lowering of voltage the source tubes are brought nearer to the counter window. It is now 4·5 mm. from the window. Fig. 5 shows the result as expected. The rotation of the source tube in the manner described above does not affect the results.

Fig. 5.

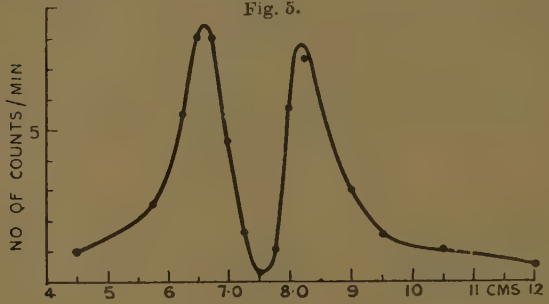

Source rotated by 90°.

7. *Influence of Thin Filters* (*Scattering*).

We had seen in a previous section that the prominence of the minima gets less pronounced as the radioactive source is moved farther and farther away from the window along the axis. Different filters such as paper and aluminium were next tried.

Curves *a*, *b*, *c*, and *d* (see fig. 6) have been taken in the order in which they are written, the arrows show the sequence in which the readings have been taken. In all these cases the value of y remains the same, namely, 0·6 cm. The position of the axis of the counter may be taken as 7·5 cm. on the scale of the carrier of the source which has been drawn as abscissæ. The minima at 7·5 cm. can be seen clearly. The curve *a*, with only a single sheet of foolscap paper as filter on window of the counter, has a pronounced minimum on the axial position. In curve *b*, with four sheets of the same paper as filter, the minimum is less pronounced; further, the maxima on either side have moved nearer to the axis. Curve *c* is for control and taken without any filter. The next curve, *d*, has been taken with four folds of Indian post-card (of about the same thick-

ness as post-cards in any other country) as filter. The minimum has almost disappeared and the maxima have moved nearer to the axis than in previous curves, *b* or *a*. It may further be noted that the intensity of the maxima has not diminished to any appreciable extent as compared to the great change brought about in the minimum.

8. *Explanation of the Phenomenon.*

If we turn to fig. 1 we can mark out a region PQ all round the point N of the needle. From the geometry of the counter it is clear that for a given energy an ion anywhere in the region NPQ has the smallest distance to cover and the chances of its reaching the needle-tip N are greatest, as inside NPQ the field is stronger than anywhere else. The primary particles that pass near the point N must be assumed to be less effective in a trigger action required for a count to be registered than those farther away which get a higher potential drop for their secondary particles before they reach the needle-point. As the needle-point is negative with respect to the outer cylinder, it follows that in a trigger action it is the *positive* ion that is effective.

The filters, by scattering the primary particles at the window, enable them to be effective in that they spread them out nearer to PQ.

It is possible that some small portions of the secondary ions could come from the walls at PQ. These must be small in our case, as otherwise it would required that the distances between the maxima should be independent of the applied voltage.

The filters used by us were placed touching the window so that the scattered particles do get inside the counter. As has actually been verified, filters placed some distance in front of the window are less effective than if they are mounted on the window.

9. *Influence of Thick Filters (absorption).*

Curves *g* and *h* (fig. 6) are with filters of 1 and 2 mm. of Al, respectively, touching the window. In addition to the disappearance of the minima, due to scattering, the effect of absorption in cutting off the particles entering the chamber is perceptible, in that the maxima have diminished in intensity considerably.

The explanation for the powerful scattering without appreciable absorption required from experimental data of curves *a*, *b*, and *d*, is in keeping with the known facts about β-rays *. Similar explanation suffices for the experiments of para. 5, where air space in front of the window is the scatterer.

Fig. 6.

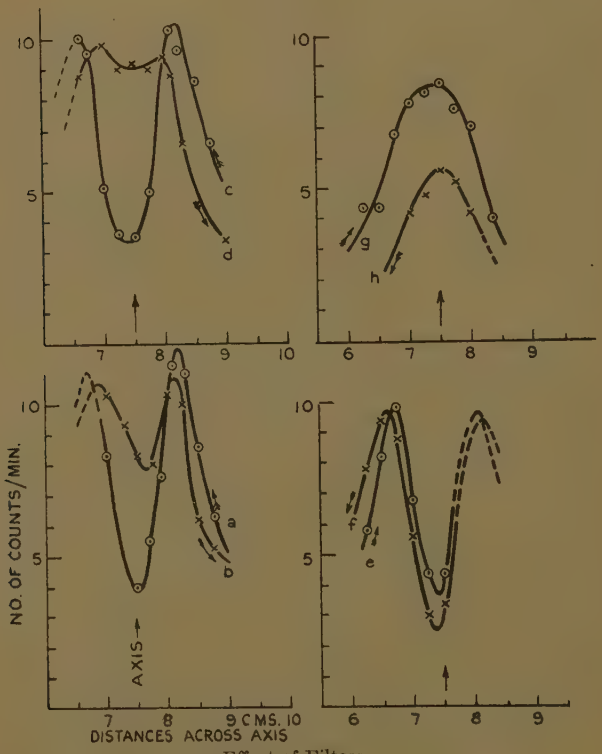

Effect of Filters.

a→ Single sheet of foolscap paper.
b→ Four sheets.
c→ Without filter.
d→ Four folds of postcard.
g→ 1 mm. of aluminium.
h→ 2 „ „
e→ Extension of window with 1 mm. collar of lead.
f→ Collar removed.

* See "Radiations from Radioactive Substances," by Lord Rutherford, Chadwick and Ellis, p. 217. Crowther, Proc. Roy. Soc., A, lxxx. p. 186 (1908); A, lxxxiv. p. 226 (1910).

10. *Influence of Window Sides (scattering).*

Will the wall surface of the opening of the window behind the mica-plate have any effect? A plate of lead nearly 1 mm. thick was placed on the window so that a hole in the lead plate, 3 mm. in diameter, came in front of the entrance hole. Curve *e* shows the result, and curve *f* the result when the lead plate was removed. The minimum is less pronounced and the maximum nearer to the axis of the counter when the lead projection window was in place (curve *e*) than when it was removed, showing the enhanced scattering caused with the lead window projection on. The enhancement is, however, small. In the actual opening behind the mica, the scattering effect must also be small, as otherwise the diminution of the distances between the maxima, as voltage on the counter is increased, would be difficult to explain, and the existence of the maxima, as well as the variation of sensitivity with pressure, support the same conclusion.

11. *Summary and Conclusion.*

The β-ray sensitiveness of a Geiger Point Counter has been investigated between the regions of its threshold value and the commencement of the saturation region. It is found that it depends on the path taken by the ray inside the counter. For positive voltages on the cage of the counter, the farther the path lies from the point (up to a limit depending on the dimensions of the counter) the more effective it is, since the secondary ions released there can acquire a greater energy. As the voltage attains that required for "saturation." the energy of the secondary particles, practically wherever liberated, seems to be enough for giving a count, so that the directional effect becomes negligible and the counts are conditioned only by the geometry of the beam. In this way it has been found possible to explain the experimental observation of regions of very high sensitivity symmetrically about the axis, reaching maximum value at some distance from the axis. The low value on the axis, or the axial dip, gradually disappears as the voltage rises to saturation (see fig. 3, p. 614). Scattering due to the material covering the window and the inner surfaces of the opening tend to lessen the axial dip and bring the maximum nearer the axis of the counter. Thin

sheets of material scatter very efficiently and tend to push the maxima to the axis (fig. 6 *a*, *b*, *c*, *d*). In *g* and *h* the effect of thick sheets of aluminium, 1 and 2 mm. respectively, are seen with the effect of absorption superimposed on that of scattering. The inner surface of the opening of the window is also shown to contribute to scattering (para. 10).

It will be interesting to know if the directional effect exists in other types of counters and also to investigate to what extent it will influence measurements in proportional counters, which work at lower voltages than those used by us.

LXII. *The Effect of Heat Treatment on the Tribo-electric Properties of Quartz and of Metals.* *By* P. A. Mainstone, *M.Sc., F.Inst.P., Lecturer in Physics, University College of North Wales* *.

IN two previous communications † the author has examined in some detail the effect of moderate heat treatment on the production of frictional charges between the polished surfaces of a metal and of a very light rubber of fused quartz. The metal was in most cases palladium, but results were also obtained with nickel and aluminium. The most striking result of such measurements was found to be that with the moderate heat treatment possible (up to about 300° C. or 350° C.) the normal negative charge produced by the friction of quartz on any metal was often reversed in sign in the presence of a small quantity of gas. It was at first believed that this effect was produced only by the presence of hydrogen, and in the case of palladium some correlation between the tribo-electric and photo-electric effects was looked for when the metal was heated in hydrogen. It was subsequently found, however, that the reversal of charge was characteristic of oxygen and not of hydrogen, and that when the former was carefully excluded from the heating chamber the presence of hydrogen made but little difference in the tribo-electric charge.

* Communicated by Professor E. A. Owen, M.A., Sc.D.

† Phil. Mag. xvi. pp. 1083–1096 (1933); xix. pp. 278–290 (1935).

With the heating chamber previously used the temperature range could not easily be extended above 350° C. Moreover, the operation of the rubber through a ground-joint was in some ways inconvenient. A new form of apparatus was therefore devised, in which the rubbing took place inside a tube of " Pyrex " glass which could be inserted into a small heating furnace, the rubbing operation being performed magnetically instead of mechanically.

Apparatus.

The disposition of the apparatus was as shown in fig. 1. The heating tube, about 2 inches in diameter and 15 inches

Fig. 1.

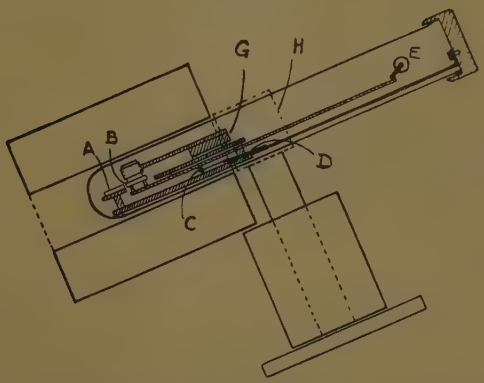

A. Earthed polished plate. B Insulated polished plate. C. Vitreosil plate. D. Steel spring. E. Excentric rod (viewed laterally). G. Carriage with soft iron armature. H. Pole pieces of magnet.

in length, was supported so as to lie at a small angle to the horizontal with its lower end within the heating furnace. The two polished metal surfaces (earthed and insulated respectively) were arranged to lie approximately at the centre of the furnace, while the quartz rubber was operated by an arm attached to a small carriage provided with a soft iron armature. The armature lay near the upper end of the furnace, where it could be excited by the transverse field of a small electromagnet. The carriage, which moved on the inclined surface between two fixed stops, was drawn up by the magnetic field,

and allowed to fall under gravity when the field was switched off. Since a large number of rubs are necessary before any definite value of the charge per single rub can be obtained, an automatic slow make and break, as well as a hand-operated switch, was included in the circuit of the electromagnet.

Much difficulty was experienced both in respect of the insulation necessary for one of the polished metal surfaces and of the efficient magnetic control of the rubber. The ultimate arrangement is shown in fig. 2. The earthed polished surface A is carried on a plate of copper, while the insulated surface B is supported at the end of an aluminium arm attached to an insulating plate C of "vitreosil," the latter thus lying at a cooler part of the tube. By means of a spring D the insulated surface was normally kept a little below the level of the earthed

Fig. 2.

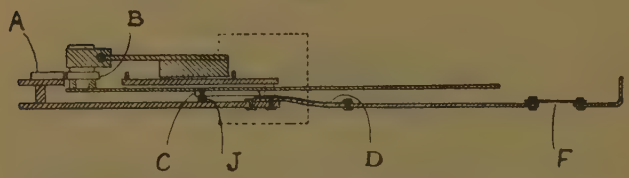

A. Earthed polished plate. B. Insulated polished plate. C. Vitreosil plate, hinged at J. D. Steel spring. F. Mica heat insulator.

surface, but by the pressure of an excentric rod E, operated through a ground-glass joint near the cool end of the tube, the two surfaces could be made exactly coplanar. The rod E also furnished a means of connexion to the electroscope. The carriage carrying the armature was arranged to run on two very small copper rollers, with side strips to prevent lateral motion. When the best adjustment was once obtained the device on the whole gave but little trouble.

The entire holder, which was of copper, was attached by an aluminium strip to a brass cap closing the upper end of the tube, with, however, a short section of mica at F for heat insulation purposes. The joint around the cap was made airtight with plasticine; this could be easily broken and remade, and was found to maintain a high vacuum with no difficulty. Cooling of the exposed

part of the tube was obtained by a wrapping of copper-foil provided with radiating vanes and surrounded by sufficient turns of a water-cooling spiral.

Preliminary Results.

Using palladium surfaces in the first instance it became apparent that when the temperature was raised to the region of 400–450° C. a positive charge appeared even in the best vacuum obtainable, *i. e.*, using an oil-diffusion pump. The surfaces, however, generally showed on removal some contamination, which was obviously due to the contact and the to-and-fro passage of the rubber. This contamination could be in part removed by rubbing with soft leather, but in general the normal negative charge on the metal could only be restored by repolishing both the metal and the quartz.

A brief period of heating to about 300° C. in air or in oxygen always gave a reversal of charge. When the surfaces were allowed to cool in the same atmosphere it was impossible to restore the negative charge by brief periods of heating to 450° C. *in vacuo*. If, however, the air or oxygen was removed immediately after heating the reversal of charge was less marked, and in some cases a negative charge could be restored after a large number of rubs.

In view of the failure to avoid completely any tarnish of the surfaces on heating the quartz rubber itself was removed during the heating and replaced when the surfaces had cooled. The effect was now quite different. Using nickel surfaces these remained untarnished after heating, and the normal negative charge, practically undiminished in value, was still observed. Even after heating in air at a pressure of several centimetres no reversal of charge was found.

The apparatus was modified such that the quartz rubber could be removed from contact with the metal surfaces during heating but restored again on cooling without opening the heating-tube. In some cases the rubber was withdrawn so as to rest on a glass surface, in others it was lifted through 2 or 3 mm. from the metal surfaces. The effect of such separation was very doubtful, a reversal of charge being observed in many cases.

It is clear that the characteristic changes in the frictional charge due to heating are in reality due to

changes on the surface of the quartz, and not on that of the metal, as previously considered. The effect of heating of the quartz surface when separated from the metal surfaces was thus examined as exhaustively as possible.

Effect of Heating of Quartz Surface.

In the first series of measurements the quartz was removed from contact with the metal and placed alongside in an inverted position, so that its rubbing surface was freely exposed. It was then necessary to reopen the tube on cooling in order to restore the rubber to its normal position. The short exposure of the surfaces to the outer air could hardly be regarded as affecting the values of the subsequent charges.

A typical series of results representing the effect of heating *in vacuo* is shown in Table I. During heating

TABLE I.

Charges on Nickel after Heating of Rubber *in vacuo*.

	Charge.
1. Metal and rubber freshly polished	−32
2. Separated surfaces heated at 450° C.	+32
3. All surfaces freshly polished, and heated at 400° C.	+28
4. Quartz freshly polished and surfaces heated at 350° C.	+ 5
5. Quartz freshly polished and surfaces heated at 300° C.	−20

the apparatus was kept exhausted by an oil-diffusion pump, the pressure being observed by a Pirani gauge. The lowest pressure, as given by the calibration of the gauge with a McLeod gauge, was 2×10^{-4} mm. The duration of heating was from one to two hours in each case, and the charge was measured after cooling to room-temperature.

It is clear that the reversal of charge occurs above temperatures in the 300°–350° range, *i. e.*, above the limit of the temperatures reached in the earlier experiments.

The effect of heating in air at a few centimetres pressure was similar, except that the reversal of charge occurred after heating at rather lower temperatures. This was in accordance with the results of the earlier experiments.

Effect of Impurities in the Apparatus.

Even at the lowest pressures reached there were present in the apparatus vapours from the oil-pumps as well as from tap-grease. The former were known to affect

the phosphorus pentoxide present in the apparatus, and it was clearly desirable to know whether the effect of heating of the rubber was due to such vapours. Accordingly an oil-vapour trap cooled by solid CO_2 and ether was introduced between the pumps and the apparatus. Taps near the heating chamber were greased with Apiezon "L" grease, although some of the original grease had in places spread into the connecting tubes of the apparatus, and could not well be removed without cutting down almost the entire apparatus. A separate heating chamber free from this defect was afterwards added.

TABLE II.

Charges on Nickel after Heating of Rubber when Oil-vapour Trap was used.

	Charge.
1. All surfaces freshly polished	−27
2. Separated surfaces heated at 475° C.	+15

This result was approximately verified on repetition, and its significance appears to be clear. The presence of the slight trace of oil vapour is in part, but not entirely, the cause of the change of the quartz surface.

Effect of Heating Quartz in Separate Chamber.

Owing to the presence of impurities referred to above it was felt necessary, as an alternative to rebuilding the apparatus, to add a small extension, comprising heating tube, drying tube, and Pirani gauge, each part of the extension being carefully cleaned before assembling. The extension could be cut off from the original apparatus by a tap, on which Apiezon grease was used, and a second oil-vapour trap was introduced between this tap and the heating tube. Apiezon wax was used for the necessary joints as well as for the metal cap closing the end of the heating tube.

In the first instance a heating tube of Pyrex glass was used, and the quartz was heated up to about 400° C. No appreciable difference from the previous results was observed. Later a silica tube was used, when the temperature could be raised to 800° C In every case in which the temperature was raised above 300° C. the subsequent *in vacuo* charge at room-temperature was positive. The results are summarized in Table III.

It is evident that under the conditions of the experiments it is impossible to prevent changes on the surface of the quartz. As previously mentioned, the lowest pressure as recorded by the Pirani gauge was of the order 10^{-4} mm., although quite possibly it was of a still lower order. Whether the surface films giving rise to these effects are due to adsorbed layers or to gases given off from the quartz itself cannot be decided with certainty. The number of molecules striking the surface at a pressure of 10^{-4} mm. is still very high, but at a temperature of 800° C. the evaporation from the surface must also be very high, and it seems doubtful whether a large part of the surface can be covered with gas due to this case

TABLE III.

Charges on Nickel after Heating Quartz *in vacuo* in Separate Furnace.

Temperature of heating.	Subsequent *in vacuo* charge at room-temperature.
350° C.	+22
500	+15
650	+20
800	+20

alone. It is more likely that gas absorbed by the quartz is only partly liberated at this temperature, and that the slow passage of gas to the surface as the quartz cools may account for the reversal of charge.

Until apparatus is designed in which the quartz can be heated at pressures much below 10^{-4} mm. there seems to be no possibility of eliminating the observed change in its tribo-electric properties.

Effect of Separate Heating of Metal Surfaces.

In view of the behaviour of the quartz surface after heating it was clearly essential to carry out separate heating of the metal surfaces up to temperatures as near the melting-point as possible. The first such measurements were made after heating the low melting-point metals tin, zinc, and bismuth. In each case short periods of heating at gradually increasing temperatures were given, the charge at room-temperature being measured after

each such heating. For each metal the results were very similar. The quartz rubber became considerably contaminated by friction with the soft metal, and the contact between the two became much closer than was usual in the case of a hard metal such as nickel. The movement of the rubber over the metal became slow and difficult, and comparatively large charges were observed. Thus, in the case of tin the *in vacuo* charge rose from −30 on freshly polished surfaces to −40 after heating at a temperature just below the melting-point; in the case of zinc and bismuth the effect of heating gave changes which, although appreciable, bore no resemblance to those obtained in the case of quartz.

TABLE IV.

Metal.	*In vacuo* charge.		Highest temperature reached.
	Before heating.	After heating.	
Tin	−30	−40	225° C.
Bismuth	−20	−35	260
Zinc	−32	−15	400
Aluminium	−23	−30	650
Copper	−27	−15	800
Nickel	−32	−15	800
Palladium	−30	−13	800

Metals with higher melting-points were heated in a silica tube in the extension of the apparatus already referred to, and the same precautions for the elimination of impurities were observed. The metals examined were aluminium, copper, nickel, and palladium, and except in the case of aluminium the highest temperature reached during heating was 800° C. The results are summarized in Table IV.

The contrast between the behaviour of the metals and that of quartz is very marked. It would appear that the metal surfaces are practically unaffected, even at temperatures approaching their melting-points, by the small amounts of gas or vapour present. As already mentioned, heating in a considerable amount of air produced no marked change in some cases. In the case of copper the tribo-electric properties remained unchanged so long as the surface was free from oxidation.

The temperature ranges employed in these investigations might be considerably extended, but it seems unlikely that any markedly different results would be obtained until the changes on the quartz surface are fully understood.

Summary.

1. The tribo-electric property of quartz is normally positive with respect to most metals. After heating at temperatures above 350° C., and at a pressure of 10^{-4} mm., it becomes electrically negative. The technique employed for the removal of impurities during heating has failed to prevent this reversal.

2. The metals tin, bismuth, zinc, aluminium, when heated almost to their respective melting-points, and the metals copper, nickel, palladium, when heated to 800° C., show no reversal of their tribo-electric properties.

LXIII. *The Geodesic Postulate in General Relativity. By* Prof. V. V. Narlikar *and* Jaipat Singh, *Benares Hindu University, India* *.

Abstract.

It is argued that the geodesic postulate is not implicit in the relativity equations. A certain indeterminacy about the motion of the particle in Schwarzschild's solution is indicated. If the field equations are also to give the motion as suggested by Einstein the geodesic postulate must be abandoned, in which case the difficulty still remains whether a singularity in a solution does represent a mass-particle or not. If the geodesic postulate is to be retained, and if at the same time Einstein's suggestion is accepted, then certain tracks must reduce to geodesics in the limit, provided the singularities represent masses. This may serve as a test whether a singularity represents a mass or not.

A MASS-PARTICLE has not yet been successfully introduced into the scheme of general relativity. The geodesic postulate has been tentatively accepted

* Communicated by the Authors.

in order to obtain the motion of a small mass whose disturbing influence is negligible. Since two of the three crucial tests of the general theory are hinged upon the geodesic postulate it may be worth while considering some implications of this postulate and its probable place in a complete theory of relativity.

The first point that has to be emphasized is that the geodesic postulate is not implicit in the relativity equations of gravitation. It may be of some interest to note that Tolman [1], in his recent exposition of relativity, departs from most of the earlier expositions in not deducing the geodesic postulate from the equations

$$(T_\mu^\nu)_\nu = 0. \quad . \quad . \quad . \quad . \quad . \quad . \quad . \quad . \quad (1)$$

An examination of (1) for a perfect fluid for which

$$T_\mu^\nu = (\rho + p)\, g_{\mu\sigma} v^\sigma v^\nu - p g_\mu^\nu \quad . \quad . \quad . \quad . \quad (2)$$

is rather interesting. We have, from (1) and (2),

$$(\rho+p) g_{\mu\sigma} v^\nu (v^\sigma)_\nu + g_{\mu\sigma} v^\sigma [(\rho+p) v^\nu]_\nu - \frac{\partial p}{\partial x^\mu} = 0. \quad . \quad (3)$$

Taking p as negligible compared to ρ, and then

$$[(\rho+p) v^\nu]_\nu = 0, \quad . \quad . \quad . \quad . \quad (4)$$

being the analogue of the hydrodynamic condition of continuity, we obtain

$$g_{\mu\sigma} v^\nu (v^\sigma)_\nu = 0. \quad . \quad . \quad . \quad . \quad . \quad . \quad . \quad (5)$$

Since $g_{\mu\sigma}$, $\mu \neq \sigma$, are of the first order of smallness, while $g_{\mu\sigma}$, $\mu = \sigma$ are finite, we have

$$v^\nu (v^\sigma)_\nu = 0, \quad . \quad . \quad . \quad . \quad . \quad . \quad . \quad . \quad (6)$$

which are the well-known equations of a geodesic. It is true that (1) gives rise to (6) when suitable assumptions are made, but it does not follow at all that a discrete mass moves along a geodesic. What we have proved in deriving (6) is that the flow at any point (x, y, z, t) in a perfect fluid is along a geodesic.

In deducing (6) for a discrete mass one cannot express the energy of a particle by

$$T^{ij} = \rho \dot{v}^i \dot{v}^j \quad . \quad . \quad . \quad . \quad . \quad . \quad . \quad (7)$$

as Eddington [2] and others have done. (7) may describe a particle, provided we define ρ precisely as a function

which is non-zero in the neighbourhood of the track and zero elsewhere. Hence, until the track becomes known the function ρ remains unknown, and so it is fallacious to proceed to obtain the geodesic as the path of a mass-particle from (7). It may be remarked also that in solving the problem of one mass-particle one does not represent the energy by any tensor of the form (7).

In Schwarzschild's solution a discrete particle is given by the hypersurface $r=2m$ in polar coordinates. From this we know about the motion of a particle only this much, that $dr/ds=0$. $d\theta/ds$, $d\phi/ds$ remain unknown, the only relation satisfied by them being

$$1=(2m)^2[d\theta/ds)^2+\sin^2\theta(d\phi/ds)^2]. \quad . \quad . \quad . \quad (8)$$

(8) follows if we put $r-2m=u^2=0$ in the line-element [3]

$$ds^2=-4(u^2+2m)du^2-(u^2+2m)^2(d\theta^2+\sin^2\theta d\phi^2)+\frac{u^2\,dt^2}{u^2+2m} \quad . \quad . \quad . \quad (9)$$

Hence if the motion is to become known from the field equations it must be admitted that the Schwarzschild solution has a degree of indeterminacy in virtue of (8). This feature of Schwarzschild's solution deserves careful study before a solution of the n-body problem is attempted on the lines suggested by Einstein and Rosen [4].

The geodesic postulate seems to us to be important for three of its special features :—(i.) It gives for the path a tensor equation ; (ii.) a geodesic reduces in natural coordinates to an analytical statement of Newton's first law ; and (iii.) a geodesic also gives the analogue of the Newtonian equations of a test-particle in a field of potential V, viz.,

$$\ddot{x}=-\frac{\partial V}{\partial x},\ \ddot{y}=-\frac{\partial V}{\partial y},\ \ddot{z}=-\frac{\partial V}{\partial z} \quad . \quad . \quad . \quad (10)$$

In spite of these three satisfactory features the geodesic postulate seems to be redundant, since, according to Einstein, both matter and motion should be given by the field equations. Thus a solution of

$$g^2R_{\mu\nu}=0 \quad . \quad . \quad . \quad . \quad . \quad . \quad . \quad (11)$$

is expected to give full information about the motion of n particles. Suppose a regular solution of (11) is obtained with n singularities, the field becoming Euclidean at infinity. A singularity does not necessarily mean

a mass-particle. We know *, for instance, that a static axially symmetrical solution is possible with two fixed singularities which cannot certainly represent masses, as they would be accelerated under their mutual interaction. Thus, although a singularity need not necessarily mean a mass-particle, it is generally agreed that a mass-particle is represented by singularity in the field. It may be possible to remove the singularity in the neighbourhood of a particle by a suitable transformation, but in the coordinate system used to represent the field of the particle at a great distance the particle will appear as a singularity. Let the constants m_1, m_2, $\ldots m_n$ be associated with the n singularities in such a manner that when $m_r=0$ the rth singularity disappears. Let the singularity corresponding to m_r be represented by the world-line

$$x=\theta_r(t),\ y=\phi_r(t),\ z=\psi_r(t). \quad . \quad . \quad . \quad (12)$$

Suppose that as $m_r \to 0$ we have in the limit

$$x=\lim_{m_r \to 0} \theta_r(t)=\theta_r'(t), \quad . \quad . \quad . \quad . \quad . \quad (13)$$

and similarly

$$y=\phi_r'(t),\ z=\psi_r'(t).$$

If m_1, m_2, etc. are masses, (13) should give the path of a test-particle introduced into the field of the $n-1$ masses from which m_r is absent. Hence if the geodesic postulate is to be consistent with the idea that the field equations (11) are to give both matter and motion, (13) must be a geodesic in the field of the other $(n-1)$ masses.

The following conclusion is therefore inevitable: either the geodesic postulate must be discarded, or, on grounds of consistency, the identification of (13) with a geodesic in the field of the remaining masses should be permissible for $r=1, 2, \ldots . n$. In view of the remarkable success of the geodesic postulate on the one hand, and the perplexing ambiguity on the other, due to singularities which are not mass-particles, we hope that the above identification may give rise to a criterion by which singularities of no physical meaning will be detected, and a sure footing given to the geodesic postulate in the logical structure of relativity. The identification of a

* Attention may be drawn in this connexion to the letter published by Einstein and Rosen in the 'Physical Review' (2nd series), March 1st, 1936.

limiting track with a geodesic explains why the path of a planet is very approximately a geodesic in the field of the sun.

[*Note (added later)*.—Since this paper was written Einstein and Rosen have revised some of their conclusions regarding the two-body problem and the part played by singularities. *Vide* (3) and (4).—V. V. N. and J. S.]

References.

(1) R. C. Tolman, 'Relativity, Thermodynamics, and Cosmology' (1934).
(2) Sir A. S. Eddington, 'The Mathematical Theory of Relativity' (1924). See also Becquerel, 'Le Principe de Relativité' (1922), pp. 209–214, where an alternative method due to Jacques Rossignot is given.
(3) Einstein and Rosen, Phys. Rev. 2nd ser. vol. xlviii. no. 1, p. 73.
(4) Einstein and Rosen, *loc. cit.*

LXIV. *Notices respecting New Books.*

A Comprehensive Treatise on Inorganic and Theoretical Chemistry. By J. W. Mellor. Vol. XV. (Longmans, 1936. Price £3 3*s*.)

THE present, and penultimate, volume of Mellor is devoted to nickel, ruthenium, rhodium, palladium, osmium, and iridium, of which nickel and palladium have, perhaps, particular interest for the physicist. The wealth of reference is as formidable as ever, but it is a pity that the treatment is not a little more critical. We are told, for instance, in one paragraph that the internal friction of solid nickel is given as $1{\cdot}55\times10^{15}$ and 2×10^{8} c.g.s. units respectively by two different groups of workers. Surely the fact that one estimate is ten million times the other might call for a word of explanation. Obsolete and indefinite terms, like magnetic power, used by workers of a hundred years ago, are quoted in heavy type, and not infrequently it is impossible to say even what the work in question is about without referring to the paper cited. Incidentally Poisson's Ratio is printed, in heavy type, in different parts of the book, which looks as if it were deliberate. In spite of blemishes, however, the work is an indispensable reference book, which contains a prodigious amount of information, accessible to skilful enquiry, and this latest volume is surprisingly up-to-date.

[*The Editors do not hold themselves responsible for the views expressed by their correspondents.*]

FIG. 7.

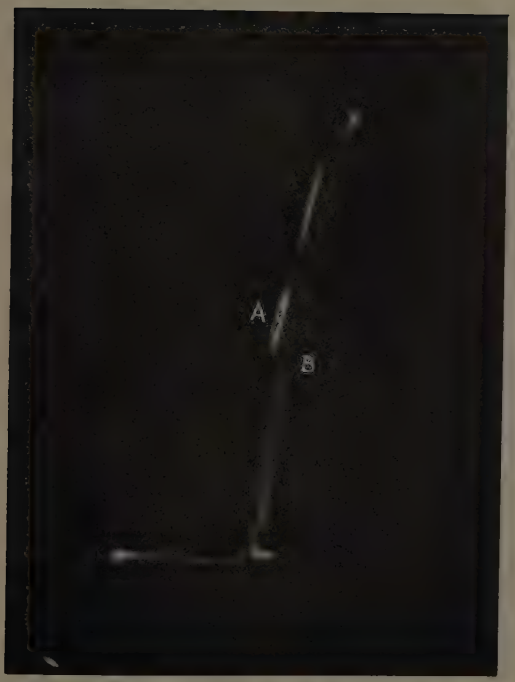

Characteristic showing that both glow and corona forms of the discharge are possible at the same current (pressure 3·4 cm. of mercury).

FIG. 9.

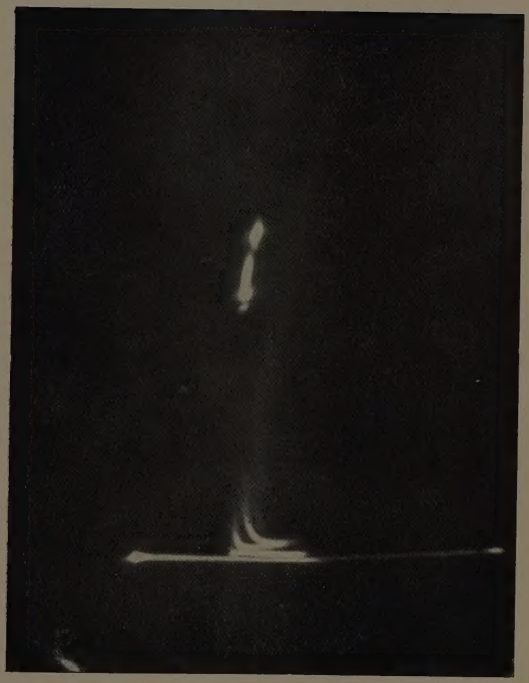

Characteristics at pressure of 7·9 cm. of mercury.

FIG. 2.

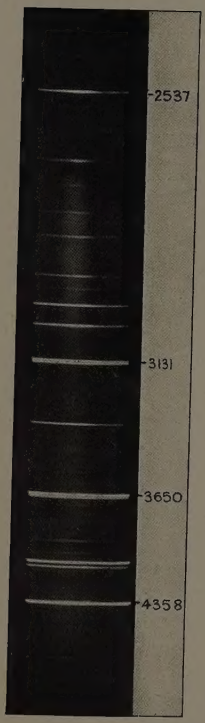

Fluorescent spectrum of cyclohexane at 16° C. excited by mercury arc-lamp.